



**Politecnico
di Torino**

Politecnico di Torino

Master's degree in Environmental and Land Engineering

A.A. 2023/2024

Graduation session: July 2024

“Numerical Modeling of Managed Aquifer Recharge (MAR) Systems”

Advisor:

Prof. Alessandro Casasso

Candidate:

Cosimo Giuseppe Carrozzo
(ID 303982)

Table of Contents

Abstract	5
1 Introduction.....	6
1.1 Groundwater Management	7
1.2 Climate change impact.....	11
2 Managed Aquifer Recharge (MAR).....	14
2.1 Managed aquifer recharge typologies.....	15
2.1.1 Spreading methods.....	15
2.1.2 Induced bank infiltration.....	16
2.1.3 Well, shaft and borehole recharge	17
2.1.4 In-channel modification	17
2.1.5 Runoff harvesting.....	18
2.2 Implementation criteria of MAR.....	18
2.2.1 Hydrogeological characteristics.....	19
2.2.2 Water availability	20
2.2.3 Water source type and climate	20
2.2.4 Water quality	21
2.3 The role of groundwater modelling for MAR.....	22
3 Methodology.....	24
3.1 Sensitivity analysis in groundwater modelling	24
3.2 The FEFLOW software	26
3.3 Base model settings	28
3.4 Boundary conditions assignment	34
3.5 Material Properties assignment.....	37
3.6 Problem settings assignment.....	38
3.7 Sensitivity analysis-investigated parameters	40

4	Results and discussion.....	42
4.1	Configuration I.....	42
4.1.1	Trench-Well 1	43
4.1.2	Trench-Well 2.....	45
4.1.3	Trench-Well 3.....	47
4.1.4	Trench-Well 4.....	48
4.1.5	Trench-Well 5.....	50
4.1.6	Trench-Well 6.....	51
4.2	Configuration II.....	52
4.2.1	Wells-Well 1	53
4.2.2	Wells-Well 2.....	54
4.2.3	Wells-Well 3.....	56
4.2.4	Wells-Well 4.....	57
4.2.5	Wells-Well 5.....	58
4.2.6	Wells-Well 6.....	60
4.3	Discussion.....	61
4.4	Estimation of the possible increase of abstracted flow rate with MAR.....	62
4.4.1	Storage efficiency	64
4.5	Impact of the variation of the MAR injected flow rate	66
4.5.1	Storage efficiency	68
4.6	Possible future developments.....	70
5	Conclusions	72
	References.....	74

Abstract

The depletion of water in aquifers, driven by exploitation for agricultural, energy, and urban purposes to meet overall demand, is accelerating globally. This phenomenon is further exacerbated by climate change, which has significantly affected the hydrological cycle in various parts of the world, directly impacting aquifers that are an integral part to this cycle. To address this issue, engineering systems such as Managed Aquifer Recharge (MAR) have been developed and implemented in various parts of the world, particularly in arid regions and areas where water stress is caused by excessive agricultural use. These systems are characterized based on their specific structures and various configurations can be employed based on the needs, considering installation and management costs as well as construction.

To understand the factors that are crucial for the implementation of these systems, numerical models are widely used. These models allow for a simplified and concrete representation of reality and provide valuable information for the development of these systems. This study presents the results obtained from a sensitivity analysis performed using FEFLOW numerical model. Specifically, the response of an unconfined aquifer to seasonal injection through an MAR system was analysed in two configurations. The analysis focused on identifying which factors used in the model implementation most significantly influence aquifer recharge, thereby contributing to an increase in extraction rates during the irrigation season. The hydraulic conductivity turned out to be the most influential factor on recharge, while the distance of the extracting well from the MAR system had a minor influence. In contrast, the hydraulic gradient and the type of MAR system had a negligible influence.

1 Introduction

Water, particularly freshwater, has been and continues to be managed to support the social and economic growth of the population, sustaining the key sectors of development such as agricultural, industrial and energetic sectors. However, rapid population growth coupled with the expansion of the sectors mentioned above has led to extensive utilisation of this resource, compromising its spatial and temporal availability thus, altering its quantity and quality. Along with these factors, the role and impact of climate change must be considered, as it further alters the distribution and the availability of the freshwater. For instance, in arid and semiarid areas, both surface freshwater and groundwater are diminishing due to overexploitation and the climate change effect¹. Clearly, the management of water is of vital importance. Understanding the global distribution of this resource is key to optimizing its management strategies. Freshwater constitutes about 2.5% of the total water on the planet, with approximately 68.7% stored in glaciers, 30.1 % as groundwater and only 1.2% as surface water distributes across lakes, rivers, soil and other sources². This distribution is schematized in Figure 1.1.

Human societies usually manage surface water resources with a good understanding, whereas groundwater resources remain a greater challenge in terms of conceptualization. These encompass multiple stakeholders and decision-makers with conflicting objectives, operating within complex, evolving systems. These systems involve interconnected social, economic, and ecological elements, adding layers of uncertainty due to limited data, information, and knowledge³. Due to the interconnectedness of various elements and the heavy reliance on groundwater usage as a water resource, an integrated approach becomes imperative for its management. Furthermore, optimizing its utilization to prevent wastage and promote reuse systems is essential, ensuring a high degree of water quality and availability. With this aim, engineering techniques such as Managed Aquifer Recharge (MAR) have been developed to ensure the long-term sustainability of groundwater by recharging reserves using water from surface water bodies, rainwater, or properly treated wastewater before injection⁴, storing it for use during droughts, thereby optimizing water management. This process not only mitigates the adverse effects of over-extraction and climate variability but also supports groundwater level stabilization, prevents land subsidence, and conserves natural ecosystems. Implementing MAR requires a thorough understanding of site-specific hydrogeological conditions, potential contamination risks, and the necessity of long-term monitoring to ensure its efficacy and sustainability. Naturally, this approach represents just one among the numerous strategies essential for ensuring the sustainable utilization of this crucial resource—water.

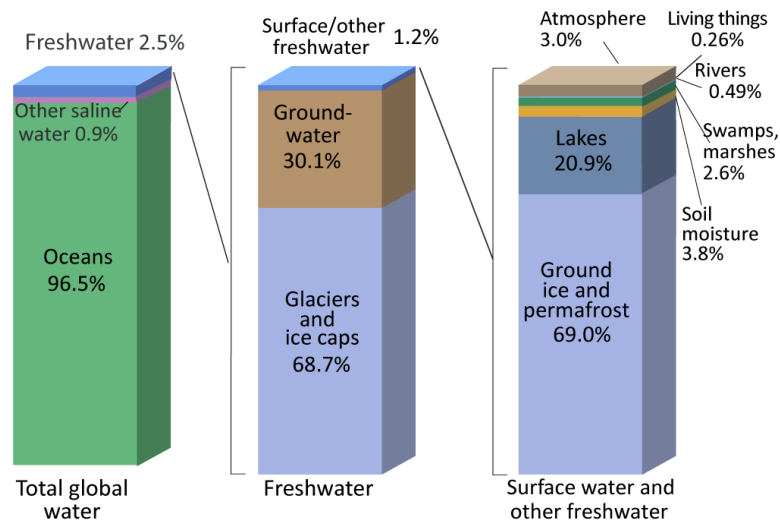


Figure 1.1 Water distribution. Source: Gleick, P. H. (1993). *Water in crisis*.

1.1 Groundwater Management

Before exploring the development and various applications of MAR technologies, a brief focus on the management and utilization of groundwater is necessary, as they directly influence the implementation of this technology. Groundwater constitutes the most substantial accessible reservoir of freshwater, contributing to approximately one-third of global freshwater withdrawals⁵. Usage of groundwater exceeds that of surface water in numerous regions worldwide, a trend anticipated to rise further owing to increasing demand. However, knowledge about aquifer systems remains relatively constrained compared to surface freshwater, primarily due to the inherent complexity of these extensive systems^{6,7}. The utilization of the groundwater resource exhibits temporal and spatial variability based on its intended purposes. Seasonal consumption is observed in agricultural irrigation, whereas its frequency rises significantly when employed for domestic use³. For instance, within humid regions like Japan and Northern Europe, groundwater finds primary application in industrial and domestic sectors. On the other hand, in countries which do not belong to those zones such as India, Pakistan, Saudi Arabia, southwestern USA, China, Iran and Mexico, groundwater is used predominantly for agricultural needs, particularly irrigation⁸. With the introduction of efficient pumps and the expansion of rural electrification, global extraction of groundwater increased from 312 km³/year in the 1960s to 743 km³/year by 2000⁹, with the 70% of this extraction used for irrigation. In Figure 1.2 trends in water consumption and groundwater abstraction by sector from the year 1900 to 2010 are reported.

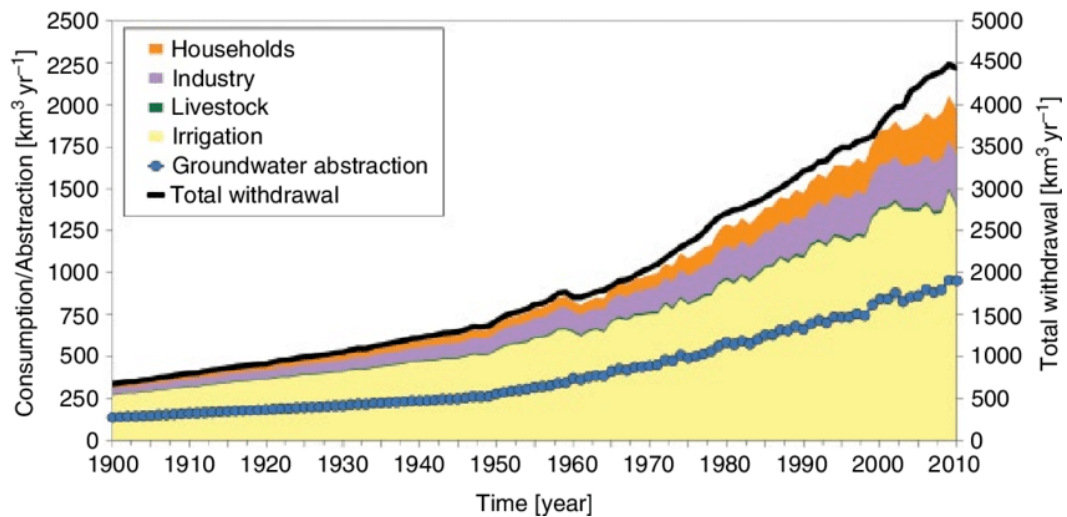


Figure 1.2 Historical trends of global human water use and groundwater abstraction (1900-2010). Source: Wada, Y. (2016). Modelling groundwater depletion at regional and global scales: Present state and future prospects.

In regions where the extraction rate exceeds the aquifer's recharge rate for a significant duration, a resultant decline in the water table occurs leading to water depletion, influencing ecosystems dependent on groundwater and subsequently altering the natural discharge. This, in turn, directly impacts all users of this resource who compete for its utilization¹⁰. Additionally, particularly in developing nations, groundwater monitoring is often neglected for the already mentioned reasons. Consequently, this leads to a high rate of water usage and, frequently, contamination. This contamination is linked to both the reduction in available water quantity, resulting in increased contaminant concentrations into the aquifer due to inadequate management and lack of monitoring. These situations can persist unnoticed even for centuries, impacting not only present users but also future generations. Thus, it is evident that a holistic approach is necessary for managing groundwater, considering all factors influencing these complex systems. This is why Integrated Groundwater Management (IGM) has been developed and applied to coordinate the management of aquifers, considering social, environmental, and economic aspects. A powerful tool utilized in this approach is modelling, allowing the representation of the complexity of the problem with suitable simplifications and boundary conditions. It relies on field-collected data and available observations to provide an accurate representation of reality. This enables the development of management strategies based on a certain level of understanding.

In the world, there are four main issues that influence the management of groundwater, namely:

- depletion of water,
- degradation of water quality,
- water-energy nexus,
- transboundary groundwater conflicts³.

Among the four mentioned, water depletion undoubtedly stands as the most significant challenge in managing groundwater. Over the years, this term has taken on various meanings; in fact, the concept was first associated with the term “safe yield” to define "the net annual supply which may be developed by pumping and artesian flow without persistent lowering of the ground-water plane"¹¹. However, this definition has undergone several modifications over the years, encompassing the effects of potential reductions in groundwater availability on connected ecosystems. This shift in definition tends towards the concept of sustainability, aligning with the principles of IGM¹². Therefore, groundwater sustainability has been defined as a responsible management of the groundwater resource which aims to prevent adverse environmental, social and economic effects. Moreover, it necessitates the achievement of an equilibrium between withdrawing and replenishing over time, aiming to ensure the ongoing availability of groundwater which may cause harm to society or environment¹³. Different studies have been conducted to assess the depletion rate in different parts of the world. Among these studies, the one conducted by Wada et al. illustrates how the area's most susceptible to groundwater depletion worldwide are arid and semi-arid regions. This is linked to various factors such as high population density in these areas and extreme variations in rainfall, which limit natural groundwater recharge. The results of this study are presented in Figure 1.3., where total global groundwater depletion of the hot spot areas reaches $283(\pm 40) \text{ km}^3 \text{ per year}^{10}$.

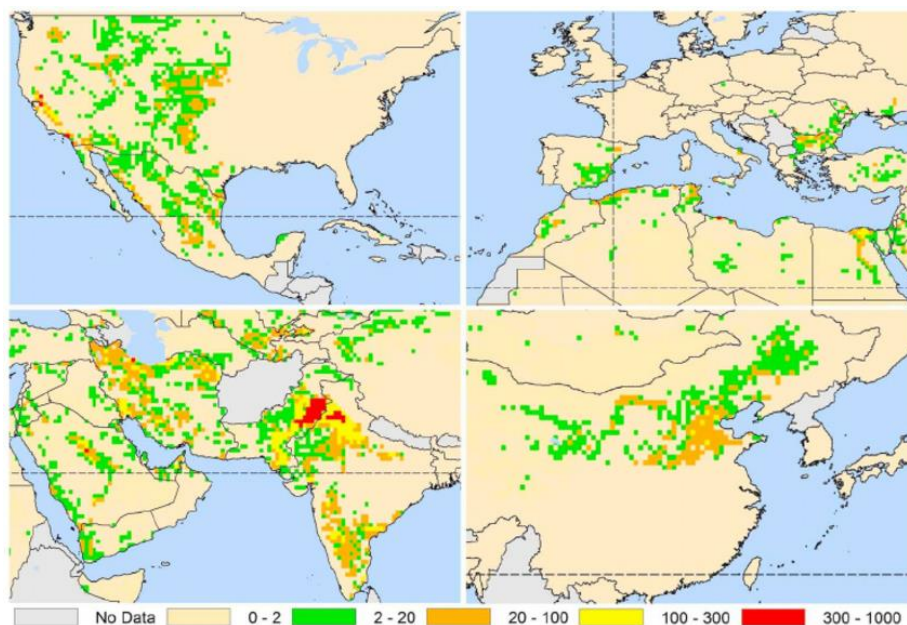


Figure 1.3 Groundwater depletion in the regions of USA, Europe; China and India and Middle East for the year 2000 (mm:yr⁻¹). Source: Wada, Yoshida, et al. "Global depletion of groundwater resources."

Regarding the degradation of water quality, it can derive both from natural or anthropogenic causes. An aquifer is considered contaminated if the concentration of one or more substances exceeds a certain threshold, representing a risk to all the interconnected systems. These substances primarily derived from industrial and agricultural activities, which release salts, chemicals and microorganisms into the environment¹⁴. Exceeding a certain concentration threshold of these substances will cause contamination due to chemicals, microorganisms or aquifer salinization. In the first case, agricultural activities, which disperse fertilizers and pesticides in fields that are carried by irrigation water¹⁵, alongside industrial activities that may release heavy metals and solvents, lead to an increase in the concentration of these substances beyond the established limits in the subsoil and, consequently, in the aquifer system through water percolation¹⁶.

Contamination due to microorganisms derived from leakage of sewage from treatment plants, or from seepage of leachate from landfills, that could reach the aquifer through various pathways¹⁴. Salinization, on the other hand, refers to the increase in salt concentration in soil or aquifer beyond a certain threshold. While this phenomenon in soils is associated with irrigation water used in agricultural fields¹⁷, in aquifers, it is linked to the seawater intrusion, which is particularly relevant in coastal regions. Due to high groundwater extraction rates, hydraulic gradient forms, facilitating the movement of seawater towards the freshwater in the aquifer when it is hydraulically connected to the sea¹⁸. This phenomenon has already affected coastal aquifers around the world, such as Spain, Australia, Lebanon and many other countries. Moreover, it is expected to intensify due to rising sea levels caused by climate change³. The effects of climate change on aquifers will be further explored in the section 1.2.

With the aim of reducing greenhouse gas emissions to mitigate the climate change effects, several alternative technologies to fossil fuels for energy production have been developed and utilized over the years, with a continuous increase in renewable energy sources. Some of these sources directly rely on groundwater systems; technologies such as Aquifer Thermal Energy Storage (ATES), geothermal plants, or even biofuels are directly involved in the management of this resource¹⁹. This highlights the close relationship between water and energy. Furthermore, it is crucial to consider that the use of unconventional gas, such as shale gas, involves extraction techniques like hydraulic fracturing, which use large quantities of water, competing with other users and potentially causing water contamination due to additives used during the operations²⁰. Moreover, another connection between these two elements arises from the groundwater extraction: due to the potential decline in water table levels, more energy will be required in the near future for pumping²¹.

The last significant issue concerning aquifers systems is transboundary conflicts. These extensive systems can span across multiple neighbouring states or regions, leading to competition over the use of groundwater. Often, these aquifers are located in geopolitically unstable contexts, becoming an additional problem among involved parties which could potentially escalate into a conflict²². A representation of these transboundary aquifers is reported in Figure 1.4.

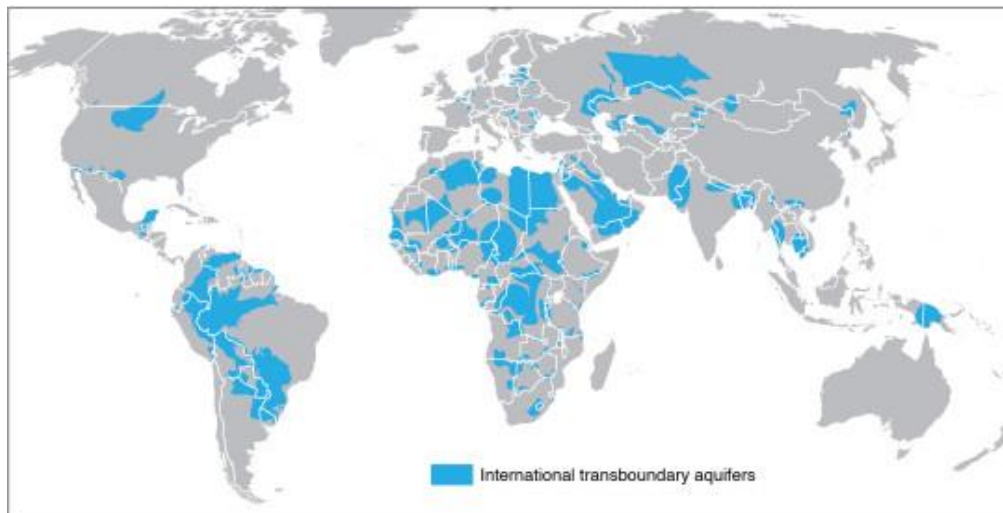


Figure 1.4 Source: Puri and Aureli 2009: *Atlas of transboundary aquifers*

1.2 Climate change impact

As mentioned in the section 1.1, there are several factors influencing the management of groundwater, affecting its quality and quantity. Among the four main issues highlighted, there is a common element which is exacerbating the impact on groundwater: climate change.

A result of anthropogenic greenhouse gas emissions the Earth's system is rapidly changing. Indeed, as a direct consequence of this increase in greenhouse gas concentrations in the atmosphere, the planet's average temperature has risen significantly, resulting in an increase of 1.1 °C in the period 2011-2020 compared to the mean temperature value registered in the period 1850-1900²³. Over the years, significant attention has been given to surface water bodies, particularly on their management as a response to climate change³. However, climate change is affecting all the Earth's system components, including aquifer systems. Consequently, the recharge frequency and the groundwater levels are and will increasingly be affected by these changes, leading to a variation in the availability and quality of groundwater²⁴. Moreover, the recharge of groundwater depends on the frequency and distribution of precipitations, whether in the form of rain or snow; it depends on the evapotranspiration, therefore, on the amount and type of vegetation which cover a certain

area, and it depends on the land use. Climate change and climate variability also affect all these interconnected elements. For instance, an increase in winter temperatures will lead to more melted ice from glaciers, increasing recharge into the aquifer or the rivers streamflow. However, it will also reduce the amount of snow accumulation during the winter season, leading to a decrease in available water in summer needed to sustain the river low flow²⁵. Consequently, this could further stress aquifers due to excessive water extraction needed for irrigation. The response of an aquifer to the pressure exerted by climate change also depends on the type of aquifer considered. Unconfined aquifers, in general, tend to be more sensitive to changes in climatic conditions compared to confined aquifers²⁶. Furthermore, also the geology, hydrogeology, hydrology and biology properties will play a role in affecting the groundwater recharge and quality in response to these climate pressures³.

Changes in groundwater recharge consequently has direct effects on its quality. The main risk is linked to the decrease in groundwater level due to the overexploitation and the rising sea levels caused by global temperatures increases, which could lead to the intrusion of saltwater into the aquifer along the coastal regions¹⁸. Furthermore, due to the increase in the extreme events such as droughts and floods, an increase in groundwater pollution is expected due to contaminants carried by rivers during a flood event or, on the other hand, due to the increase in concentrations of wastewater or other toxic compounds in water owing to its decrease in volume during droughts²⁷. However, due to the complexity of aquifer systems, it is challenging to state whether a change in water availability is directly attributable to climate change or simply due to excessive usage, or perhaps a combination of both factors.

Global hydrological models have been used in order to estimate the groundwater depletion rate. The results demonstrate that this rate is exceeding 20 mm year⁻¹ (2001–2010) in major aquifer systems such as the High Plains and California Central Valley aquifers (USA), Arabian aquifer (Middle East), North-Western Sahara Aquifer System (North Africa), Indo-Gangetic Basin (India), and North China Plain (China) and is primarily induced by human activities. In contrast, groundwater depletion at lower rates (<10 mm year⁻¹) is occurring in the Amazon Basin (Brazil) and Mekong River Basin (South East Asia), primarily attributable to climate variability and change²⁸. An analysis on a global scale using Gravity Recovery and Climate Experiment (GRACE) satellites measurements in the period 2002–2016 across 37 major aquifer systems reveals the presence of 34 trends in the terrestrial water storage (TWS). The drivers are categorized as natural interannual variability, unsustainable water consumption, or climate change. This study has demonstrated how human usage and climate change are impacting the freshwater availability²⁹. The terrestrial water storage trends are reported in Figure 1.5.

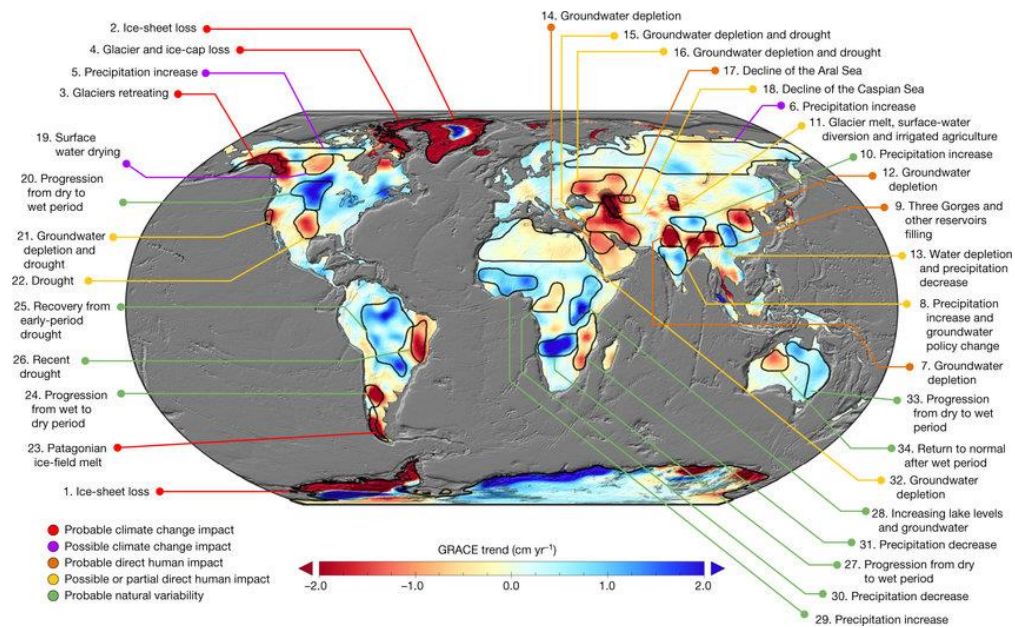


Figure 1.5 Annotated map of terrestrial water storage trends. Source: Rodell et al. 2018 “Emerging trends in global groundwater distribution”

Global Climate Models (GCMs) are used to obtain projected climate change impacts on groundwater. The depletion rate is projected to increase from $204(\pm 30) \text{ km}^3 \text{ year}^{-1}$ in 2000 to $427(\pm 56) \text{ km}^3 \text{ year}^{-1}$ by 2099¹⁰. Other studies indicate that in that northern Europe will experience increased winter rainfall, resulting in greater groundwater recharge within a shorter duration. Conversely, summers are predicted to be drier, leading to prolonged periods of limited or no groundwater recharge. In Southern Europe, the overall recharge rate will decrease, potentially leading to water stress compared to the current situation²⁶. Worldwide withdrawals of total groundwater are estimated to rise from $952 \text{ km}^3 \text{ year}^{-1}$ in 2010 to $1621 \text{ km}^3 \text{ year}^{-1}$ by 2099, whereas, the non-renewable groundwater withdrawals are estimated to rise from $304 \text{ km}^3 \text{ year}^{-1}$ in 2010 to $597 \text{ km}^3 \text{ year}^{-1}$ by 2099³⁰.

As evident, urgent actions are needed to address the future challenges concerning groundwater management. Among various developed techniques and systems, Managed Aquifer Recharge (MAR) has progressively gained attention over the years. It stands as one of the strategies to implement for supporting sustainable, long-term groundwater management.

2 Managed Aquifer Recharge (MAR)

Managed Aquifer Recharge (MAR) is an intentional process aimed at recharging groundwater, allowing for an increase in both quantity and quality. This ensures the availability of groundwater for future use. This method helps to overcome the disadvantages which affect the most common water storage systems in surface reservoirs, which include issues like water losses due to evaporation, exposure to potential contamination, and the requirement for significant land space needed for the reservoir construction³. The excess of surface water directed into an aquifer in these systems may derive from various sources such as river water, storm water, desalinated water, rainwater, treated effluent and water coming from another aquifer³¹. The evolution of these systems has undergone several stages, experiencing substantial modifications and changes due to technological advancements and progressive theoretical discoveries. These advancements have to a better understanding of aquifers and their responses to alterations in water flow, affecting their initial state.

During the initial phase, which goes from 221 BC to 1850 AD, prototypes of MAR were primarily employed to ensure groundwater availability for agricultural purposes, particularly irrigation³². Subsequently, they found application in residential context as well. Examples of early MAR prototypes include the "Amunas" utilized by the Wari civilization in Peru and "Careo" in Spain, both representing early types of infiltration channel prototypes³³.

The second phase dates back to the industrialization era in Europe, from 1850 to 1950. Due to the increasing water demand driven by population growth and the necessity to avoid the potential contamination of water resources, MAR systems found extensive application during this period. Notably, significant theoretical advancements occurred during these years. The formulation of Darcy's law in 1856, together with Dupuit's formula (1863)³¹, the theories of steady-state flow in pumping wells and, subsequently, the transient-state flow theory in pumping wells introduced by Theis in 1935, marked pivotal turning point in the evolution of these systems³⁴.

Due to the extensive destruction left by World War II, from 1950 to 1990, MAR systems represented one of the solutions employed to ensure greater availability and quality of water needed for the recovery of industrial and agricultural activities and for domestic use. The third phase of the development of these systems is attributed to this period. The significant progress during this time was also due to advancements in theoretical field. In fact, the transient theory for pumping wells was formulated during this period, thanks to the contributions of important figures in the field, such as Hantush and Jacob³¹.

The fourth phase goes from 1990 to the present day. Various applications of MAR systems have been implemented worldwide in recent years. Particularly, in more developed countries, these systems use more precise utilization techniques compared to those in developing countries. This difference arises from advanced technological and theoretical knowledge, which also involves the use of modelling software and field data collection for aquifer characterization³⁵.

Nowadays, these systems are increasing by 5% each year³⁶, and they will increasingly be employed due to the increasing water demand and the significant variability in the availability of this resource, exacerbated by climate change.

The implementation and design of MAR systems depend on various factors that are both site-specific and tailored to specific needs.

2.1 Managed aquifer recharge typologies

Depending on the chosen design, the methods of water infiltration into the aquifer and the treatment processes may vary. Based on the method of aquifer recharge and storage technique, MAR systems are classified into five main groups:

1. spreading methods,
2. induced bank infiltration,
3. well, shaft and borehole recharge,

which are techniques referring to water infiltrated, whereas

4. in-channel modification
5. runoff harvesting

which are techniques referring to intercepting water.

The choice of the suitable MAR type depend on the characteristics of the local hydrological and hydrogeological conditions, aquifer type, topography, land use, ambient groundwater quality, and the intended purpose of the recovered water³⁷.

2.1.1 Spreading methods

Spreading methods allow for the infiltration of large water volumes at a relatively low cost through straightforward management procedures. This method is employed when an unconfined aquifer is situated close to the ground surface, enabling significant quantities of water to filter into it through permeable sedimentary soil and rocks. Consequently, the water is extracted with the aid of a pumping well when required. The specific MAR methods which belong to this group are soil aquifer treatment (SAT), infiltration ponds, flooding, ditches and furrows and excess irrigation methods. A schematic representation of this method is reported in Figure 2.1. The installation of

these methods requires a large area of flat land or terrain without steep slopes, particularly in the case of infiltration ponds and flooding methods. Moreover, water dispersed on the ground may carry contaminants if not adequately treated or if filtration through the soil is insufficient to retain these compounds. Consequently, these substances may reach the aquifer, and due to the required time interval for soil filtration, water might incur significant mass losses through evaporation³⁸.

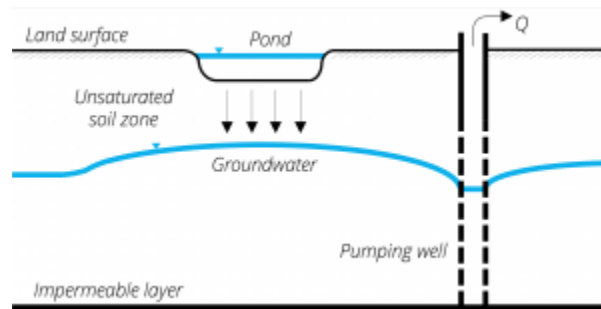


Figure 2.1 Schematic representation of spreading method (infiltration ponds). Source: DEEPWATER-CE

2.1.2 Induced bank infiltration

This method aims to improve both the quantity and quality of water. However, its installation is more complex as it involves strategically placing pumping wells near surface water bodies with low quality levels. Thus, the water is filtered through the ground by the capture zone created by the well's pumping, as it is visible in Figure 2.2. Estimating the travel time accurately during the system's design phase is crucial for retaining pollutants in the soil. It's estimated that to achieve a high level of purification, a travel time exceeding a month is required³⁹. Moreover, intensive monitoring during operations is also necessary. Specific MAR method which belong to this category are river or lake bank infiltration and dune filtration³⁸.

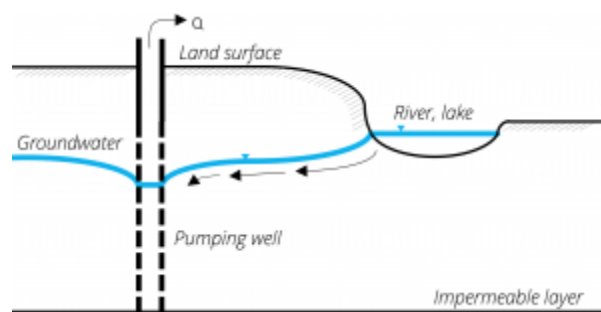


Figure 2.2 Schematic representation of induced bank infiltration (river/lake bank infiltration). Source: DEEPWATER-CE

2.1.3 Well, shaft and borehole recharge

With this method, it's possible to directly inject water into the aquifer using an injection well, in areas where the soil permeability does not allow for the use of the methods mentioned above or where a confined aquifer exists. Subsequently, the water can be recovered through the same well or using another located at a certain distance from the injection well. In the first case, the specific MAR method is named Aquifer Storage and Recovery (ASR), while in the latter case, it is named as Aquifer Storage, Transfer, and Recovery (ASTR), reported in Figure 2.3. For this method as well, the design and construction phases are complex, requiring continuous monitoring during system operation. Moreover, water sources with high-quality levels are needed in the process³⁸.

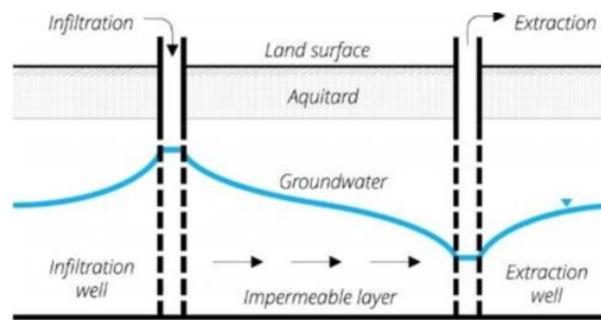


Figure 2.3 Schematic representation of well, shaft and borehole recharge (aquifer storage transfer and recovery). Source: DEEPWATER-CE

2.1.4 In-channel modification

The in-channel modification typologies belong to the category of MAR systems that facilitate aquifer recharge by diverting rivers, channels, and intermitted water flows through the construction of various dams like sand storage dams or subsurface dams. These dams are designed to modify the flow, retaining a certain amount of water that will recharge the underlying aquifer through infiltration. In this case, since no injection wells are utilized, the aquifer beneath the water flow must be unconfined and the soil above which the system is installed must be permeable, allowing the water to reach the aquifer³⁸. The schematic representation is reported in Figure 2.4.

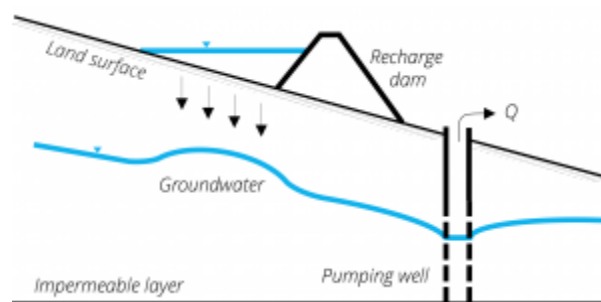


Figure 2.4 Schematic representation of in-channel modification (recharge dams). Source: DEEPWATER-CE

2.1.5 Runoff harvesting

In these MAR systems, water is directed into specific storage tanks and subsequently allowed to infiltrate through permeable soil to reach the unconfined aquifer. It is a system that can be employed at various scales, from a single house, whose schematic representation is visible in Figure 2.5, to a residential context. Usually, these types of systems do not have high costs and are characterized from simple constructions. Moreover, they allow for the restoration of the hydrological cycle in urban settings⁴⁰.

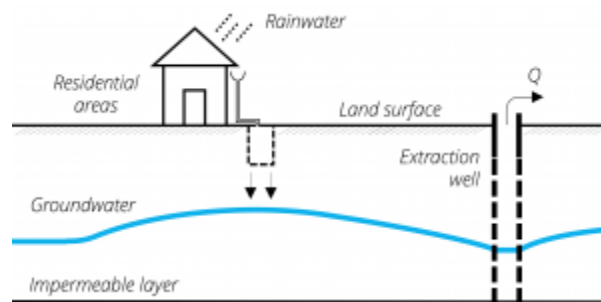


Figure 2.5 Schematic representation of runoff harvesting (rooftop rainwater harvesting). Source: DEEPWATER-CE

2.2 Implementation criteria of MAR

As reported in the previous paragraph, there are various MAR schemes and strategies that can be implemented to manage water resources, improving their availability and quality according to specific needs. However, the development and the choice of these MAR strategies is heavily influenced by various elements which are site-specific. This necessitates following criteria based on specific site characteristics such as hydrology, climatic variability, water resource availability and type, geology, regulations, and many others. This paragraph will analyse all these criteria that influence the implementation of MAR systems and therefore, which of these systems are best suited based on these characteristics.

The MAR selection criteria can be summarised in four main categories:

1. hydrogeological characteristics,
2. water source availability,
3. water source type and climate,
4. water quality ⁴.

2.2.1 Hydrogeological characteristics

Soil and subsurface characterization play a pivotal role in determining which MAR system to employ in a particular location. Understanding the type of aquifer in the area, its water storage capacity, and the infiltration process are the key objectives in this phase of system design. Particular attention is needed for the characterization of the vertical hydraulic conductivity which usually must be higher with respect the horizontal one, since directly affect the vertical infiltration. Moreover, other important information is needed, such as the boundary conditions of the site, in order to understand if there are inflow or outflow of water, and the aquifer parameters. All this information will be used to model the zone in which the MAR system should be installed, in order to simulate the response of the system to potential modifications in the quantity and method of water recharged into the aquifer. A critical distinction is needed between soil and subsurface characteristics as they can vary significantly, influencing water infiltration differently and thereby affecting the selection of the appropriate MAR system to be installed. Some criteria guide the choice of MAR systems based on the soil type where installation is required. Soils can be classified into four Hydrologic soil groups (HSG): sandy loam or HSG-A (>90% of sand), silt loam or HSG-B (50-90% sand and 10-20% clay), sandy clay loam or HSG-C (<50% sand and 20-40% clay) and clay loam or HSG-D (<50% sand and >40% clay). Studies demonstrated that in sandy loam and silt loam HSGs the high infiltration rate makes the installation of MAR systems unnecessary generally, since the soil allow the water to infiltrates naturally. Whereas, in places where sandy clay loam is present, it has been demonstrated that also an high number of MAR systems are installed due to the lower infiltration rate which characterize the soil⁴. A schematic representation of the MAR types distribution as a function of the soil type is reported in Figure 2.6.

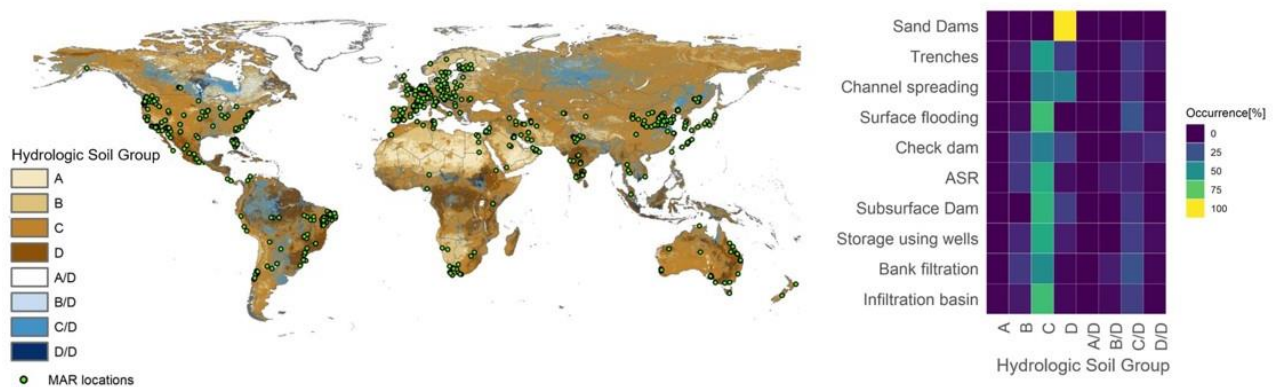


Figure 2.6 Schematic representation of Hydrologic soil groups on the left and MAR type distribution depending on the HSG on the right. Source: S. Alam et al. "Managed aquifer recharge implementation criteria to achieve water sustainability"

However, the permeability of the deeper part of the soil considered can vary significantly compared to the upper layer, affecting the choice of the MAR scheme that needs to be installed. Consequently, a subsurface characterization must be included in the analysis. Data are obtained through pumping test, water availability and water balance.

2.2.2 Water availability

The availability of water in a specific location can be determined directly by the difference between long-term precipitation and evapotranspiration in a particular basin. However, other parameters directly influence the water availability such as the terrain characteristics (elevation, slope), vegetation, land use, and flow availability. Thus, MAR systems can be implemented to improve water quality, which occurs in areas with high water availability, or to increase water quantity in areas with low water availability. Obviously, the implementation of MAR systems strongly depends on the climate of the area, which influences the water balance.

2.2.3 Water source type and climate

The implementation of MAR systems also depends on the type of water source available in the area. The origin of this water can vary and is generally classified into four main groups: surface water (lakes, rivers), rainwater, wastewater, and groundwater. Moreover, considering the climate of the area is crucial in determining the type of MAR scheme to install. Generally, climates are categorized into five main classes: hyper-arid, arid, semi-arid, dry-sub-humid, and humid⁴¹. Considering the climatic zone and the water resource helps determine the most suitable MAR system to implement. According to a study conducted by S. Alam et al.⁴, which analysed 1127 MAR sites worldwide to understand how these systems varied based on climatic regions and water resources, it was evident that surface water is the most commonly used water resource for MAR implementation across all climatic regions, followed by rainwater. Additionally, it was observed that contaminated groundwater is primarily used in semi-arid, dry-sub-humid, and humid areas, while wastewater is mainly utilized in hyper-arid zones. A schematization of the results obtained is reported in Figure 2.7.

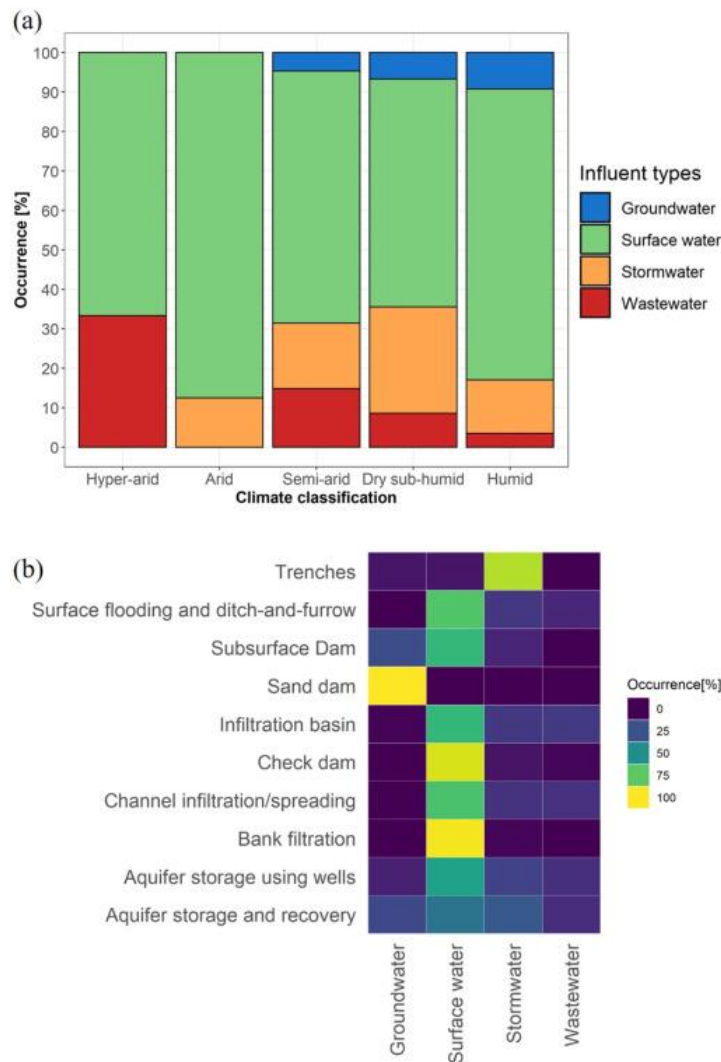


Figure 2.7 Source water categorized according to (a) climate classification (b) MAR type. Source: S. Alam et al. "Managed aquifer recharge implementation criteria to achieve water sustainability".

2.2.4 Water quality

The last criterion to consider for implementing MAR systems is water quality. To assess water quality, several parameters need analysis, including salinity, the presence of particulates, organic and inorganic compounds, nutrients, and pathogens. The removal capacity of potential pollutants and the consequent improvement in water quality vary based on the MAR system used. For instance, Soil Aquifer Treatment (SAT) is effective in removing organic carbon, unlike Aquifer Storage and Recovery (ASR) systems. This is because geochemical and microbiological processes in the unsaturated zone purify water filtered through the soil, eliminating compounds present in the water source. Therefore, appropriately evaluating the residence time during the MAR system's design phase to enable contaminant removal is crucial.

However, the presence of compounds and sediments in the water can cause physical and biological clogging of subsurface pores, reducing water infiltration⁴². Parameters to consider for assessing the

purification capacity of the unsaturated zone include reduction potential, pH, organic matter content, and mineralogy. Furthermore, besides the capacity to remove potential contaminants from water filtered into the aquifer, MAR systems can be used to dilute contaminated groundwater by injecting appropriately treated or uncontaminated water from other sources⁴³. This strategy helps reduce the concentration of pollutants like nitrogen, pathogens, or organic contaminants⁴⁴. Finally, implementing MAR systems requires tailoring the approach based on the type of contaminant and its potential risk since certain compounds might not be adequately removed by the subsurface, requiring pre-treatment before injection. This approach ensures an effective strategy for managing specific contaminants and mitigating potential risks associated with them within the aquifer system⁴.

2.3 The role of groundwater modelling for MAR

The deployment of a Managed Aquifer Recharge (MAR) project is affected by a multitude of factors outlined in preceding sections. To ensure the successful execution of the project, it is imperative to adopt an approach based on the implementation criteria, adopting a methodology which is enriched by prior successful MAR projects. Although each project exhibits unique site-specific characteristics, gaining information and experience from past implementations fosters strategic decision-making and increase the likelihood of success of the current project. The implementation options are always integrated within the Integrated Groundwater Management (IGM) and are divided into six phases according to the Standard Guidelines for Artificial Recharge⁴⁵:

- I. Preliminary activities
- II. Field investigation
- III. Design
- IV. Construction and start-up
- V. Operation and maintenance
- VI. Closure

The initial steps typically involve collecting and assessing data, as well as conducting a preliminary study that utilizes models to generate a conceptual assessment of the proposed MAR project. Moreover, modelling can be used for scenario analysis and future predictions, representing a valuable tool to assess the feasibility of a MAR project in a specific location.

The assessment of a MAR project necessitates the utilization of different models, depending on the specific evaluation objectives. These models serve to simulate various hydrological processes, such as groundwater flow, unsaturated flow, solute transport, reactive transport, and watershed dynamics. Each model is designed to provide insight into specific aspects of the MAR system, assisting in decision-making and optimizing project outcomes. As example, groundwater flow models represent primarily the saturated soil zone and are typically based on the Darcy's law, describing the water movement through the porous media. In contrast, unsaturated flow models focus on the areas where the porous media is not fully saturated and utilize the Richards' equation to simulate the water movement through the unsaturated soil³⁵.

Therefore, modelling can help to evaluate the advantages and disadvantages of a specific MAR scheme, helping in evaluating its feasibility and the optimal design⁴⁶. Moreover, the use of model allow to quantify the recovery efficiency, determining the amount of water with specific quality standards that can be retrieved, evaluating the residence time of the infiltrated water⁴⁷. The movement of injected water and its interaction with natural groundwater are computed to measure the resulting groundwater level changes and the affected area when MAR is developed.

Finally, a sensitivity assessment can help to understand which are the main hydrological and operational factors which impact the effectiveness of a MAR project, simulating the best and the worst-case scenario. Nonetheless, modelling offers a unique opportunity to integrate future climate change scenarios, water usage patterns, and management strategies into the feasibility assessment. Among the model typology reported above, groundwater flow models are most used for MAR assessment followed by the unsaturated flow models³⁵.

Typically, models specifically designed for MAR implementation are not developed. Among the available options, prevalent choices for groundwater and saturated flow modelling include MODFLOW⁴⁸, FEFLOW⁴⁹, and SEAWAT⁵⁰. Meanwhile, MIKE-SHE⁵¹, MARTHE⁵², and HYDRUS⁵³ are commonly employed for unsaturated flow modelling purposes.

It is important to note that models provide a simplified representation of the complexity which characterizes the natural systems, thus uncertainty and errors affect the final results.

3 Methodology

The primary aim of this study was to perform a sensitivity analysis of the parameters that mostly affect the performance of Managed Aquifer Recharge (MAR) systems through numerical flow modelling. In particular, the MAR system simulated is aimed at replenishing the aquifer during the non-irrigation season using water from agricultural canals that are not used out of the irrigation season. This investigation is crucial for determining water availability during the subsequent irrigation season.

The sensitivity analysis was conducted on a simplified model, which did not use an actual stratigraphic configuration but instead an assumed one. Representative parameters available in the literature were used to approximate reality. The parameters selected for the sensitivity analysis were: the MAR typology considered, the distance of the extracting well from the MAR system, the hydraulic gradient, and the hydraulic conductivity. These were hypothesized to be the major factors affecting aquifer recharge. The software selected to perform the study is FEFLOW. This approach ensures that the study serves as a foundation for future research that will integrate site-specific data, starting from the insights gained from this sensitivity analysis.

3.1 Sensitivity analysis in groundwater modelling

Sensitivity analysis (SA) serves as a valuable supplementary tool in groundwater flow modelling, helping to evaluate the significance of different governing flow parameters in determining the behaviour of a particular flow scenario⁵⁴. It is the study of how the outputs of a system are related to (and are influenced by) its inputs⁵⁵. In numerous applications, the utilized models can be classified into two main categories: statistical models and process-based models. Statistical models function by mapping inputs to outputs^{56,57}, while process-based models solve a set of differential or other mathematical equations that govern the spatiotemporal behaviours of the underlying processes^{58,59}. These models serve as powerful tools for understanding and simulating complex systems, offering insights into how various factors interact and influence outcomes⁵⁵. The inputs of interest, often known as 'factors' in sensitivity analysis, encompass a broad range of elements within the model framework. These factors may consist of model parameters, forcing variables, boundary and initial conditions, selections of model structural configurations, as well as assumptions and constraints. On the other hand, outputs can take various forms, including functions of model responses that may exhibit spatiotemporal variability. Objective functions, such as error functions in model calibration, are also considered among the outputs of interest⁵⁵. In groundwater modelling, sensitivity analysis serves as a valuable tool for calibrating simulation models. It allows for the determination of tolerances on parameters such as transmissivity and

storativity, based on acceptable levels of error in hydraulic head. Additionally, sensitivity analysis aids in estimating the variance and confidence intervals for hydraulic heads, providing valuable insights into model performance and reliability⁶⁰.

Sensitivity analysis involves various approaches, which can generally be classified into two main categories: local SA and global SA. Local sensitivity analysis involves examining how a model's response changes when one parameter is varied while all others are held constant. This is typically done through methods like differential sensitivity analysis (DSA). In contrast, global sensitivity analysis looks at how the model's response changes when all parameters are varied simultaneously. The generalized sensitivity analysis (GSA) method is a type of global sensitivity analysis that addresses the limitations of local sensitivity analysis approaches⁶¹.

The study of sensitivity serves various purposes depending on the specific application, that can be summarized as follows:

- Establishing a response surface, which describe how model responses change with variations in input parameters.
- Identifying the most significant uncertain parameters based on their impact on model response variability, known as factor prioritization⁶².
- Examining parameter interactions to understand process dynamics and potential influences between variables⁶³.
- Ensuring consistency between the model and the physical system⁶⁴.
- Streamlining the model by identifying and eliminating non-influential parameters, reducing computation time and errors caused by over-parameterization^{65,66}.

For instance, sensitivity analysis in flow modelling and groundwater management, enables the assessment of optimal well locations and pumping rates, considering various constraints such as local drawdown limitations, hydraulic gradients, and water production targets. By systematically analysing the sensitivity of these factors, decision-makers can make informed choices to enhance groundwater management practices and ensure sustainable resource utilization⁶⁷.

In this study, FEFLOW software was selected to perform sensitivity analysis. The aim was to determine the key parameters influencing groundwater recharge when utilizing a Managed Aquifer Recharge (MAR) system. Together with the introduction of the case study, a comprehensive introduction to FEFLOW is provided in the next chapter. This introduction aims to describe briefly the software capabilities and features pertinent to the subsequent analysis conducted.

3.2 The FEFLOW software

The analysis was performed with the finite-element code FEFLOW (Finite Element subsurface FLOW system), one of the most sophisticated numerical models available for simulating flow and transport processes in porous media, under both saturated and unsaturated conditions. The modelling platform features an advanced graphical environment allow for simulating underground flow dynamics in complex situations, contaminant transport in the aquifer, and heat transport.

The use of a finite element approach, as opposed to the finite difference method used by classical numerical groundwater flow models such as MODFLOW, ensures extreme flexibility in spatial discretization of the domain and provides a better representation of natural elements and anisotropic conditions. FEFLOW also allows for the representation of discrete features such as single or multiple fractures. In addition to its superior domain representation compared to other common simulation codes, FEFLOW offers further significant advantages and capabilities in representing local dynamics. These include the ability to completely desaturate calculation layers, which is strategically important in cases of high gradients.

The applications span various fields, with some examples including: flow transport in fractured media, intrusion of salt water, design of remediation interventions, contamination transport, management and allocation of groundwater, groundwater/surface water interaction, and geothermal energy and heat transport⁶⁸.

To perform sensitivity analysis through FEFLOW, several steps are required, but the first step, regardless of the complexity of the analysis to be performed, is to generate a conceptual model or base model. The conceptual model serves as an ideal representation of hydrogeology within the groundwater flow system. It represents the optimal approach to describe the functioning of the aquifer. Furthermore, it provides a visual representation of the complex natural aquifer system before constructing the numerical model. To build a robust conceptual model, the following elements are essential:

- ✓ Groundwater flow directions
- ✓ Hydrologic boundaries (including recharge areas, rivers, lakes, wetlands, etc.)
- ✓ Geologic formations
- ✓ Hydrologic parameters (e.g., soil conductivity, storage, porosity)
- ✓ Well conditions (including extraction or injection details such as location, screen, depth, and rates)
- ✓ Observations of groundwater head and groundwater quality⁶⁹.

The construction of a model in FEFLOW involves a series of essential steps. These steps are fundamental in ensuring the accuracy and reliability of the simulation results. They provide a structured approach to setting up the model and analyzing the behaviour of the system under consideration. In this thesis, the process of model construction in FEFLOW is delineated into the following key stages:

1. Prepare input data, including importing shapes, wells, surfaces, XYZ points, cross-sections of the ground layer, and digitizing new GIS layers.
2. Define the super element mesh and 2D mesh.
3. Identify slice elevations.
4. Assign property zones.
5. Define flow boundaries.
6. Run the simulation and analyze the results, checking the visualization outcomes.

The conceptual model serves as the foundation of the FEFLOW code, offering several advantages:

- **Independence of Boundary and Model Input:** the conceptual model is not dependent on the numerical grid or mesh, allowing for the design of multiple conceptualizations of the site without constraints. This independence facilitates easy modifications even after construction.
- **Flexibility in Design:** multiple grids or meshes with different sizes can be selected based on project requirements. This flexibility enables the adaptation of the conceptual model to varying needs and scenarios.
- **Conversion to Numerical Model:** the conceptual model can be converted into a numerical model with a numerical grid. This conversion process facilitates the transition from conceptualization to detailed numerical simulation.
- **Adaptability to Project Needs:** the simulator can be adjusted or customized to accommodate specific project requirements. If the existing numerical model is unsuitable, a new one can be developed with a different grid or configuration.
- **Ease of Modification:** the conceptual model allows for easy and efficient modifications, ensuring that the model can be updated or refined as needed throughout the project lifecycle.

Overall, the conceptual model provides a versatile and adaptable framework for developing and refining numerical simulations within the FEFLOW code⁶⁹.

3.3 Base model settings

As mentioned earlier, FEFLOW employs the finite element method to solve the partial differential equations, in two or three variables, that characterize the mathematical model. To solve the problem, FEFLOW subdivides the larger system into simpler and smaller parts called finite elements through a process of discretization, which leads to the generation of the so-called mesh of the considered geometric space. In order to generate the finite element mesh for constructing the model, the initial step involves constructing the supermesh. This reference structure contains all the essential geometric information required by the algorithm for mesh generation. FEFLOW provides the option to generate either a 2D or a 3D supermesh, depending on the analysis requirements and the available data. For the purpose of this study, the 2D supermesh option has been selected. This involves the use of polygons, lines, and points to define the reference geometric entities. In the study, the reference supermesh was defined using a regular polygon with a side length of 5000 m. Considering the analysis objective, six extraction wells were incorporated into the domain, represented as points in the Supermesh. These wells were positioned at distances of 1700 m, 1900 m, 2100 m, 2300 m, 2500m, and 2700 m respectively, from the lower boundary of the polygon, and at a distance of 2500 m from the lateral edges.

The final geometrical entity to be considered before mesh generation is the MAR system, through which the aquifer is recharged. Specifically, two different configurations were analysed based on the MAR system considered:

- The first configuration in which the MAR system is a trench, represented in the supermesh by a rectangle with a base of 1000 m and a height of 1 m.
- The second configuration in which the trench is replaced with a series of eleven injecting wells, each spaced 100 m apart for a total distance of 1000 m.

The vertical distance among the represented MAR systems from the first pumping well is 200 m.

The comparison between the two reference scenarios are reported in Figure 3.1 and Figure 3.2.

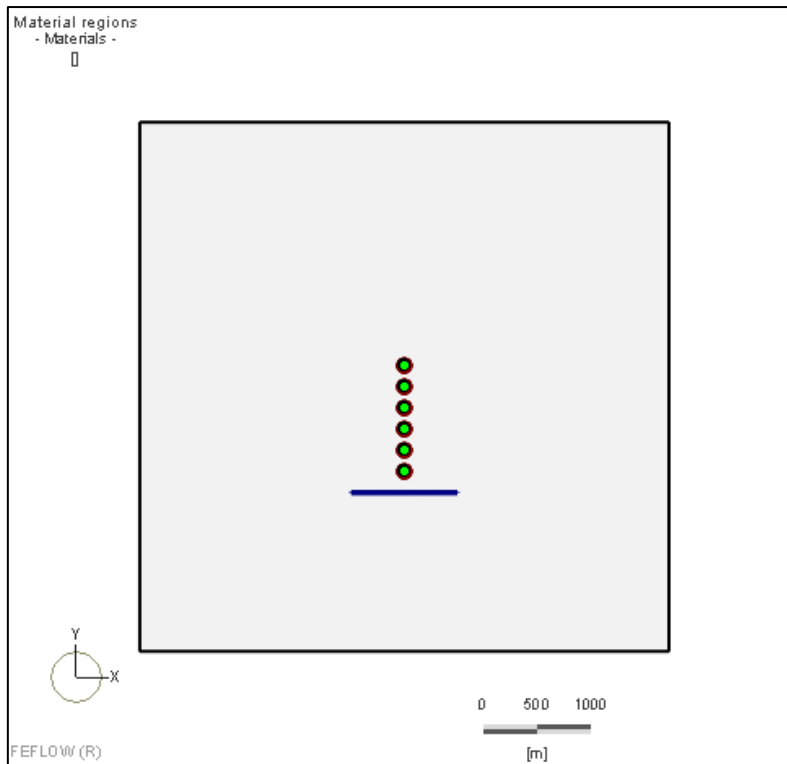


Figure 3.1 Supermesh with an injecting trench

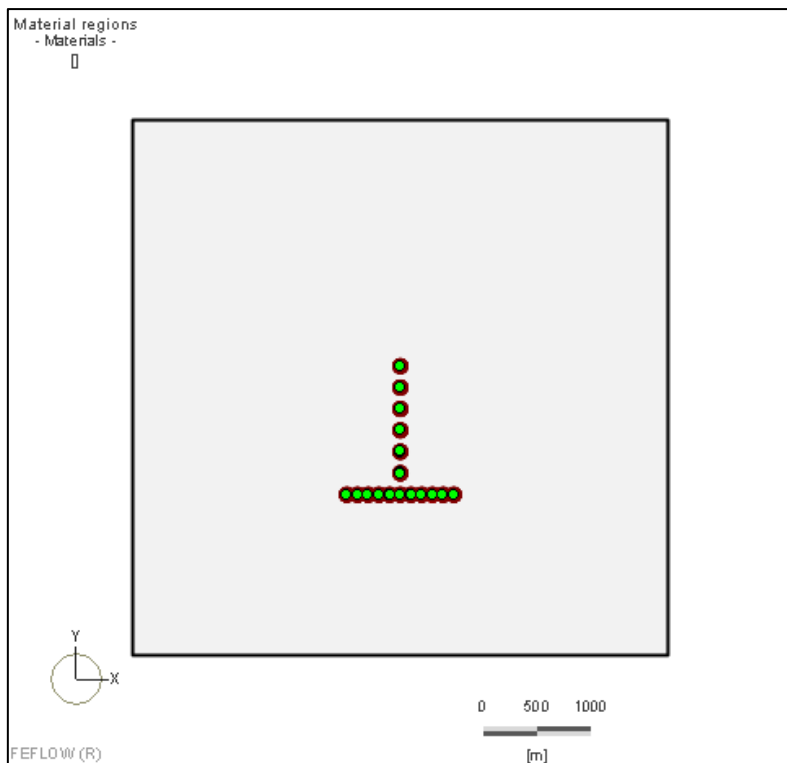


Figure 3.2 Supermesh with a series of injecting wells

To ensure an optimal discretization around the wells, crucial for accurately solving the flow equations in the vicinity of these points, each well is represented by seven points. Six of these points are positioned at the vertices of a hexagon, while the seventh point is located at the centre of the well as reported in Figure 3.3. In the image, r_b represents the borehole radius, while Δ denotes the distance at which each of the six measurement points is positioned from the centre. This Δ value must approximate the virtual radius $r_{virtual}$. The node distance Δ is calculated using the following formula:

$$\Delta = \exp\left(\frac{2\pi}{n \tan\left(\frac{\pi}{n}\right)}\right) \cdot r_b$$

Eq. 1

Where n represents the number of nodes, in this case equal to 6.

This configuration allows for a more refined meshing strategy, enhancing the model's ability to capture the dynamics of flow behaviour around the wells.

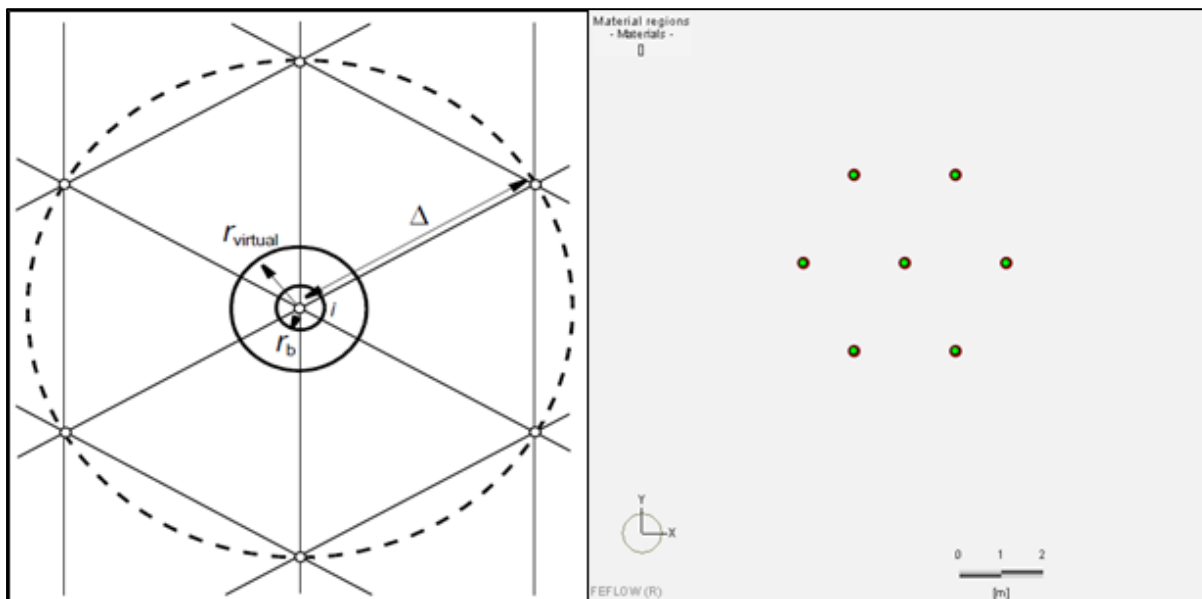


Figure 3.3 Well points representation in the supermesh

After that the 2D domain has been defined with all the internal elements, the finite-element mesh generation was carried out. The finite-element mesh generation can be performed with different algorithms which are available on FEFLOW. Considering the geometrical characteristics of the domain and the purpose of this study, the mesh generation has been carried out with the Triangle algorithm. The process has been performed for both the supermesh domain and the results are reported in Figure 3.4 and in Figure 3.5.

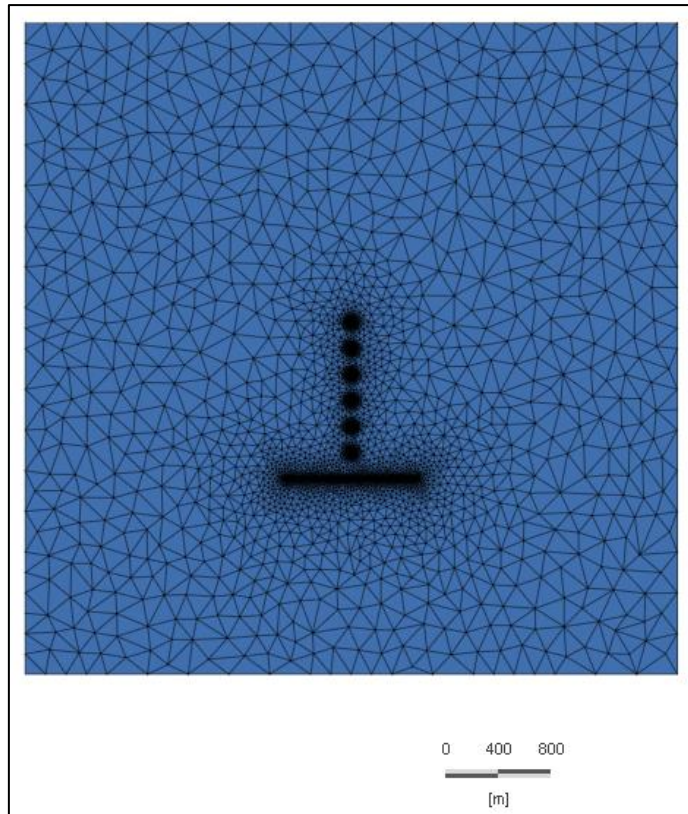


Figure 3.4 2D Finite-element mesh with trench as a MAR system

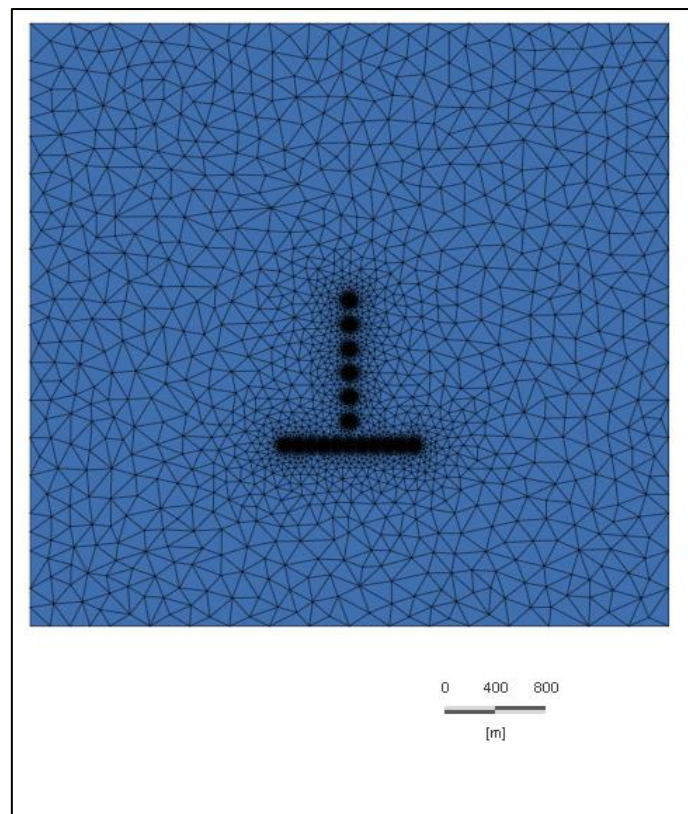


Figure 3.5 2D Finite-element with wells as a MAR system

From the figures shown above, it can be observed that the finite element discretization of the domain becomes denser around the geometric elements representing the extraction wells and injection trench in the first configuration, and the extraction and injection wells in the second one. It is important to have a higher density of finite elements around those points because they represent areas of significant interest and activity in the numerical model. A greater density of finite elements allows for better spatial resolution and a more accurate representation of phenomena occurring near extraction and injection points, such as flow distribution, for example. This is crucial for a correct assessment of hydrogeological behaviour and, consequently, for a more accurate sensitivity analysis of the system and the precision of predictions provided by the model. In Figure 3.6 it is possible to observe these details.

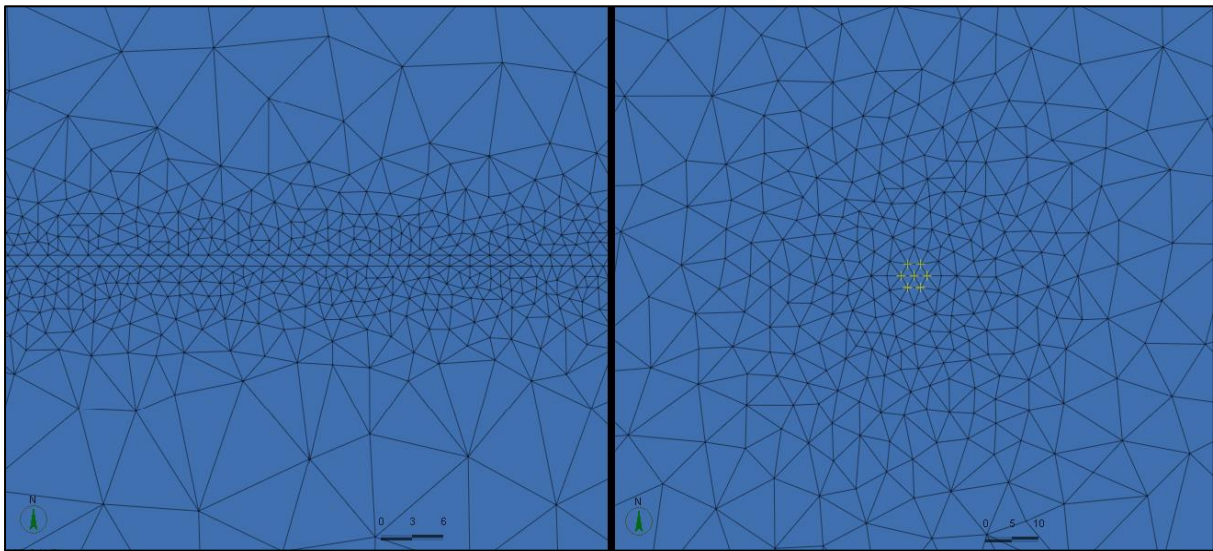


Figure 3.6 Zoom on well and trench

Once the domain discretization process was completed, it was possible to switch from the 2D model to the 3D model. In both cases, the 3D model consists of three layers with different thicknesses. Starting from the upper layer towards the lower one, the thickness of these layers is 30m, 20m, and 10m respectively. The upper layer represents the vadose zone, whereas, the middle layer represents the unconfined aquifer. The lowest layer is an impermeable stratum, acting as a barrier that prevents further downward movement of water.

Additionally, each slice in the model has an inclination, which is inferred by the model using the elevation of the vertices of the domain. The representation of the domain is reported in Figure 3.7.

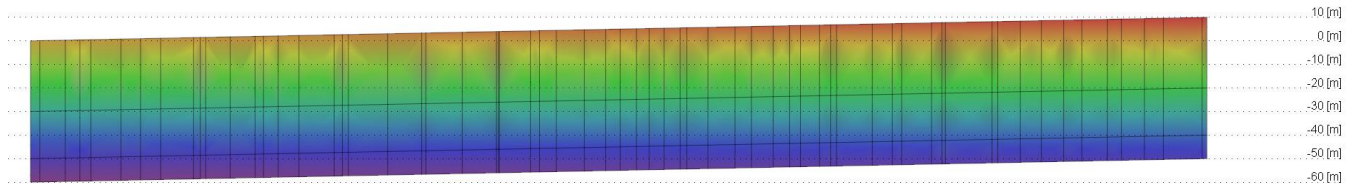
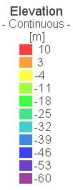


Figure 3.7 Cross-section of the model along the y-axis

The summary of all the geometric settings is reported in the Table 1.

Table 1 Problem Geometry

Width [m]	5000
Height [m]	5000
Number of layers	3
Number of slices	4
Depth layer 1 [m]	30
Depth layer 2 [m]	20
Depth layer 3 [m]	10
Element type	Triangular prism
Element per layer	13357
Nodes per Slice	6717





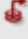
After finalizing the 3D configuration, the next step involved improving the characterization of the conceptual model by incorporating essential information required for conducting sensitivity analysis. This implied defining boundary conditions and specifying material properties pertinent to the model.

3.4 Boundary conditions assignment

In FEFLOW, the default boundary condition is characterized by a state of "no flow," indicating that there is no water movement permitted across the boundary. However, if there is a necessity to enforce specific conditions within the model, it becomes imperative to explicitly define a boundary condition at the respective node. By setting boundary conditions at designated nodes, the model can accurately simulate and reflect the desired hydraulic behaviour and interactions within the system. FEFLOW provides the capability to set boundary conditions for fluid flow, mass transport, and heat transport. In this case, only the Fluid-Flow boundary conditions have been specified. Boundary conditions can be established both at the outer boundaries and within the internal framework of the FEFLOW model. These conditions are specified at the nodal level, although certain types, such as Fluid-flux BC and Fluid-transfer BC, require application across multiple nodes.

FEFLOW offers four categories of boundary conditions, all of which can function either in steady-state condition or transient conditions in conjunction with time series. The implementation of these boundary conditions may be subject to additional physical constraints. The different boundary conditions categories are reported in Table 2.

Table 2 Boundary Conditions categories; Source: FEFLOW 8.0 Documentation

Symbol	Boundary Condition	Short Description	Examples
	<u>Hydraulic-head BC</u>	Fixed hydraulic head (1 st kind/Dirichlet boundary condition).	<ul style="list-style-type: none"> Well-known groundwater level at boundary Surface water body perfectly connected to the aquifer
	<u>Fluid-flux BC</u>	Fixed flux (Darcy flux) across a model boundary (2 nd kind/Neumann boundary condition).	<ul style="list-style-type: none"> Lateral inflow into the aquifer from a slope
	<u>Fluid-transfer BC</u>	Fixed reference water level with additional transfer rate (3 rd kind/Cauchy boundary condition)	<ul style="list-style-type: none"> River/lake with clogging layer Partly clogged drain
	<u>Well BC</u>	Fixed abstraction/infiltration at a single node or along a well screen.	<ul style="list-style-type: none"> Pumping/infiltration well
	<u>Multi-layer wells</u>	Fixed abstraction/infiltration along a well screen.	<ul style="list-style-type: none"> Pumping/infiltration well

In the conceptual model developed for this study, the initial implementation focused on Hydraulic-head boundary conditions. Specifically, a hydraulic head of 20 m and 10 m was imposed in the southern and northern boundary of the model, respectively, to achieve a hydraulic gradient of 0.002. Consequently, constraints were applied to the nodes representing the pumping wells utilized during the irrigation season. This was accomplished using the Multi-layer wells boundary condition, which offers the capability to specify a fixed or time-varying pumping rate along a well screen. The depth of the wells was assumed to coincide with the sum of the thickness of the first two layers. This parameterization was carried out using the Multi-layer wells editor, which facilitates the definition of various well characteristics, including pumping rate, well depth, and well radius. The corresponding menu is illustrated Figure 3.8.

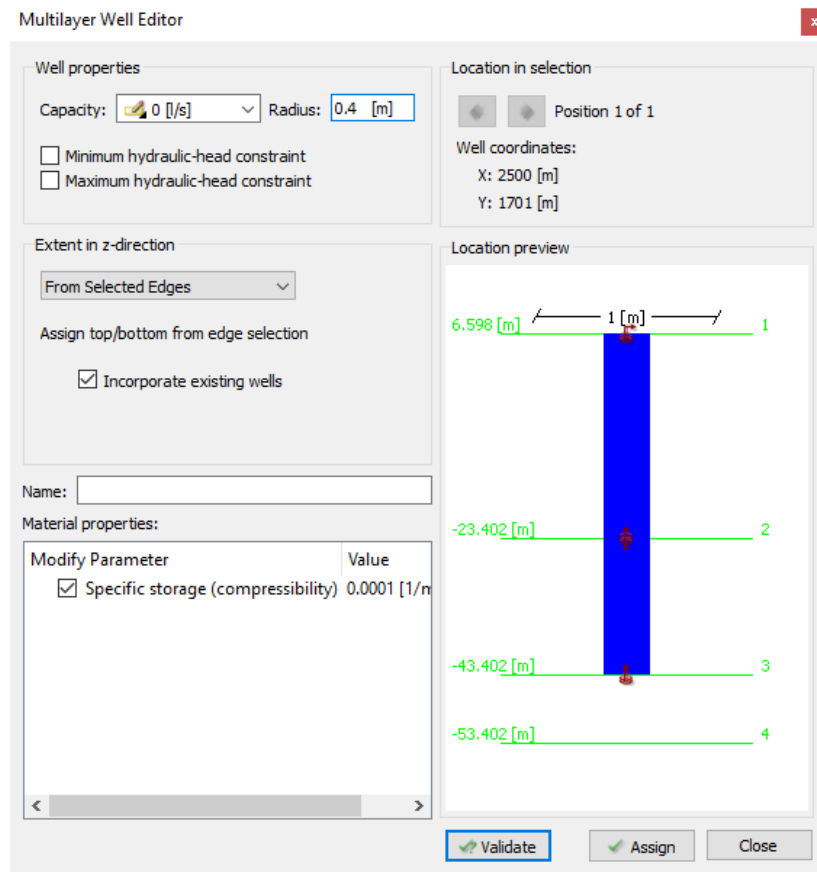





Figure 3.8 Multi-layer well editor

The radius of the wells was set equal to 0.4 m. Regarding the wells capacity or pumping rate, it was imposed that during the irrigation season, spanning 120 days, the capacity must be maintained at 25 l/s for each well, whereas during the non-irrigation season, the capacity was set to 0 l/s. The last requirement to be addressed concerns the Managed Aquifer Recharge system situated within

the model domain. As outlined in section 3.3, the analysis is divided into two separate configurations: one featuring the MAR system represented by a trench, and the other by a series of eleven wells. These configurations demand distinct characterization, given the differing methods through which water infiltrates the aquifer via these systems. In the initial configuration, the trench has been represented within the model as a Fluid-flux boundary. A flux boundary condition implies the application of a predetermined flux, specifically the Darcy flux, to nodes encompassing the faces of elements in a 3D model. Flux boundary conditions are employed in situations where the gradient or inflow/outflow velocity is known. In this specific case, given the known injection rate of the MAR system, set at 250 l/s, it was possible to calculate the Darcy flux applied to each node contained into the trench. In contrast, within the second scenario, the eleven wells representing the MAR system have been assigned a multilayer boundary condition. Each well was characterized with a radius of 0.4 m, a screen depth equivalent to the cumulative thickness of the initial two layers, and a capacity (injection rate) of 23 l/s, thereby ensuring a total injection rate of 250 l/s, similarly to the conditions established in the first configuration. In both cases, groundwater recharge is implemented during the non-irrigation season, lasting a total of 245 days. The Table 3 presents a summary of all the boundary conditions applied to the conceptual model in both configurations prior to the sensitivity analysis to be conducted.

Table 3 Boundary conditions settings

Boundary Condition	Configuration I			Configuration II				
	Mesh Element	Value		Mesh Element	Value			
<u>Hydraulic-head BC</u> 	Southern Boundary (node elements)	20 [m]		Southern Boundary (node elements)	20 [m]			
	Northern Boundary (node elements)	10 [m]		Northern Boundary (node elements)	10 [m]			
<u>Fluid-flux BC</u> 	Trench (node elements)	21.95 [m/d]		/	/			
<u>Multi-layer wells BC</u> 		Capacity [l/s]	Radius [m]	Screen depth [m]		Capacity [l/s]	Radius [m]	Screen depth [m]
	Extraction Well (vertical edge)	25	0.4	50	Extraction Well (vertical edge)	25	0.4	50
Injection Well (vertical edge)					23	0.4	50	

3.5 Material Properties assignment

Material properties describe important characteristics of the porous medium to be simulated at an elemental level. FEFLOW allows assigning material properties to the finite-element mesh using different methods, including those that account for changes over time. Several parameters can be imposed directly as material properties, while others are inferred or derived from the values inserted into the model or from the default values provided by the software. For example, the default value for Drain/Fillable porosity in the software was set equal to 0.2. In this study, this value was maintained, following the default settings. The only parameter that was modified was the conductivity. The principal direction of conductivity coincided with the Cartesian coordinates

in both cases. Therefore, the conductivity imposed was along the x direction (K_x), the y direction (K_y), and the z direction (K_z). The values imposed on the model were based on the fact that the first layers had to exhibit the same behaviour in terms of conductivity. These layers were considered permeable since they represented both the saturated and unsaturated zones, while the third layer was assumed to be impermeable. The assigned values are reported in Table 4.

Table 4 Material properties settings

Material Properties		Configuration I			Configuration II		
		Layer 1	Layer 2	Layer 3	Layer 1	Layer 2	Layer 3
<u>Compressibility</u> [1/m] [default]		10^{-4}	10^{-4}	10^{-4}	10^{-4}	10^{-4}	10^{-4}
<u>Drain/Fillable porosity</u> [default]		0.2	0.2	0.2	0.2	0.2	0.2
<u>Conductivity</u> [m/s]	K_x	5×10^{-4}	5×10^{-4}	1×10^{-9}	5×10^{-4}	5×10^{-4}	1×10^{-9}
	K_y	5×10^{-4}	5×10^{-4}	1×10^{-9}	5×10^{-4}	5×10^{-4}	1×10^{-9}
	K_z	5×10^{-4}	5×10^{-4}	1×10^{-9}	5×10^{-4}	5×10^{-4}	1×10^{-9}
<u>Transmissivity</u> [m ² /s]		0.01	0.01	2×10^{-8}	0.01	0.01	2×10^{-8}

Once the conductivity values have been inserted into the model, the software is capable of computing the transmissivity T as:

$$T = K \cdot d$$

Eq. 2

Where K represents the hydraulic conductivity and d the saturated water thickness, which was set to be equal to 20 m when the boundary conditions of the model domain were imposed. Transmissivity is a measure of how much water can be transmitted horizontally.

3.6 Problem settings assignment

The problem settings assignment represents the most crucial aspect in achieving the desired conceptualization of the model. The initial requirement posed by the problem settings editor is whether the model will simulate flow via:

- The saturated groundwater flow equation; or
- Unsaturated or variably saturated media.

In this study, the saturated flow option was selected to simplify the model calculations. This choice implies that groundwater flow will be described by Darcy's law. Another crucial decision involves

selecting whether the simulation should be conducted under steady-state or transient conditions. Steady-state conditions are appropriate for systems with fixed boundary conditions and material properties, providing a representation of the system in equilibrium. In contrast, transient conditions are suitable for simulations covering a specific time period with varying characteristics. Given the objective of this study—to observe the aquifer response to seasonal recharge and extraction—transient conditions were selected for the simulation. Consequently, FEFLOW allows the selection of whether the aquifer to be modelled is fully confined or unconfined, the unconfined option has been selected. Additionally, there is the possibility to define the slices that constitute the model. Four options are available to assign to each slice: *Free*, *Phreatic*, *Confined*, and *Dependent*. In the model under analysis, the Phreatic option was chosen for the first slice, while the Dependent option was selected for the other two slices.

In *Phreatic* mode, the model stratigraphy is fixed, meaning elements can become dry or partially saturated. Unlike the unsaturated mode, the calculation of the unsaturated zone is much simpler, and typically only one phreatic surface is possible. For each partially saturated element, the partial saturation is determined by dividing the saturated thickness of the element by its total thickness. The conductivity values in all directions are then reduced proportionally to the partial saturation of the element. The *Dependent* option, on the other hand, means that the selected slice will be dependent on the nearest non-dependent slice above it. Another option that has been modified is the *Residual Water Depth*, which has been set to 0.005 meters.

In the Problem Settings menu, it is possible to define the simulation time. The menu requires to specify an initial simulation time, the type of time-step control (constant, varying, or automatic), the initial time-step length, and the final simulation time. All these settings are summarized in the Table 5, which have been used in both configurations.

Table 5 Problem Settings

Aquifer	Unconfined
Type	Saturated
Projection	3D phreatic aquifer (fixed mesh)
Residual water depth for unconfined aquifer [m]	0.005
Time Class	Transient flow
Time Stepping	Adams-Bashforth/Trapezoid rule (AB/TR) predictor-corrector (Automatic)
Initial simulation time [d]	0
Initial time-step length [d]	0.001
Final simulation time [d]	365

3.7 Sensitivity analysis-investigated parameters

As mentioned in the section 3.1, sensitivity analysis is an optimal tool in evaluating which parameters have the strongest influence on the groundwater flow domain. To understand which parameters mostly affect the aquifer response to groundwater recharge, various scenarios have been investigated. The sensitivity analysis was conducted on the following factors:

- The type of groundwater injection, comparing trench versus wells.
- The distance of the activated extraction well from the trench or wells.
- Changing the hydraulic conductivity value compared to the initial condition.
- Changing the hydraulic gradient value compared to the initial condition.
- Changing the injected flow rate through MAR system

Each iteration was repeated to identify which combinations of selected factors provided the optimal increase in pumping rate compared to conditions without recharge. This process involved systematically varying the factors to evaluate their impact on the efficiency of the MAR system. The goal was to determine the most effective configurations for maximizing groundwater replenishment and enhancing pumping capacity. The results of these iterations provide critical insights into the design and operational parameters that can improve MAR performance.

From now on, all investigated scenarios will be reported, with results presented through graphs that describe the evolution of the hydraulic head in time at the monitored wells for each possible combination. These visual representations will illustrate how different factors influence the

hydraulic response of the aquifer under various configurations. The analysis has been divided based on the type of MAR system investigated. The first configuration to be examined involves using a trench as the MAR system. This section will explore all possible combinations of factors, including variations in the distance from the trench/wells of the activated well, hydraulic conductivity, and hydraulic gradient.

4 Results and discussion

In the following paragraph, the results obtained through the sensitivity analysis are presented. The presentation is divided into two parts based on the MAR system configuration considered. Configuration I refers to the model where the MAR system is represented by a trench, while configuration II refers to the model where the MAR system is represented by a series of eleven wells.

The results are detailed for each of the six extracting wells located downstream of the MAR system at different distances, under both conditions of activated recharge and no recharge. This comparison helps to determine the effect of the injected water on the drawdown at the considered wells. Finally, the parameters investigated for each well are the hydraulic conductivity and the hydraulic gradient.

4.1 Configuration I

In the following sections, the results obtained for all extraction wells located at various distances from the recharging trench are presented. The behaviour of the hydraulic head curve is consistent across each iteration. The primary variation observed is a general reduction in the hydraulic head as the distance between the well and the trench increases. This trend is attributed to the positioning of the wells closer to the northern boundary of the system, downstream from the trench, along the direction of the hydraulic gradient. The graphs reported in the following figures describe this behaviour, reporting the evolution of the hydraulic head over a simulation period of 365 days. The red curves represent this evolution for a hydraulic conductivity value of $K_x = K_y = 5 \times 10^{-4} m/s$, which is the value that was initially set in material properties (section 3.5) as reference parameter, whereas the black curves correspond to a hydraulic conductivity value of $K_x = K_y = 1 \times 10^{-3} m/s$. The dotted lines indicate the "no recharge" condition, meaning the MAR system was inactive during the simulation. In contrast, the continuous lines represent the scenario with the trench activated, injecting water at the established rate. It is evident that the primary difference between the red and black curves lies in the aquifer response to water extraction or injection. The variations in the black curves are less steep compared to the red ones, indicating a faster response of the aquifer to perturbations due to the higher hydraulic conductivity. The quicker response of the aquifer also results in a less pronounced decrease or increase in hydraulic head at the well, thus defining a narrower range of variation compared to the case with lower hydraulic conductivity. By knowing the hydraulic head value on day 210, which is the day at which the trench is switched off, it was possible to calculate the difference between the drawdown values

of the curves with and without trench activation, thereby determining the gain in terms of reduced drawdown. The tables reported at the end of each section, representing the various iteration performed, show the difference in hydraulic head (Δh) at the selected Extraction-Well on day 210 between the active trench condition and the non-active trench condition.

4.1.1 Trench-Well 1

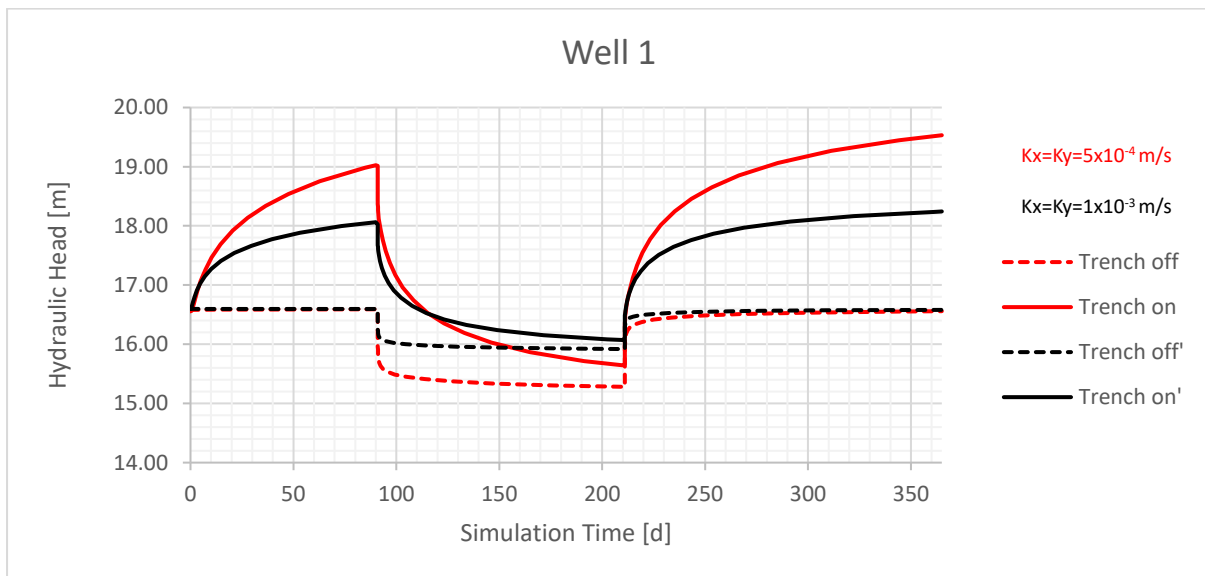


Figure 4.1 Evolution of the Hydraulic head in time at the Well 1 (distance from the trench $d=200 \text{ m}$). The red curve represents the hydraulic head for a hydraulic conductivity value of $K_x = K_y = 5 \times 10^{-4} \text{ m/s}$, while the black curve corresponds to a hydraulic conductivity value of $K_x = K_y = 1 \times 10^{-3} \text{ m/s}$. The hydraulic gradient for this iteration is $i = 0.002$.

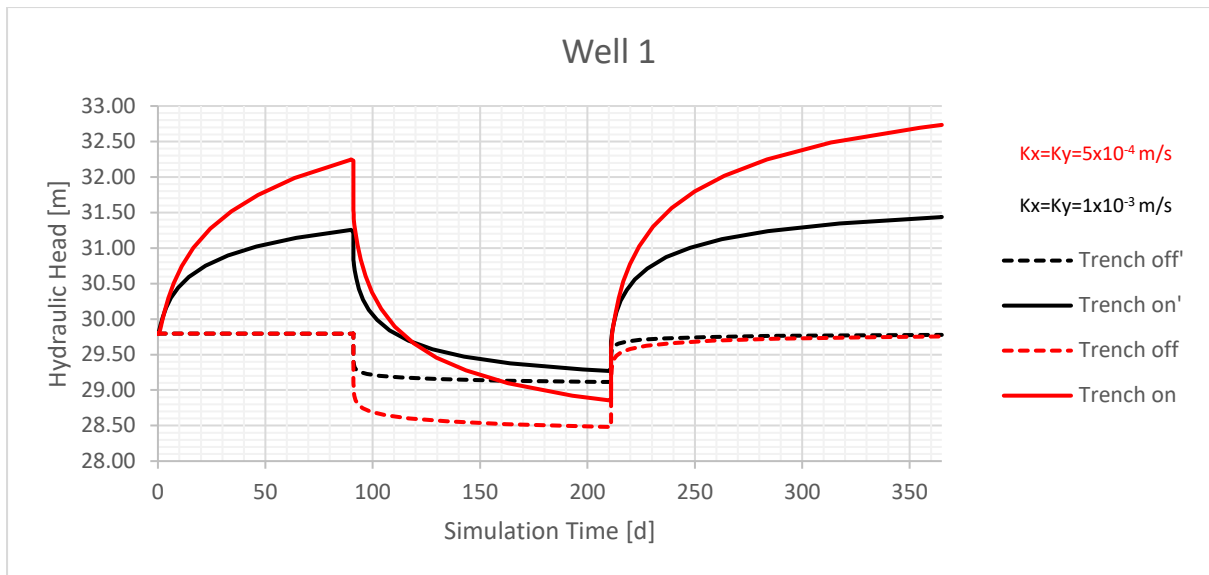


Figure 4.2 Evolution of the Hydraulic head in time at the Well 1 (distance from the trench $d=200$ m). The red curve represents the hydraulic head for a hydraulic conductivity value of $K_x = K_y = 5 \times 10^{-4} \text{ m/s}$, while the black curve corresponds to a hydraulic conductivity value of $K_x = K_y = 1 \times 10^{-3} \text{ m/s}$. The hydraulic gradient for this iteration is $i = 0.006$.

Table 6 Difference in hydraulic head (Δh) at Well 1 on day 210 between the condition with active trench and inactive trench.

Hydraulic conductivity [m/s]	Hydraulic gradient $i=0.002$			Hydraulic gradient $i=0.006$		
	Drawdown day 210 [m]		Δh [m]	Drawdown day 210 [m]		Δh [m]
	Trench off	Trench on		Trench off	Trench on	
$K_x=K_y=5 \times 10^{-4}$	1.32	0.96	0.36	1.32	0.94	0.38
$K_x=K_y=1 \times 10^{-3}$	0.68	0.53	0.15	0.69	0.53	0.16

4.1.2 Trench-Well 2

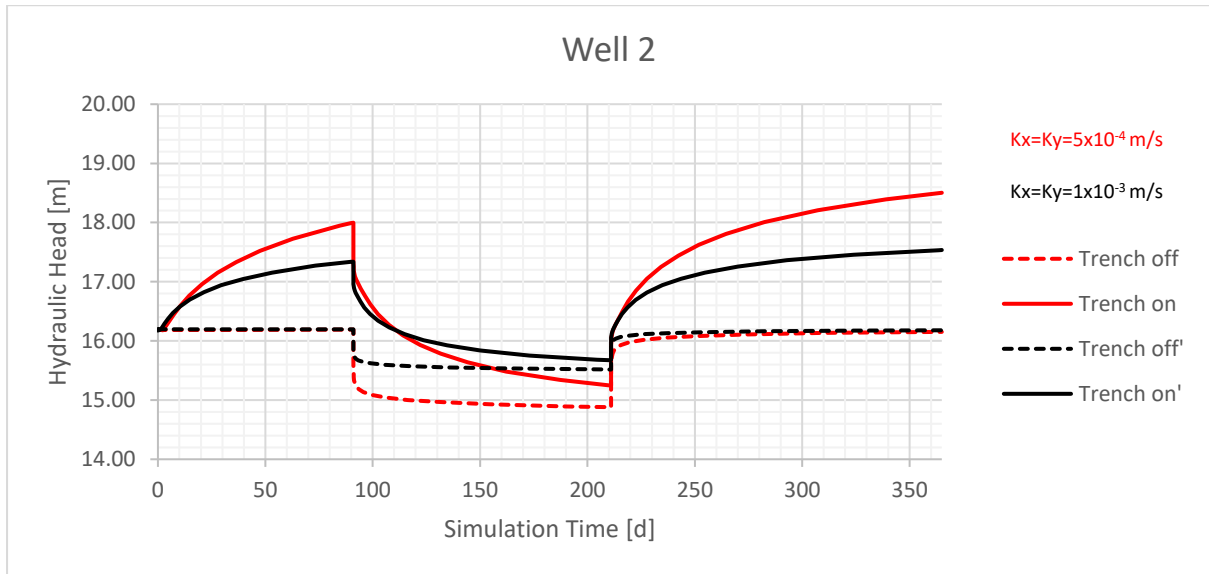


Figure 4.3 Evolution of the Hydraulic head in time at the Well 2 (distance from the trench $d=400$ m). The red curve represents the hydraulic head for a hydraulic conductivity value of $K_x = K_y = 5 \times 10^{-4}$ m/s, while the black curve corresponds to a hydraulic conductivity value of $K_x = K_y = 1 \times 10^{-3}$ m/s. The hydraulic gradient for this iteration is $i = 0.002$.

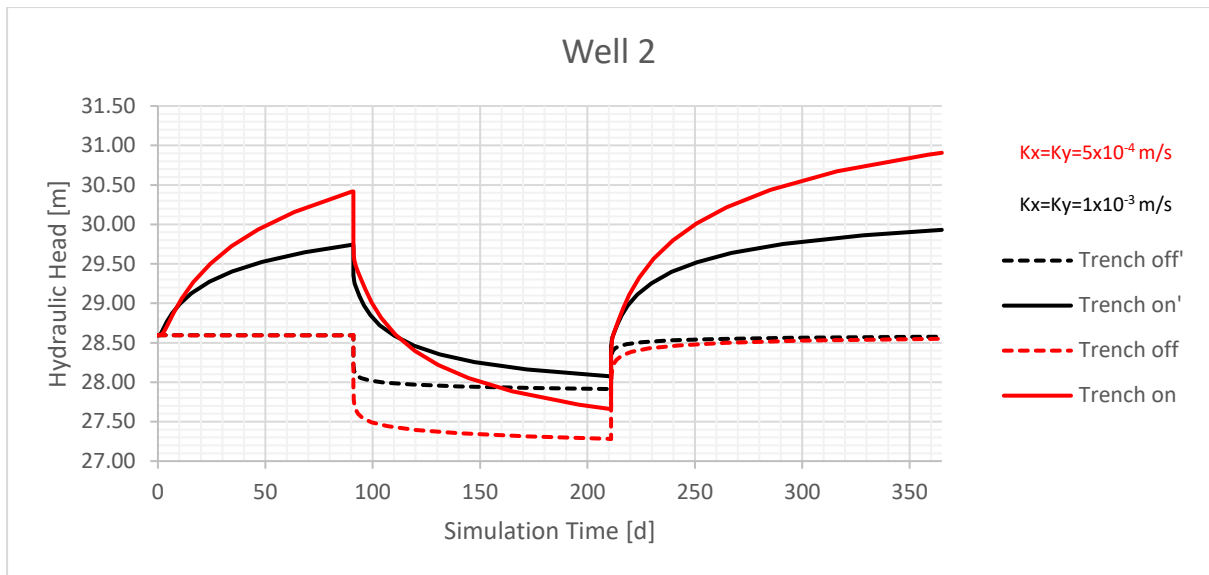


Figure 4.4 Evolution of the Hydraulic head in time at the Well 2 (distance from the trench $d=400$ m). The red curve represents the hydraulic head for a hydraulic conductivity value of $K_x = K_y = 5 \times 10^{-4}$ m/s, while the black curve corresponds to a hydraulic conductivity value of $K_x = K_y = 1 \times 10^{-3}$ m/s. The hydraulic gradient for this iteration is $i = 0.006$.

Table 7 Difference in hydraulic head (Δh) at Well 2 on day 210 between the condition with active trench and inactive trench.

Hydraulic conductivity [m/s]	Hydraulic gradient $i=0.002$			Hydraulic gradient $i=0.006$		
	Drawdown day 210 [m]		Δh [m]	Drawdown day 210 [m]		Δh [m]
	Trench off	Trench on		Trench off	Trench on	
$K_x=K_y=5 \times 10^{-4}$	1.30	0.93	0.37	1.31	0.93	0.38
$K_x=K_y=1 \times 10^{-3}$	0.66	0.50	0.16	0.68	0.51	0.17

4.1.3 Trench-Well 3

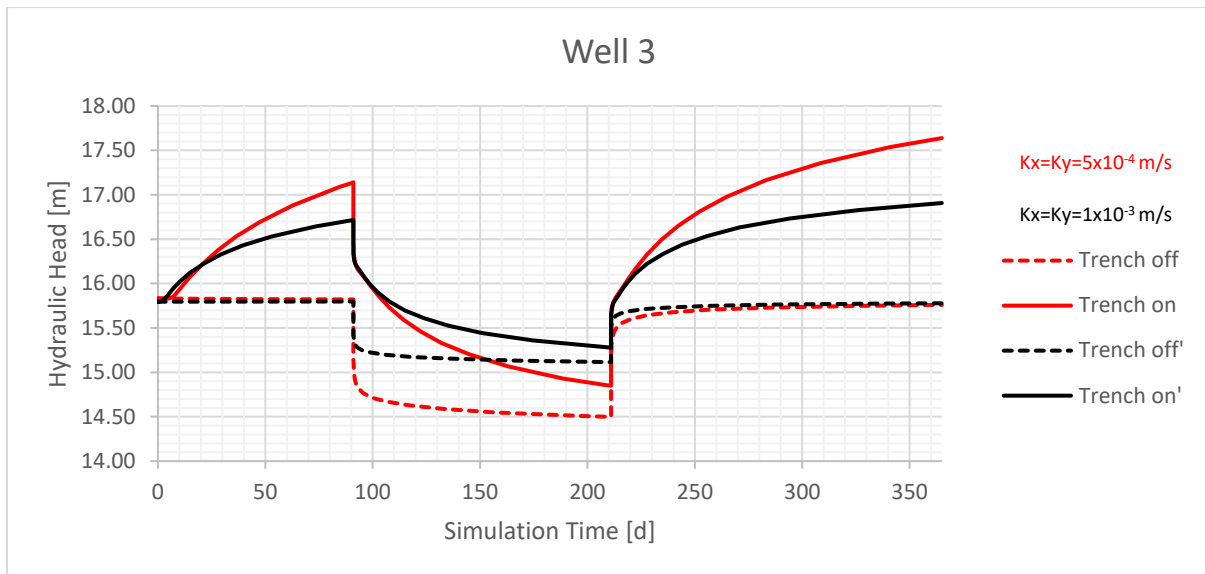


Figure 4.5 Evolution of the Hydraulic head in time at the Well 3 (distance from the trench $d=600$ m). The red curve represents the hydraulic head for a hydraulic conductivity value of $K_x = K_y = 5 \times 10^{-4}$ m/s, while the black curve corresponds to a hydraulic conductivity value of $K_x = K_y = 1 \times 10^{-3}$ m/s. The hydraulic gradient for this iteration is $i = 0.002$.

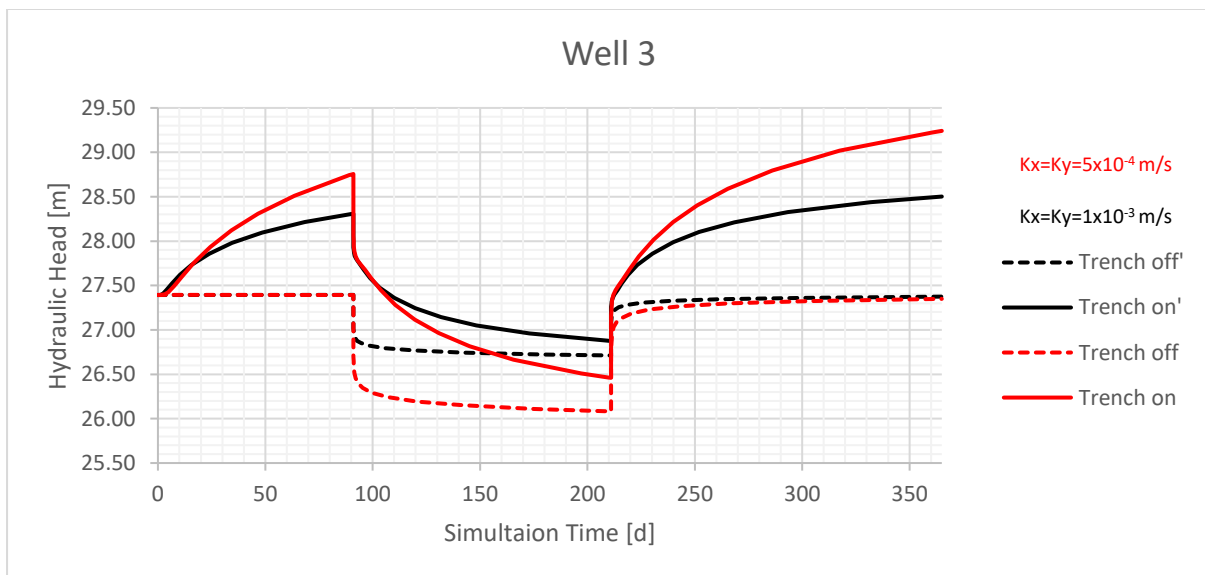


Figure 4.6 Evolution of the Hydraulic head in time at the Well 3 (distance from the trench $d=600$ m). The red curve represents the hydraulic head for a hydraulic conductivity value of $K_x = K_y = 5 \times 10^{-4}$ m/s, while the black curve corresponds to a hydraulic conductivity value of $K_x = K_y = 1 \times 10^{-3}$ m/s. The hydraulic gradient for this iteration is $i = 0.006$.

Table 8 Difference in hydraulic head (Δh) at Well 3 on day 210 between the condition with active trench and inactive trench.

Hydraulic conductivity [m/s]	Hydraulic gradient $i=0.002$			Hydraulic gradient $i=0.006$		
	Drawdown day 210 [m]		Δh [m]	Drawdown day 210 [m]		Δh [m]
	Trench off	Trench on		Trench off	Trench on	
$K_x=K_y=5 \times 10^{-4}$	1.31	0.95	0.36	1.31	0.93	0.38
$K_x=K_y=1 \times 10^{-3}$	0.69	0.52	0.17	0.68	0.51	0.17

4.1.4 Trench-Well 4

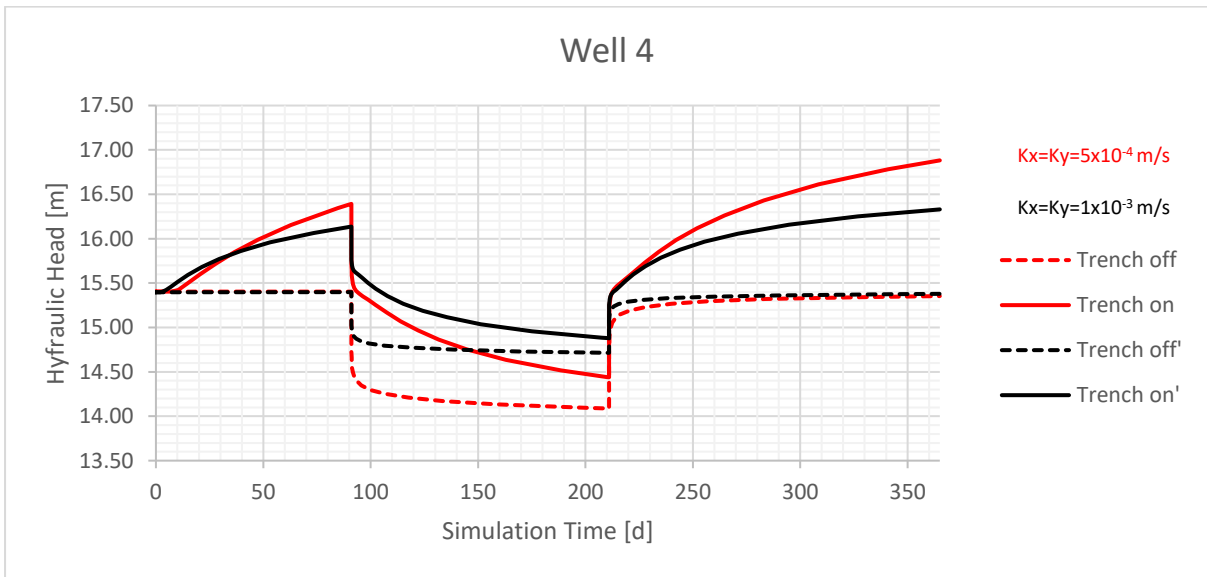


Figure 4.7 Evolution of the Hydraulic head in time at the Well 4 (distance from the trench $d=800$ m). The red curve represents the hydraulic head for a hydraulic conductivity value of $K_x = K_y = 5 \times 10^{-4}$ m/s, while the black curve corresponds to a hydraulic conductivity value of $K_x = K_y = 1 \times 10^{-3}$ m/s. The hydraulic gradient for this iteration is $i = 0.002$.

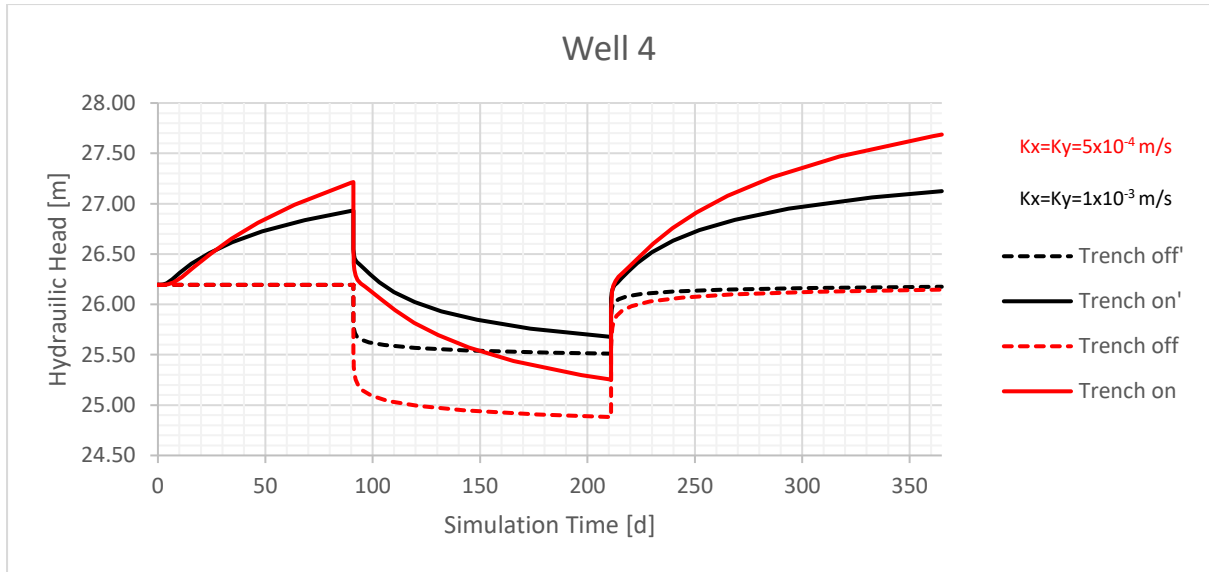


Figure 4.8 Evolution of the Hydraulic head in time at the Well 4 (distance from the trench $d=800\text{ m}$). The red curve represents the hydraulic head for a hydraulic conductivity value of $K_x = K_y = 5 \times 10^{-4}\text{ m/s}$, while the black curve corresponds to a hydraulic conductivity value of $K_x = K_y = 1 \times 10^{-3}\text{ m/s}$. The hydraulic gradient for this iteration is $i = 0.006$.

Table 9 Difference in hydraulic head (Δh) at Well 4 on day 210 between the condition with active trench and inactive trench.

Hydraulic conductivity [m/s]	Hydraulic gradient $i=0.002$			Hydraulic gradient $i=0.006$		
	Drawdown day 210 [m]		Δh [m]	Drawdown day 210 [m]		Δh [m]
	Trench off	Trench on		Trench off	Trench on	
$K_x=K_y=5 \times 10^{-4}$	1.31	0.96	0.35	1.31	0.94	0.37
$K_x=K_y=1 \times 10^{-3}$	0.69	0.52	0.17	0.51	0.68	0.17

4.1.5 Trench-Well 5

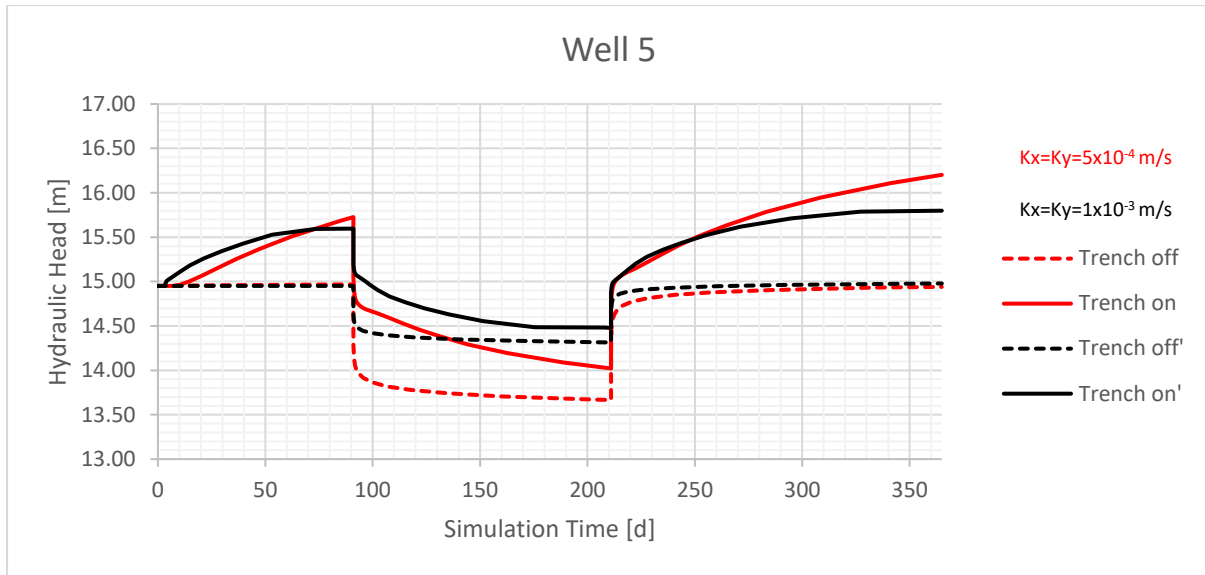


Figure 4.9 Evolution of the Hydraulic head in time at the Well 5 (distance from the trench $d=1000\text{ m}$). The red curve represents the hydraulic head for a hydraulic conductivity value of $K_x = K_y = 5 \times 10^{-4}\text{ m/s}$, while the black curve corresponds to a hydraulic conductivity value of $K_x = K_y = 1 \times 10^{-3}\text{ m/s}$. The hydraulic gradient for this iteration is $i = 0.002$.

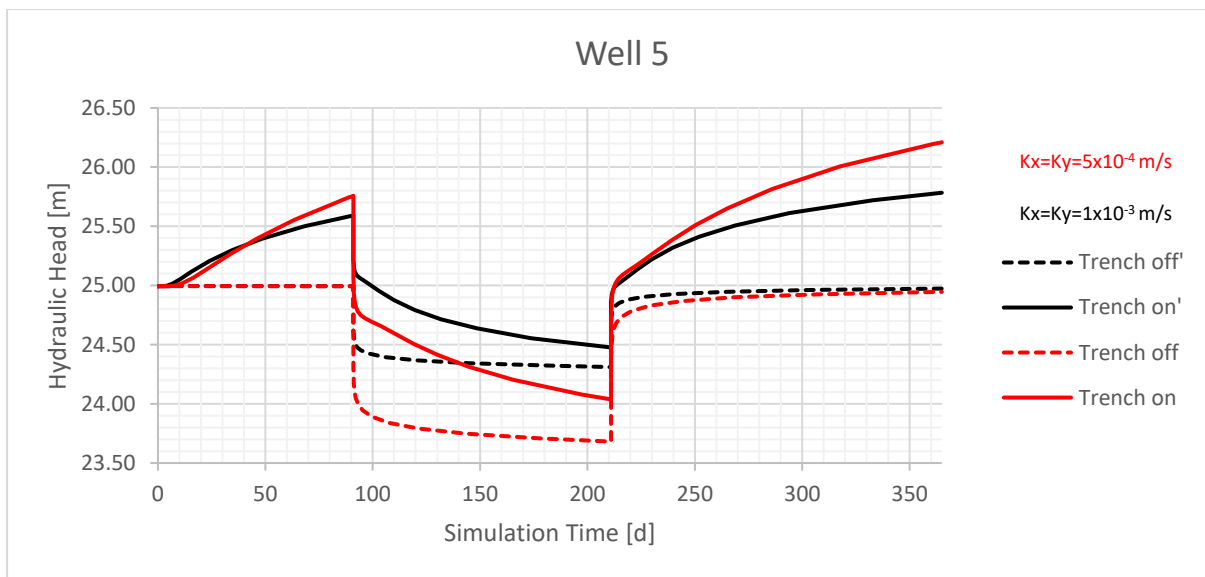


Figure 4.10 Evolution of the Hydraulic head in time at the Well 5 (distance from the trench $d=1000\text{ m}$). The red curve represents the hydraulic head for a hydraulic conductivity value of $K_x = K_y = 5 \times 10^{-4}\text{ m/s}$, while the black curve corresponds to a hydraulic conductivity value of $K_x = K_y = 1 \times 10^{-3}\text{ m/s}$. The hydraulic gradient for this iteration is $i = 0.006$.

Table 10 Difference in hydraulic head (Δh) at Well 5 on day 210 between the condition with active trench and inactive trench.

Hydraulic conductivity [m/s]	Hydraulic gradient $i=0.002$			Hydraulic gradient $i=0.006$		
	Drawdown day 210 [m]		Δh [m]	Drawdown day 210 [m]		Δh [m]
	Trench off	Trench on		Trench off	Trench on	
$K_x=K_y=5 \times 10^{-4}$	1.28	0.93	0.35	1.31	0.95	0.36
$K_x=K_y=1 \times 10^{-3}$	0.64	0.47	0.17	0.68	0.51	0.17

4.1.6 Trench-Well 6

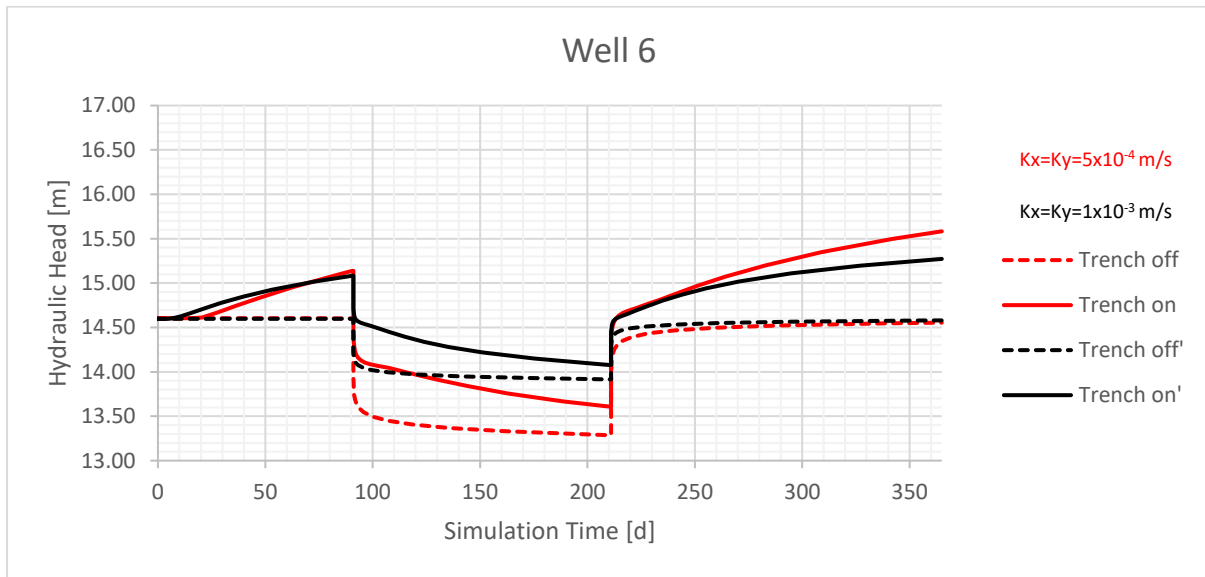


Figure 4.11 Evolution of the Hydraulic head in time at the Well 6 (distance from the trench $d=1200$ m). The red curve represents the hydraulic head for a hydraulic conductivity value of $K_x = K_y = 5 \times 10^{-4}$ m/s, while the black curve corresponds to a hydraulic conductivity value of $K_x = K_y = 1 \times 10^{-3}$ m/s. The hydraulic gradient for this iteration is $i = 0.002$.

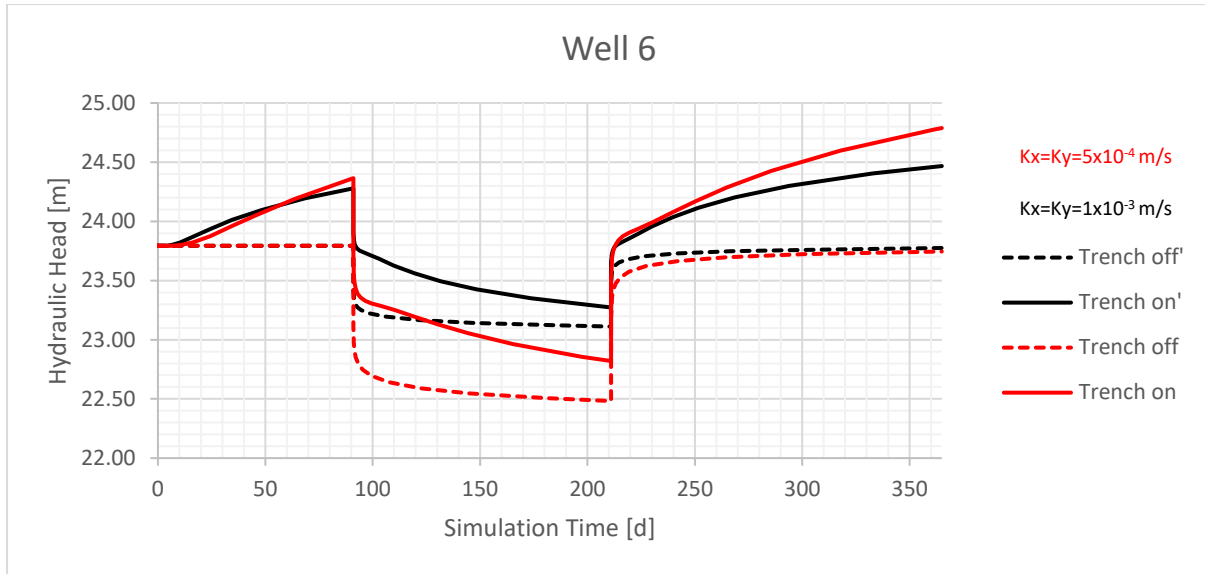


Figure 4.12 Evolution of the Hydraulic head in time at the Well 6 (distance from the trench $d=1200$ m). The red curve represents the hydraulic head for a hydraulic conductivity value of $K_x = K_y = 5 \times 10^{-4}$ m/s, while the black curve corresponds to a hydraulic conductivity value of $K_x = K_y = 1 \times 10^{-3}$ m/s. The hydraulic gradient for this iteration is $i = 0.006$.

Table 11 Difference in hydraulic head (Δh) at Well 6 on day 210 between the condition with active trench and inactive trench.

Hydraulic conductivity [m/s]	Hydraulic gradient $i=0.002$			Hydraulic gradient $i=0.006$		
	Drawdown day 210 [m]		Δh [m]	Drawdown day 210 [m]		Δh [m]
	Trench off	Trench on		Trench off	Trench on	
$K_x=K_y=5 \times 10^{-4}$	1.31	0.99	0.32	1.31	0.97	0.34
$K_x=K_y=1 \times 10^{-3}$	0.69	0.52	0.17	0.68	0.52	0.16

4.2 Configuration II

In the following sections, the results of the iterations conducted with configuration II are presented. In this configuration, the MAR system is characterized from series of 11 wells injecting at a rate of 250 l/s for a period of 245 days, similar to the previous configuration. As before, the values of the hydraulic head difference in the wells are reported, comparing the levels measured with the MAR system activated to those measured with the system deactivated for all possible combinations. From the graphs and results obtained, a behaviour similar to the previously reported configuration can be observed.

4.2.1 Wells-Well 1

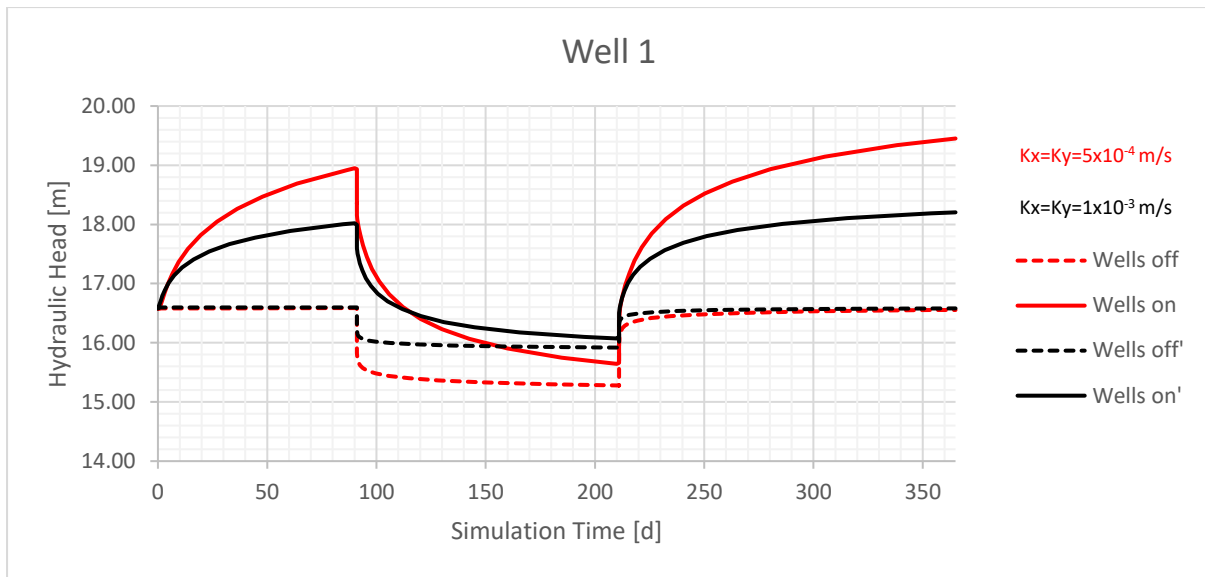


Figure 4.13 Evolution of the Hydraulic head in time at the Well 1 (distance from the wells $d=200\text{ m}$). The red curve represents the hydraulic head for a hydraulic conductivity value of $K_x = K_y = 5 \times 10^{-4}\text{ m/s}$, while the black curve corresponds to a hydraulic conductivity value of $K_x = K_y = 1 \times 10^{-3}\text{ m/s}$. The hydraulic gradient for this iteration is $i = 0.002$.

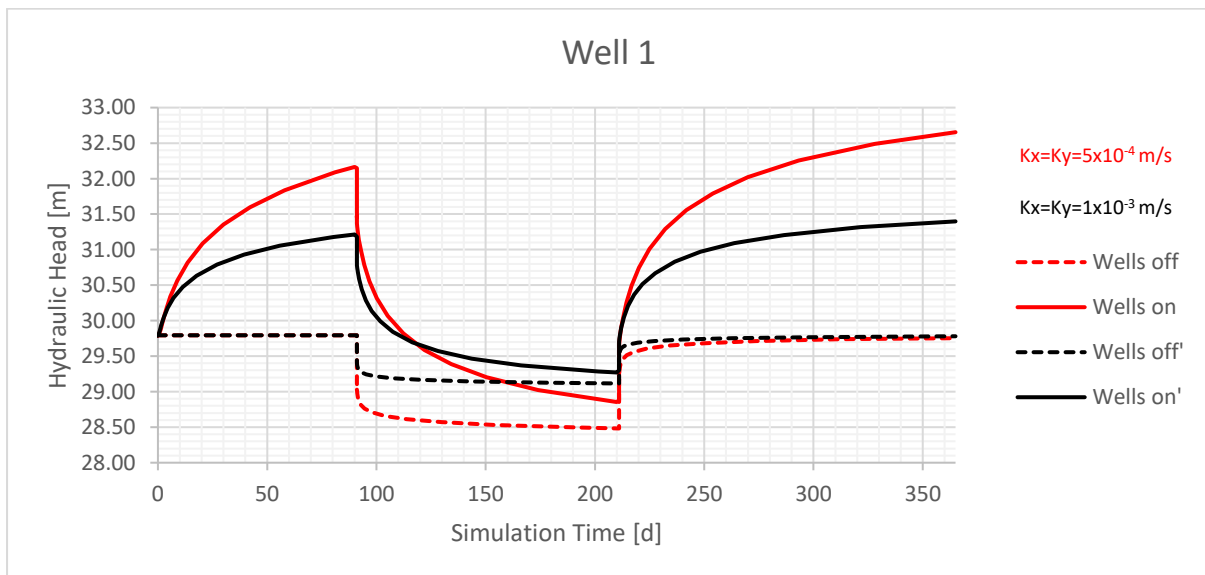


Figure 4.14 Evolution of the Hydraulic head in time at the Well 1 (distance from the wells $d=200\text{ m}$). The red curve represents the hydraulic head for a hydraulic conductivity value of $K_x = K_y = 5 \times 10^{-4}\text{ m/s}$, while the black curve corresponds to a hydraulic conductivity value of $K_x = K_y = 1 \times 10^{-3}\text{ m/s}$. The hydraulic gradient for this iteration is $i = 0.006$.

Table 12 Difference in hydraulic head (Δh) at Well 1 on day 210 between the condition with active wells and inactive wells.

Hydraulic conductivity [m/s]	Hydraulic gradient $i=0.002$			Hydraulic gradient $i=0.006$		
	Drawdown day 210 [m]		Δh [m]	Drawdown day 210 [m]		Δh [m]
	Wells off	Wells on		Wells off	Wells on	
$K_x=K_y=5 \times 10^{-4}$	1.30	0.94	0.36	1.32	0.94	0.38
$K_x=K_y=1 \times 10^{-3}$	0.66	0.51	0.15	0.68	0.53	0.15

4.2.2 Wells-Well 2

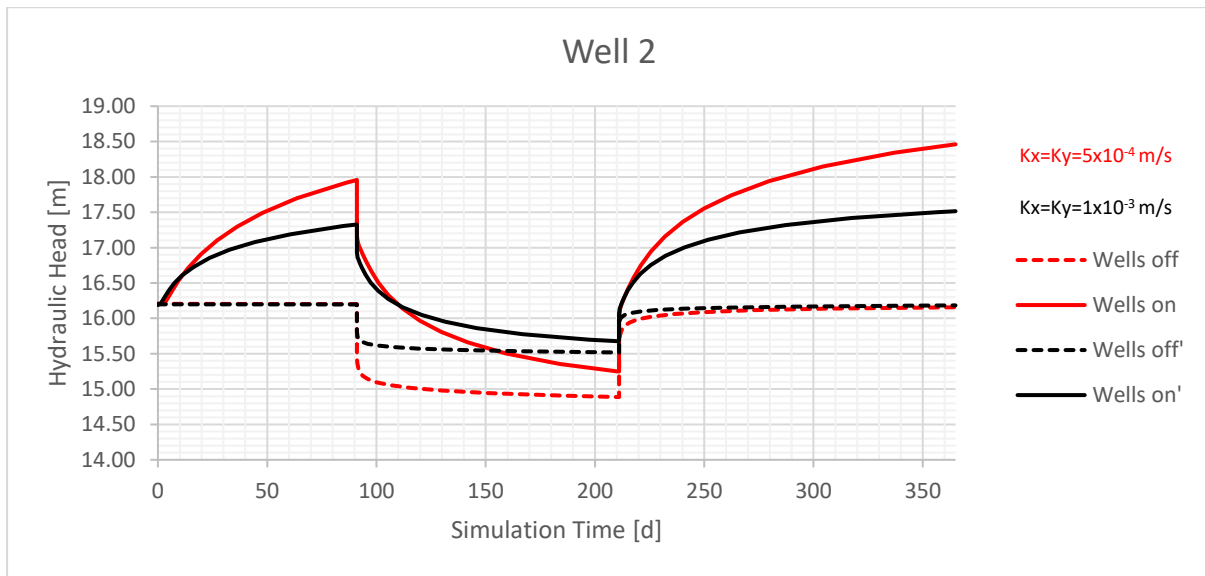


Figure 4.15 Evolution of the Hydraulic head in time at the Well 2 (distance from the wells $d=400$ m). The red curve represents the hydraulic head for a hydraulic conductivity value of $K_x = K_y = 5 \times 10^{-4}$ m/s, while the black curve corresponds to a hydraulic conductivity value of $K_x = K_y = 1 \times 10^{-3}$ m/s. The hydraulic gradient for this iteration is $i = 0.002$.

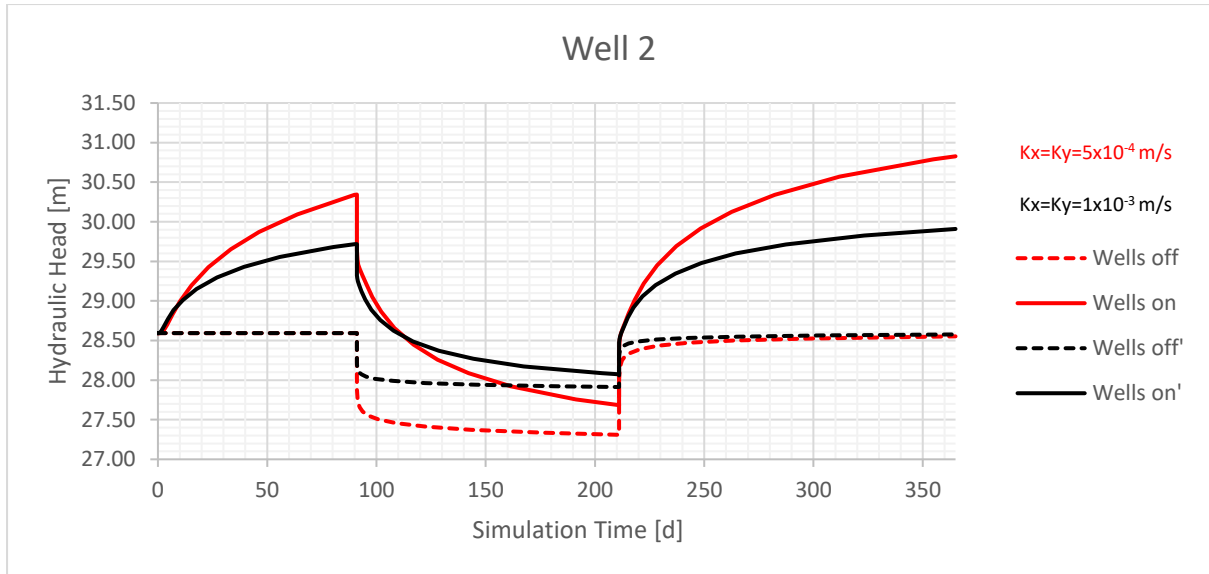


Figure 4.16 Evolution of the Hydraulic head in time at the Well 2 (distance from the wells $d=400$ m). The red curve represents the hydraulic head for a hydraulic conductivity value of $K_x = K_y = 5 \times 10^{-4} \text{ m/s}$, while the black curve corresponds to a hydraulic conductivity value of $K_x = K_y = 1 \times 10^{-3} \text{ m/s}$. The hydraulic gradient for this iteration is $i = 0.006$.

Table 13 Difference in hydraulic head (Δh) at Well 2 on day 210 between the condition with active wells and inactive wells.

Hydraulic conductivity [m/s]	Hydraulic gradient $i=0.002$			Hydraulic gradient $i=0.006$		
	Drawdown day 210 [m]		Δh [m]	Drawdown day 210 [m]		Δh [m]
	Wells off	Wells on		Wells off	Wells on	
$K_x=K_y=5 \times 10^{-4}$	1.31	0.95	0.36	1.28	0.91	0.37
$K_x=K_y=1 \times 10^{-3}$	0.68	0.52	0.16	0.68	0.51	0.17

4.2.3 Wells-Well 3

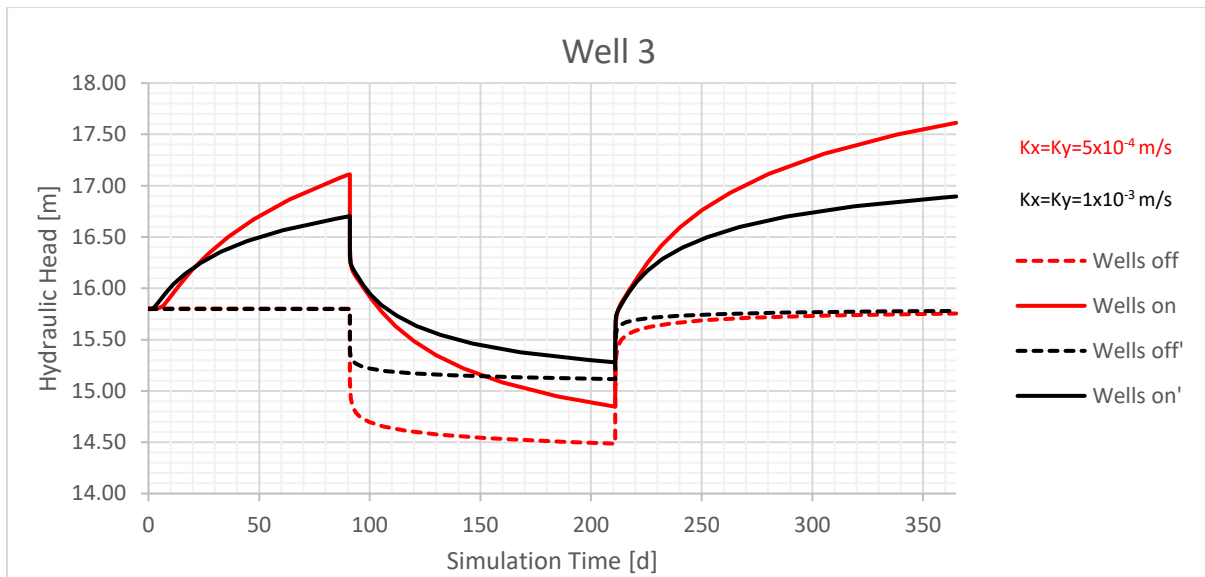


Figure 4.17 Evolution of the Hydraulic head in time at the Well 3 (distance from the wells $d=600$ m). The red curve represents the hydraulic head for a hydraulic conductivity value of $K_x = K_y = 5 \times 10^{-4}$ m/s, while the black curve corresponds to a hydraulic conductivity value of $K_x = K_y = 1 \times 10^{-3}$ m/s. The hydraulic gradient for this iteration is $i = 0.002$.

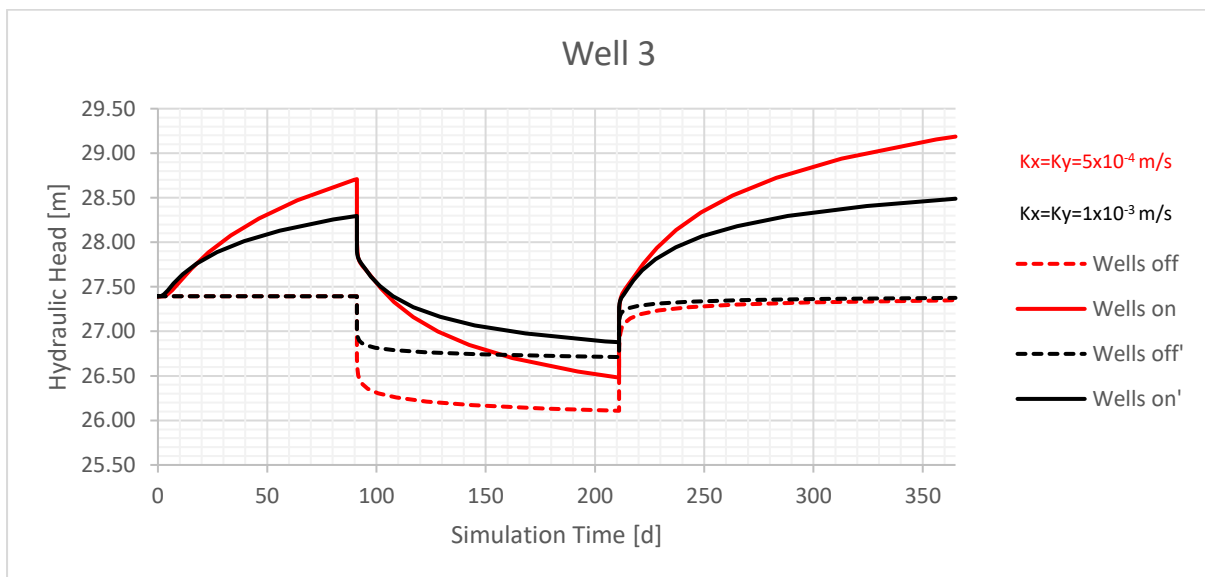


Figure 4.18 Evolution of the Hydraulic head in time at the Well 3 (distance from the wells $d=600$ m). The red curve represents the hydraulic head for a hydraulic conductivity value of $K_x = K_y = 5 \times 10^{-4}$ m/s, while the black curve corresponds to a hydraulic conductivity value of $K_x = K_y = 1 \times 10^{-3}$ m/s. The hydraulic gradient for this iteration is $i = 0.006$.

Table 14 Difference in hydraulic head (Δh) at Well 3 on day 210 between the condition with active wells and inactive wells.

Hydraulic conductivity [m/s]	Hydraulic gradient $i=0.002$			Hydraulic gradient $i=0.006$		
	Drawdown day 210 [m]		Δh [m]	Drawdown day 210 [m]		Δh [m]
	Wells off	Well on		Wells off	Wells on	
$K_x=K_y=5 \times 10^{-4}$	1.31	0.95	0.36	1.28	0.91	0.37
$K_x=K_y=1 \times 10^{-3}$	0.69	0.52	0.17	0.68	0.51	0.17

4.2.4 Wells-Well 4

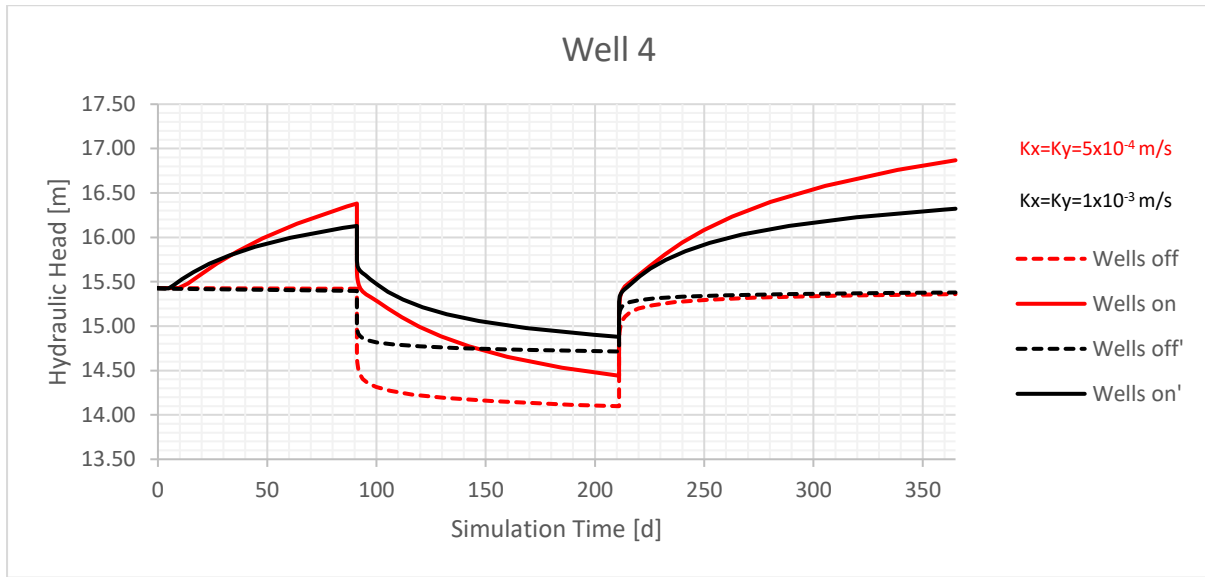


Figure 4.19 Evolution of the Hydraulic head in time at the Well 4 (distance from the wells $d=800$ m). The red curve represents the hydraulic head for a hydraulic conductivity value of $K_x = K_y = 5 \times 10^{-4}$ m/s, while the black curve corresponds to a hydraulic conductivity value of $K_x = K_y = 1 \times 10^{-3}$ m/s. The hydraulic gradient for this iteration is $i = 0.002$.

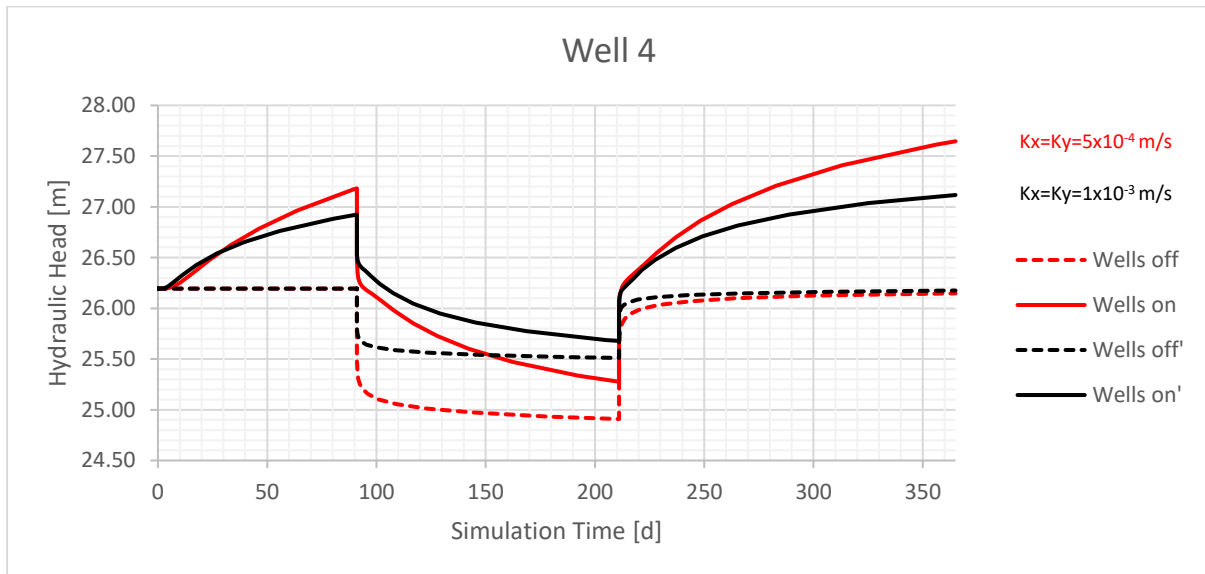


Figure 4.20 Evolution of the Hydraulic head in time at the Well 4 (distance from the wells $d=800$ m). The red curve represents the hydraulic head for a hydraulic conductivity value of $K_x = K_y = 5 \times 10^{-4}$ m/s, while the black curve corresponds to a hydraulic conductivity value of $K_x = K_y = 1 \times 10^{-3}$ m/s. The hydraulic gradient for this iteration is $i = 0.006$.

Table 15 Difference in hydraulic head (Δh) at Well 4 on day 210 between the condition with active wells and inactive wells.

Hydraulic conductivity [m/s]	Hydraulic gradient $i=0.002$			Hydraulic gradient $i=0.006$		
	Drawdown day 210 [m]		Δh [m]	Drawdown day 210 [m]		Δh [m]
	Wells off	Wells on		Wells off	Wells on	
$K_x=K_y=5 \times 10^{-4}$	1.33	0.99	0.34	1.28	0.91	0.37
$K_x=K_y=1 \times 10^{-3}$	0.72	0.55	0.17	0.68	0.51	0.17

4.2.5 Wells-Well 5

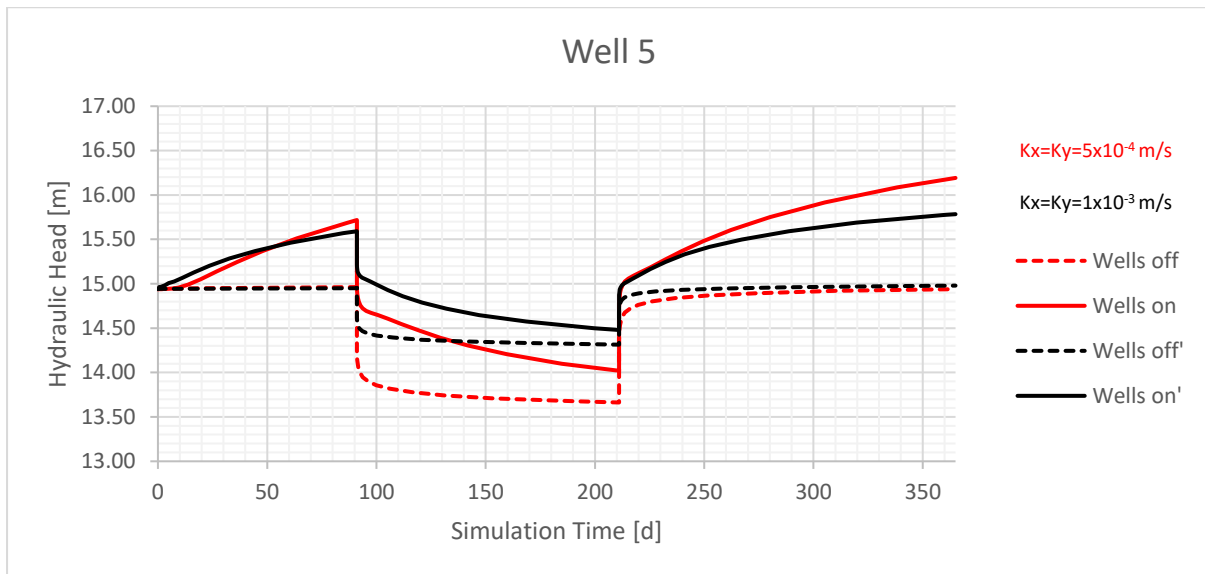


Figure 4.21 Evolution of the Hydraulic head in time at the Well 5 (distance from the wells $d=1000$ m). The red curve represents the hydraulic head for a hydraulic conductivity value of $K_x = K_y = 5 \times 10^{-4} \text{ m/s}$, while the black curve corresponds to a hydraulic conductivity value of $K_x = K_y = 1 \times 10^{-3} \text{ m/s}$. The hydraulic gradient for this iteration is $i = 0.002$.

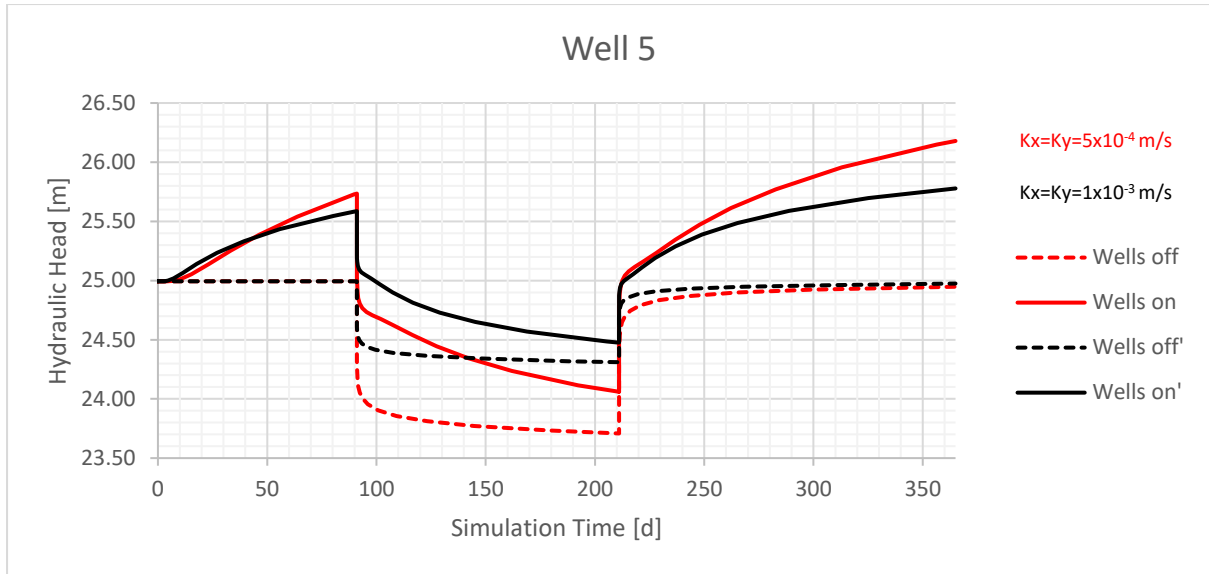


Figure 4.22 Evolution of the Hydraulic head in time at the Well 5 (distance from the wells $d=1000$ m). The red curve represents the hydraulic head for a hydraulic conductivity value of $K_x = K_y = 5 \times 10^{-4}$ m/s, while the black curve corresponds to a hydraulic conductivity value of $K_x = K_y = 1 \times 10^{-3}$ m/s. The hydraulic gradient for this iteration is $i = 0.006$.

Table 16 Difference in hydraulic head (Δh) at Well 5 on day 210 between the condition with active wells and inactive wells.

Hydraulic conductivity [m/s]	Hydraulic gradient $i=0.002$			Hydraulic gradient $i=0.006$		
	Drawdown day 210 [m]		Δh [m]	Drawdown day 210 [m]		Δh [m]
	Wells off	Wells on		Wells off	Wells on	
$K_x=K_y=5 \times 10^{-4}$	1.28	0.92	0.36	1.28	0.93	0.35
$K_x=K_y=1 \times 10^{-3}$	0.63	0.46	0.17	0.68	0.51	0.17

4.2.6 Wells-Well 6

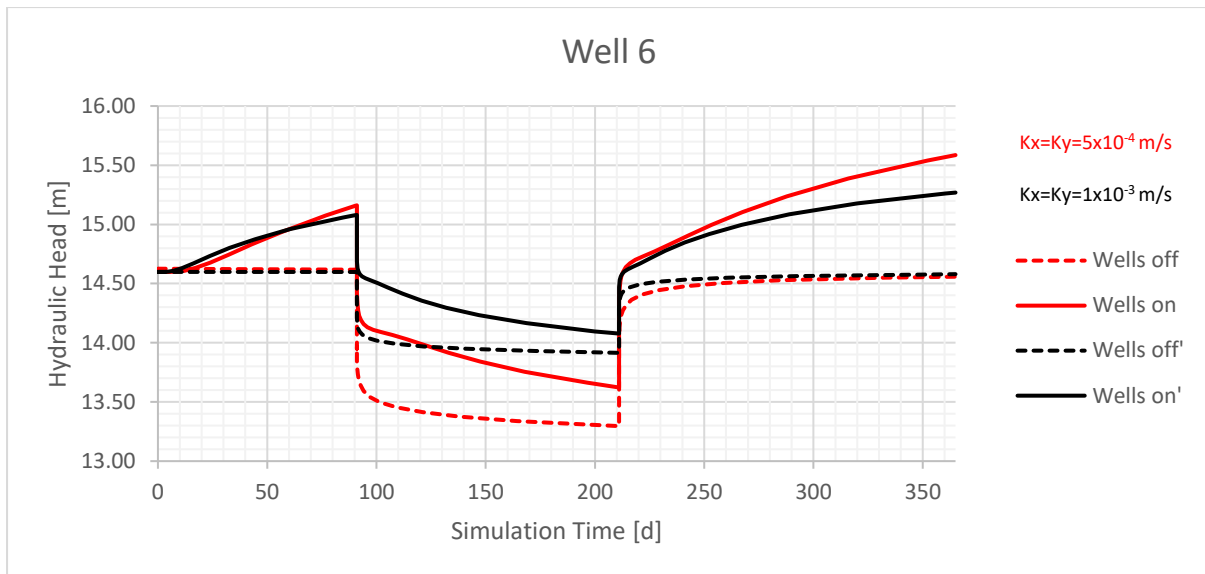


Figure 4.23 Evolution of the Hydraulic head in time at the Well 6 (distance from the wells $d=1200\text{ m}$). The red curve represents the hydraulic head for a hydraulic conductivity value of $K_x = K_y = 5 \times 10^{-4}\text{ m/s}$, while the black curve corresponds to a hydraulic conductivity value of $K_x = K_y = 1 \times 10^{-3}\text{ m/s}$. The hydraulic gradient for this iteration is $i = 0.002$.

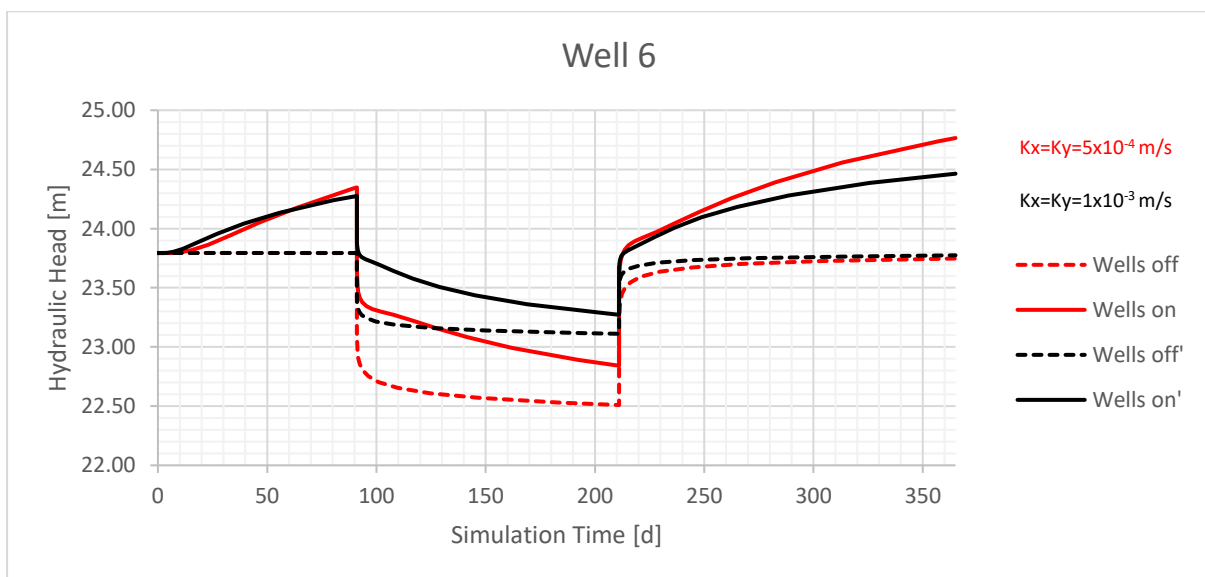


Figure 4.24 Evolution of the Hydraulic head in time at the Well 6 (distance from the wells $d=1200\text{ m}$). The red curve represents the hydraulic head for a hydraulic conductivity value of $K_x = K_y = 5 \times 10^{-4}\text{ m/s}$, while the black curve corresponds to a hydraulic conductivity value of $K_x = K_y = 1 \times 10^{-3}\text{ m/s}$. The hydraulic gradient for this iteration is $i = 0.006$.

Table 17 Difference in hydraulic head (Δh) at Well 6 on day 210 between the condition with active wells and inactive wells.

Hydraulic conductivity [m/s]	Hydraulic gradient $i=0.002$			Hydraulic gradient $i=0.006$		
	Drawdown day 210 [m]		Δh [m]	Drawdown day 210 [m]		Δh [m]
	Wells off	Wells on		Wells off	Wells on	
$K_x=K_y=5 \times 10^{-4}$	1.30	0.98	0.32	1.28	0.95	0.33
$K_x=K_y=1 \times 10^{-3}$	0.69	0.52	0.17	0.68	0.52	0.16

4.3 Discussion

From the graphs and calculations presented in the previous sections, it is evident that the behaviour and response of the aquifer to water injection via the MAR system are not significantly influenced by the configuration used, whether it is wells or a trench. The Table 18 presents the difference in hydraulic head measured under active MAR conditions, with groundwater injection, compared to the hydraulic head under non-injection conditions on day 210, obtained from all iterations performed. Analysing these values, it is evident that Well 3, located 600 meters from the injection point, shows the greatest increase in hydraulic head following groundwater injection. This optimal performance is observed when considering both the variation in hydraulic gradient, hydraulic conductivity, and distance from the MAR system, making well three the most effective among the wells analysed. However, same considerations can be made. From the graphs presented, it is evident that the factor most influencing aquifer recharge is hydraulic conductivity. As for the hydraulic gradient and the distance of the extraction well from the MAR system, at least for the values set for this sensitivity analysis, it is difficult to determine which of the two had a predominant role in aquifer recharge. Indeed, the calculations do not show a significant discrepancy between the Δh calculated with varying hydraulic gradient and varying distance. However, small differences are evident, and these differences have allowed to identify the optimal well in terms of the gain of water available for extraction during the irrigation season.

Table 18 Difference in hydraulic head measured with the MAR system active and inactive on day 210 for all extraction wells, considering various combinations of hydraulic gradient and conductivity for the two configurations.

Configuration I-Trench												
$\Delta h[m]$												
Well 1		Well 2		Well 3		Well 4		Well 5		Well 6		
$i=0.00$ 2	$i=0.00$ 6	$i=0.00$ 2	$i=0.00$ 6	$i=0.00$ 2	$i=0.00$ 6	$i=0.00$ 2	$i=0.00$ 6	$i=0.00$ 2	$i=0.00$ 6	$i=0.00$ 2	$i=0.00$ 6	
$K=5 \times 10^{-4}$ m/s	0.36	0.38	0.37	0.38	0.36	0.38	0.35	0.37	0.35	0.36	0.32	0.34
$K=1 \times 10^{-3}$ m/s	0.15	0.16	0.16	0.17	0.17	0.17	0.17	0.17	0.17	0.17	0.17	0.16
Configuration II -Wells												
$\Delta h[m]$												
Well 1		Well 2		Well 3		Well 4		Well 5		Well 6		
$i=0.00$ 2	$i=0.00$ 6	$i=0.00$ 2	$i=0.00$ 6	$i=0.00$ 2	$i=0.00$ 6	$i=0.00$ 2	$i=0.00$ 6	$i=0.00$ 2	$i=0.00$ 6	$i=0.00$ 2	$i=0.00$ 6	
$K=5 \times 10^{-4}$ m/s	0.36	0.38	0.36	0.37	0.36	0.37	0.34	0.37	0.36	0.35	0.32	0.33
$K=1 \times 10^{-3}$ m/s	0.15	0.15	0.16	0.17	0.17	0.17	0.17	0.17	0.17	0.17	0.17	0.16

4.4 Estimation of the possible increase of abstracted flow rate with MAR

Once the well with the best result was identified, a further analysis was conducted to determine the increase in extracted flow rate during the irrigation season following water injection with the MAR system. This was done to obtain a value of the process efficiency.

To achieve this, the initial attempt involved calculating the new value of extracted flow rate by multiplying the initially set value of 25 l/s by the ratio of the hydraulic head measured at Well 3 following recharge with the MAR system to that measured in the absence of recharge on day 210. This was done for both selected hydraulic conductivity values and for both configurations.

To verify the accuracy of the new selected flow rate, various iterations were conducted using FEFLOW. The evolution of the hydraulic head over time at Well 3 with the MAR system active was observed. Specifically, it was examined whether the hydraulic head value on day 210 matched the hydraulic head value measured on day 210 under "no recharge" conditions. However, after this initial iteration, the hydraulic head measured on day 210 following water injection prior to extraction did not match the levels measured on the same day under "no recharge" conditions. This indicated the potential to further increase the extraction flow rate of the well, thus invalidating the initial parameterization attempt. Consequently, a trial-and-error process was undertaken to determine the new extraction flow rate value. This trial-and-error procedure led to the determination of the flow rate values reported in the Table 19, considering all possible combinations of hydraulic gradient and hydraulic conductivity for Well 3.

Table 19 Flow rate values (Q_{new}) determined after the trial-and-error procedure for all possible combinations of hydraulic conductivity and hydraulic gradient at well 3.

MAR system considered	Q _{new}			
	i=0.002		i=0.006	
	$K_x=K_y=5 \times 10^{-4}$ m/s	$K_x=K_y=1 \times 10^{-3}$ m/s	$K_x=K_y=5 \times 10^{-4}$ m/s	$K_x=K_y=1 \times 10^{-3}$ m/s
<u>Trench</u>	32	31	32	31
<u>Wells</u>	32	31	32	31

As can be seen from the reported data, the flow rate gain in the case of $K_x = K_y = 5 \times 10^{-4}$ m/s is 7 l/s, while in the case of $K_x = K_y = 1 \times 10^{-3}$ m/s, the gain is 6 l/s. These results clearly indicate that the influence of hydraulic conductivity is predominant over the hydraulic gradient in determining the aquifer response to recharge. The following graphs depict the evolution of the hydraulic head at Well 3 under conditions of no recharge and active recharge with both

configurations. Notably, the increase in extraction flow rate causes the hydraulic head value on day 210 under active recharge conditions to decrease to the hydraulic head value on day 210 under no recharge conditions. This confirms the extraction flow rate value that can be achieved following aquifer recharge via the MAR system, as determined through the trial-and-error procedure.

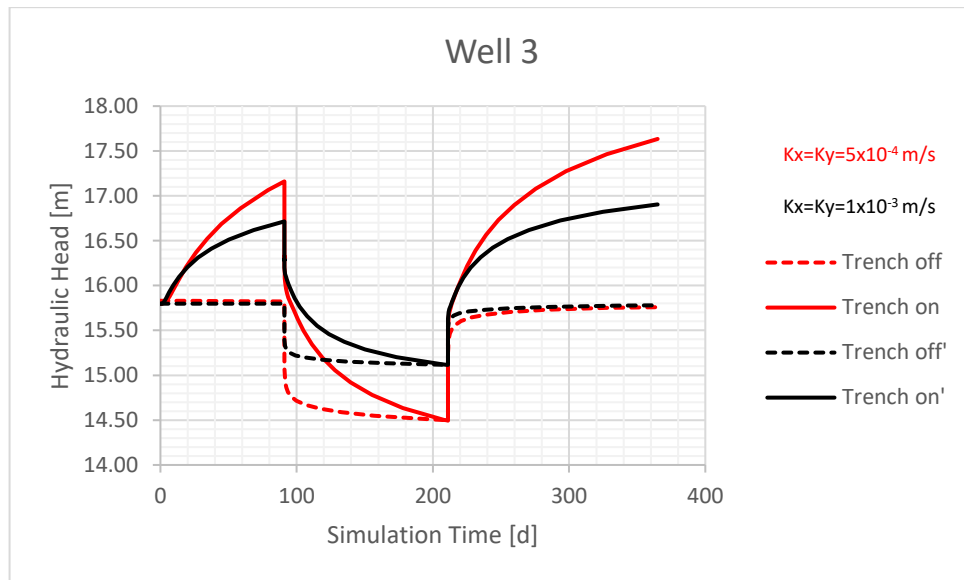


Figure 4.25 Configuration I-Evolution of the Hydraulic head in time at the Well 3 (distance from the trench $d=600$ m) determined using a trial-and-error approach. The red curve represents the hydraulic head for a hydraulic conductivity value of $K_x = K_y = 5 \times 10^{-4} \text{ m/s}$, while the black curve corresponds to a hydraulic conductivity value of $K_x = K_y = 1 \times 10^{-3} \text{ m/s}$. The hydraulic gradient for this iteration is $i = 0.002$.

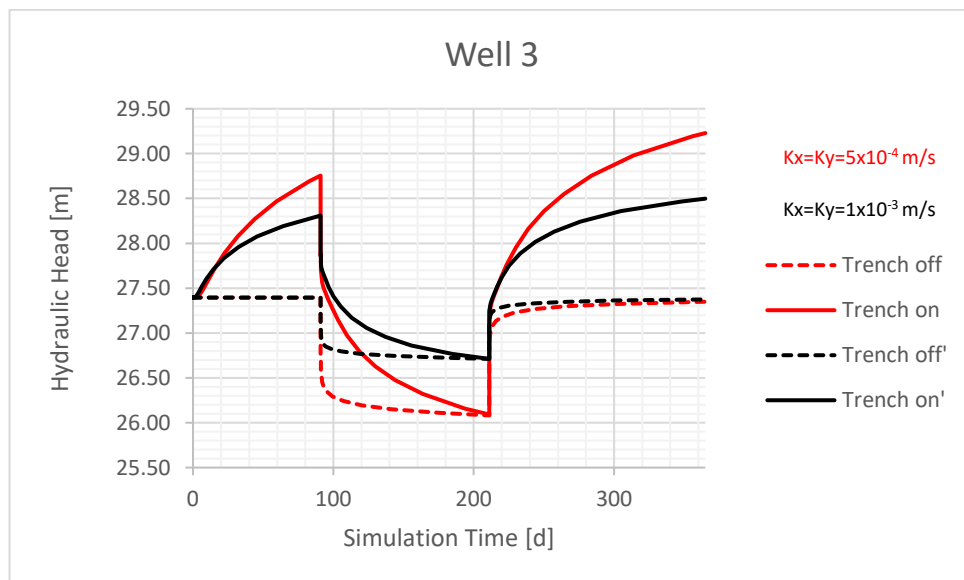


Figure 4.26 Configuration I- Evolution of the Hydraulic head in time at the Well 3 (distance from the trench $d=600$ m) determined using a trial-and-error approach. The red curve represents the hydraulic head for a hydraulic conductivity value of $K_x = K_y = 5 \times 10^{-4} \text{ m/s}$, while the black curve corresponds to a hydraulic conductivity value of $K_x = K_y = 1 \times 10^{-3} \text{ m/s}$. The hydraulic gradient for this iteration is $i = 0.006$.

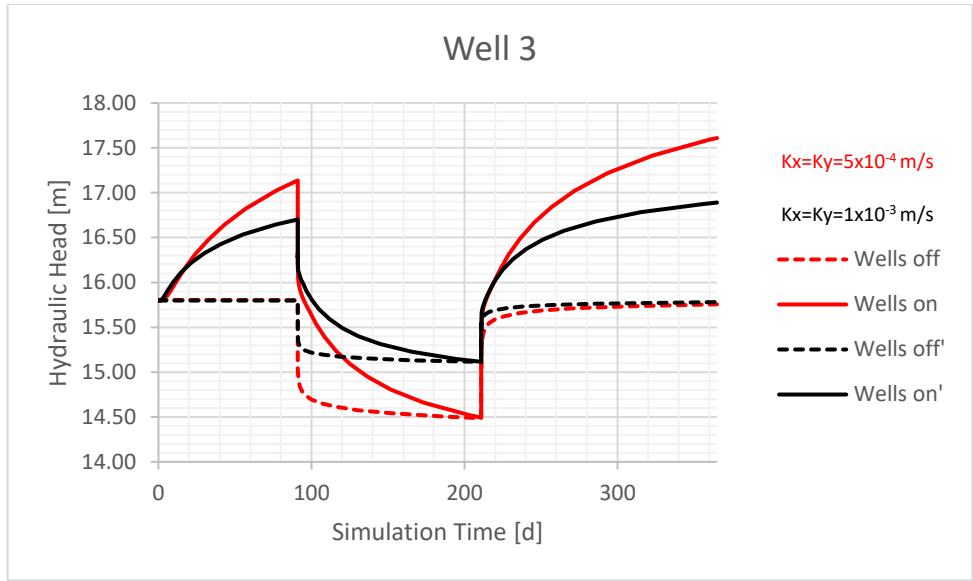


Figure 4.27 Configuration II-Evolution of the Hydraulic head in time at the Well 3 (distance from the trench $d=600\text{ m}$) determined using a trial-and-error approach. The red curve represents the hydraulic head for a hydraulic conductivity value of $K_x = K_y = 5 \times 10^{-4}\text{ m/s}$, while the black curve corresponds to a hydraulic conductivity value of $K_x = K_y = 1 \times 10^{-3}\text{ m/s}$. The hydraulic gradient for this iteration is $i = 0.002$.

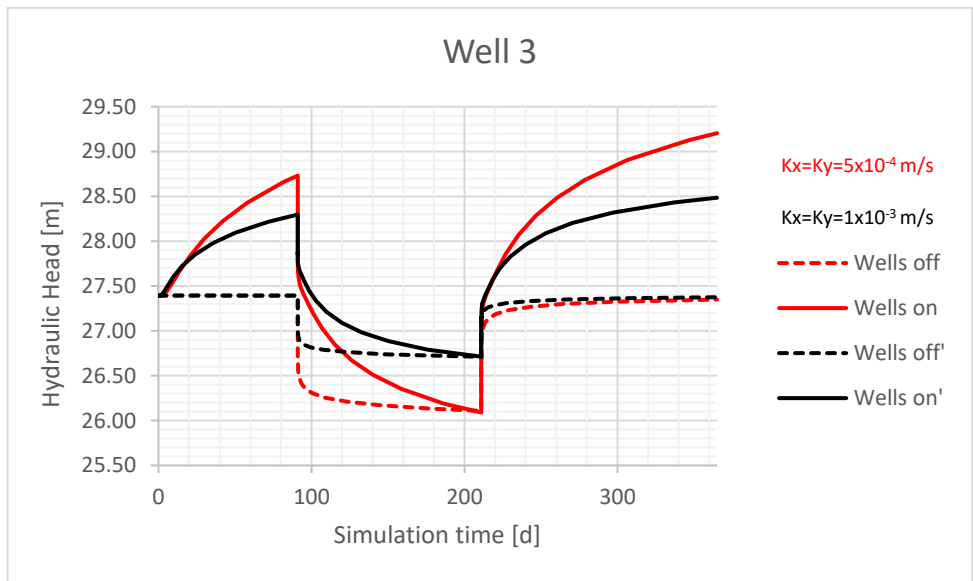


Figure 4.28 Configuration II-Evolution of the Hydraulic head in time at the Well 3 (distance from the trench $d=600\text{ m}$) determined using a trial-and-error approach. The red curve represents the hydraulic head for a hydraulic conductivity value of $K_x = K_y = 5 \times 10^{-4}\text{ m/s}$, while the black curve corresponds to a hydraulic conductivity value of $K_x = K_y = 1 \times 10^{-3}\text{ m/s}$. The hydraulic gradient for this iteration is $i = 0.006$.

4.4.1 Storage efficiency

After determining the gain in extracted flow rate at Well 3 from the analysis conducted, the storage efficiency of the MAR system was calculated. As observed in the various sections, in this case, storage efficiency does not appear to be dependent on the type of MAR system used, whether trench or injection wells, but primarily depends on the hydraulic conductivity and the distance of the extraction well from the injection point. However, it is important to note that the model used

is a simplified representation of reality; therefore, it is not possible to definitively conclude whether the type of MAR system employed does not influence aquifer recharge. Considering this, the following table summarizes the amounts of water extracted with and without recharge, and the amount of water injected into the aquifer via the MAR system, thus estimating a value for storage efficiency for both determined extraction flow rate.

Table 20 Storage efficiency of the MAR system with a recharge flow rate $Q=250$ l/s

	$K_x=K_y = 5 \times 10^{-4}$ m/s		$K_x=K_y = 1 \times 10^{-3}$ m/s	
	Value	Unit	Value	Unit
Recharge flow rate	250	l/s	250	l/s
	900	m ³ /h	900	m ³ /h
	21600	m ³ /d	21600	m ³ /d
Recharge duration	245	d/y	245	d/y
Recharge volume	5292000	m ³ /y	5292000	m ³ /y
Q extracted without MAR	25	l/s	25	l/s
	90	m ³ /h	90	m ³ /h
	2160	m ³ /d	2160	m ³ /d
Extraction duration	120	d/y	120	d/y
Volume extracted without MAR	259200	m ³ /y	259200	m ³ /y
Q extracted with MAR	32	l/s	31	l/s
	115.2	m ³ /h	111.6	m ³ /h
	2764.8	m ³ /d	2678.4	m ³ /d
Extraction duration	120	d/y	120	d/y
Volume injected	331776	m ³ /y	321408	m ³ /y
Gain in volume extracted with MAR	72576	m ³ /y	62208	m ³ /y
Storage efficiency	1.37%	/	1.18%	/

From the calculations performed, it is evident that the efficiency obtained from the two flow rate values is of the same order of magnitude in both cases, although for a flow rate of 32 l/s, the value is slightly higher. However, it is challenging to derive definitive conclusions regarding the obtained efficiency values, as it is not possible to compare them with literature data due to their absence. This arises from the inherent complexity of estimating storage efficiency in aquifers, except through modelling. In this context, the values are presented to highlight the predominant factors in the sensitivity analysis conducted.

4.5 Impact of the variation of the MAR injected flow rate

Following the obtained results, an additional test was conducted on Well 3 by varying the injection rate of the MAR system to determine if it was possible to increase the storage efficiency. Therefore, a flow rate of 100 l/s was selected for this analysis. As before, the response of the aquifer is not influenced by the type of MAR used. The obtained results are presented in the following graphs and in Table 21, where the required Δh was determined to establish the new extraction rate.

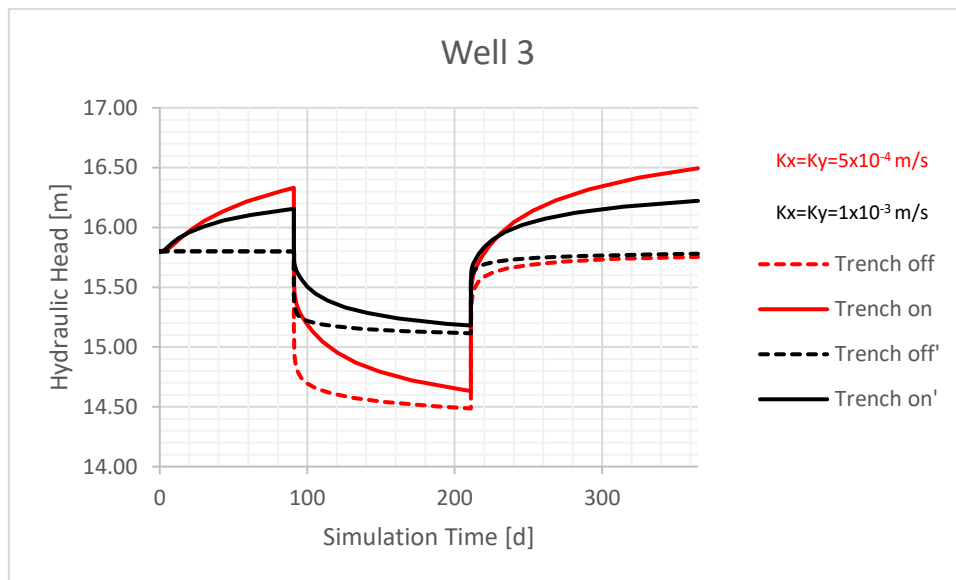


Figure 4.29 Evolution of the Hydraulic head in time at the Well 3 (distance from the trench $d=600$ m). The red curve represents the hydraulic head for a hydraulic conductivity value of $K_x = K_y = 5 \times 10^{-4} \text{ m/s}$, while the black curve corresponds to a hydraulic conductivity value of $K_x = K_y = 1 \times 10^{-3} \text{ m/s}$. The hydraulic gradient for this iteration is $i = 0.002$. The injected flow rate is $Q=100$ l/s

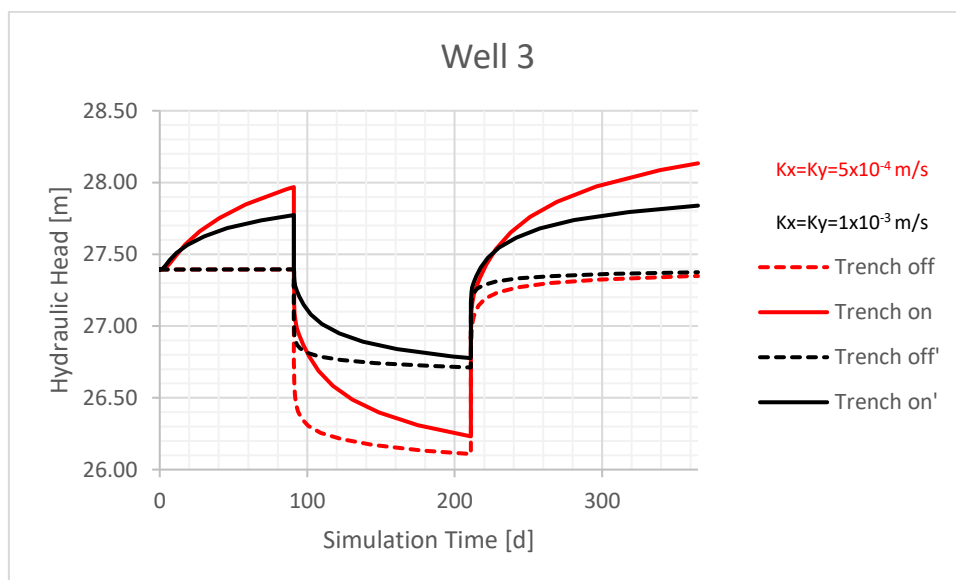


Figure 4.30 Evolution of the Hydraulic head in time at the Well 3 (distance from the trench $d=600$ m). The red curve represents the hydraulic head for a hydraulic conductivity value of $K_x = K_y = 5 \times 10^{-4} \text{ m/s}$, while the black curve corresponds to a hydraulic conductivity value of $K_x = K_y = 1 \times 10^{-3} \text{ m/s}$. The hydraulic gradient for this iteration is $i = 0.006$. The injected flow rate is $Q=100$ l/s

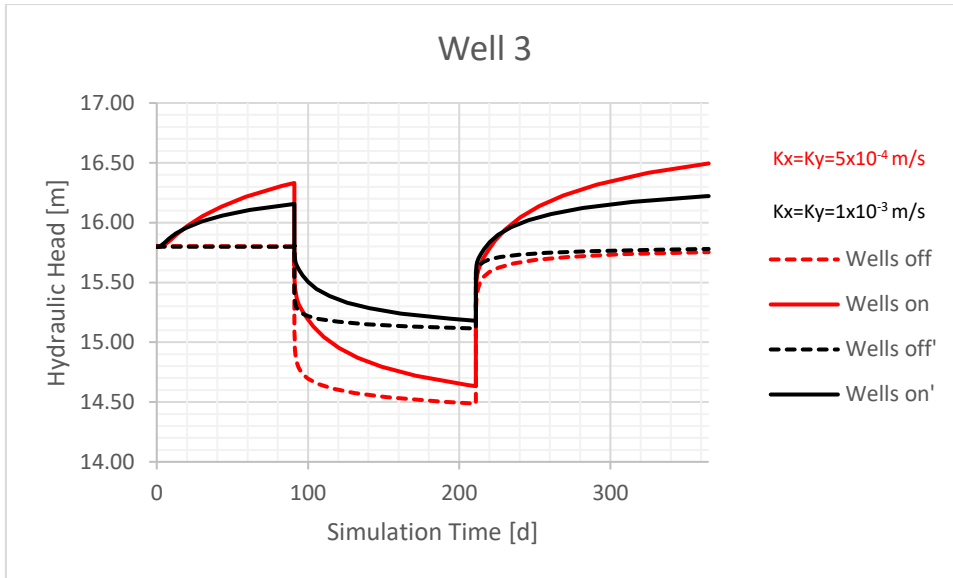


Figure 4.31 Evolution of the Hydraulic head in time at the Well 3 (distance from the wells $d=600$ m). The red curve represents the hydraulic head for a hydraulic conductivity value of $K_x = K_y = 5 \times 10^{-4} \text{ m/s}$, while the black curve corresponds to a hydraulic conductivity value of $K_x = K_y = 1 \times 10^{-3} \text{ m/s}$. The hydraulic gradient for this iteration is $i = 0.002$. The injected flow rate is $Q=100 \text{ l/s}$

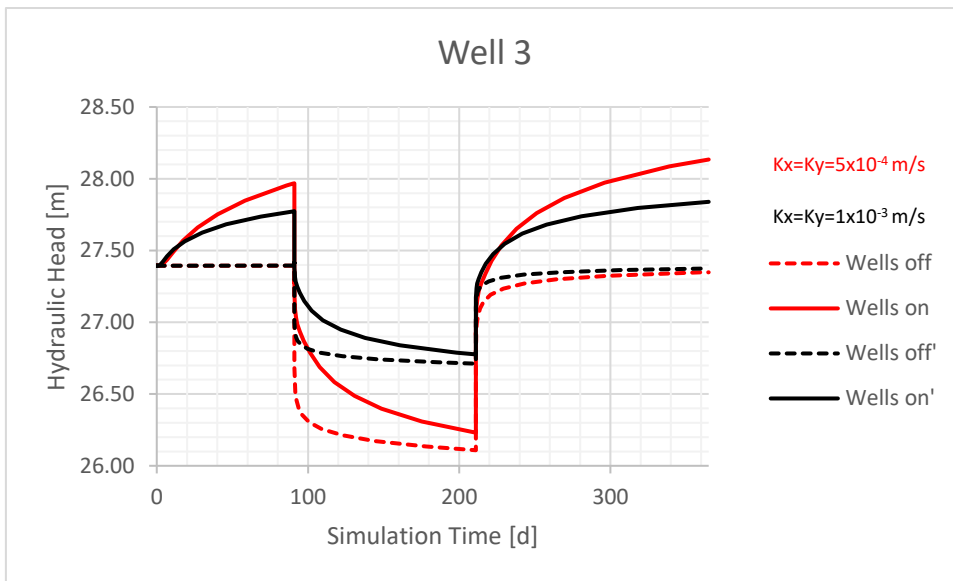


Figure 4.32 Evolution of the Hydraulic head in time at the Well 3 (distance from the wells $d=600$ m). The red curve represents the hydraulic head for a hydraulic conductivity value of $K_x = K_y = 5 \times 10^{-4} \text{ m/s}$, while the black curve corresponds to a hydraulic conductivity value of $K_x = K_y = 1 \times 10^{-3} \text{ m/s}$. The hydraulic gradient for this iteration is $i = 0.006$. The injected flow rate is $Q=100 \text{ l/s}$

Table 21 Difference in hydraulic head (Δh) at Well 3 on day 210 between the condition with active wells and inactive wells with an injected flow rate $Q=100$ l/s

Configuration I						
Hydraulic conductivity [m/s]	Hydraulic gradient $i=0.002$			Hydraulic gradient $i=0.006$		
	Drawdown day 210 [m]		Δh [m]	Drawdown day 210 [m]		Δh [m]
	Trench off	Trench on		Trench off	Trench on	
$K_x=K_y=5 \times 10^{-4}$	1.31	1.17	0.14	1.28	1.16	0.12
$K_x=K_y=1 \times 10^{-3}$	0.69	0.62	0.07	0.68	0.61	0.07
Configuration II						
Hydraulic conductivity [m/s]	Hydraulic gradient $i=0.002$			Hydraulic gradient $i=0.006$		
	Drawdown day 210 [m]		Δh [m]	Drawdown day 210 [m]		Δh [m]
	Wells off	Wells on		Wells off	Wells on	
$K_x=K_y=5 \times 10^{-4}$	1.31	1.17	0.14	1.28	1.16	0.12
$K_x=K_y=1 \times 10^{-3}$	0.69	0.62	0.07	0.68	0.61	0.07

Subsequently, the trial-and-error procedure was repeated to establish the new flow rate following aquifer recharge. At the end of the process, the values shown in the table below were obtained.

Table 22 Flow rate values (Q_{new}) determined after the trial-and-error procedure for all possible combinations of hydraulic conductivity and hydraulic gradient at well 3.

MAR system considered	Q_{new}			
	$i=0.002$		$i=0.006$	
	$K_x=K_y=5 \times 10^{-4}$ m/s	$K_x=K_y=1 \times 10^{-3}$ m/s	$K_x=K_y=5 \times 10^{-4}$ m/s	$K_x=K_y=1 \times 10^{-3}$ m/s
<u>Trench</u>	29	28	29	28
<u>Wells</u>	29	28	29	28

4.5.1 Storage efficiency

In order to verify if there was an actual gain in terms of storage efficiency, the storage efficiency for the scenario presented in the previous section was determined. The results obtained are shown in the table.

Table 23 Storage efficiency of the MAR system with a recharge flow rate $Q=100$ l/s

	$K_x=K_y = 5 \times 10^{-4}$ m/s		$K_x=K_y=1 \times 10^{-3}$ m/s	
	<u>Value</u>	<u>Unit</u>	<u>Value</u>	<u>Unit</u>
Recharge flow rate	100	l/s	100	l/s
	360	m ³ /h	360	m ³ /h
	8640	m ³ /d	8640	m ³ /d
Recharge duration	245	d/y	245	d/y
Recharge volume	259200	m ³ /y	259200	m ³ /y
Q extracted without MAR	25	l/s	25	l/s
	90	m ³ /h	90	m ³ /h
	2160	m ³ /d	2160	m ³ /d
Extraction duration	120	d/y	120	d/y
Volume extracted without MAR	259200	m ³ /y	259200	m ³ /y
Q extracted with MAR	29	l/s	28	l/s
	104.4	m ³ /h	100.8	m ³ /h
	2505.6	m ³ /d	2419.2	m ³ /d
Extraction duration	120	d/y	120	d/y
Volume injected	300672	m ³ /y	290304	m ³ /y
Gain in volume extracted with MAR	41472	m ³ /y	31104	m ³ /y
Storage efficiency	1.96%	/	1.47%	/

With the reduction of the injection flow rate, there was an increase in storage efficiency, although not significantly high, as the value remains of the same order of magnitude with a slight percentage increase. However, as mentioned earlier, it is difficult to draw conclusions about the obtained efficiency values due to the lack of comparable data.

4.6 Possible future developments

As mentioned in the section 3.7 , in order understand which parameters mostly affect the aquifer response to groundwater recharge the sensitivity analysis was conducted on:

- The type of groundwater injection, comparing trench versus wells:

From the various iterations performed, it was observed that the type of MAR selected did not influence the increase in hydraulic head in the various extraction wells, yielding similar or entirely coincident results in both cases analysed. However, it is important to consider that no tests were conducted by varying the geometric configuration of the MAR system; the same arrangement was adopted for both the trench and the series of injection wells. This factor could potentially influence the recharge process either positively or negatively.

- The distance of the activated extraction well from the trench or wells.

Regarding the distance of the extraction well from the adopted recharge system, this appears to have a certain influence on the hydraulic head measured at the well of interest following the recharge. It was a factor that allowed for the determination of which well experienced a greater increase in hydraulic head in all the combinations of factors considered. The analysis determined that the optimal distance from the injection point is 600 meters, despite Well 2, situated 400 meters from the MAR system, also exhibiting a significant increase in hydraulic head. Conversely, Wells 5 and 6, located 1000 meters and 1200 meters from the MAR system respectively, were the least affected by recharge. These wells displayed flatter curves compared to the others, indicating minimal impact from the recharge process.

- Changing the hydraulic conductivity value compared to the initial condition.

The variation in hydraulic conductivity emerged as the most significant factor influencing the increase in hydraulic head levels in the extraction wells following the recharge. Specifically, under conditions of low hydraulic conductivity—set as the initial condition—the increase in hydraulic head was more pronounced, although it remained within the same order of magnitude as the scenario with higher hydraulic conductivity. It is crucial to note that the simulations were conducted using an isotropic model. This means that the hydraulic conductivity values were uniform in all directions and layers of the model, with changes occurring based on the specific scenario considered.

- Changing the hydraulic gradient value compared to the initial condition.

The variation in the hydraulic gradient impacting the hydraulic head levels post-recharge was notably significant only in the case of low hydraulic conductivity. Analysis of the iterations revealed

that with both a higher hydraulic gradient and a low hydraulic gradient, the hydraulic head at the extraction wells increased marginally by approximately 0.02 meters.

- Changing the injected flow rate through MAR system

Once the well most significantly affected by recharge had been determined, the final parameter analysed was the recharge rate. Specifically, the recharge rate was reduced to assess whether an increase in storage efficiency could be achieved. Although there was an increase, it was not substantial enough to be considered optimal, as it remained within the same order of magnitude. However, as previously mentioned, this outcome is attributed to the nature of aquifers, which are open systems highly influenced by boundary conditions.

It might be beneficial, for instance, to investigate whether a different configuration of the MAR system and its parametrization could guide the “recharge wave” produced by injection more effectively, avoiding dispersions, towards the downstream recharge wells. Certainly, the structure of the aquifer and the specific characteristics of the considered area are crucial factors influencing dispersion.

However, it is important to note that a simplified model was used for this study. Among the various simplifications assumed, stable boundary conditions were set. These conditions significantly influence the model's behaviour, and consequently the aquifer's behaviour, leading to results that may differ considerably from a non-steady-state situation. One of the assumptions made was to set a hydraulic head boundary condition stationary upstream and downstream of the model, which determined the distribution of the hydraulic head across the entire domain. It is easy to imagine how introducing non-steady-state boundary conditions could introduce variability in the hydraulic head at the wells of interest. However, it is always worth considering how crucial this influence is for the study's objectives. Given that the main goal was to observe the aquifer's response following MAR injection, this aspect was disregarded.

Additionally, starting from this study, it is possible to conduct a more site-specific analysis by incorporating the stratigraphy of the area of interest. In the case of a favourable configuration, this could positively influence recharge. Hydraulic conductivity values obtained directly from the site could be included in FEFLOW, allowing for interpolation. It is also possible to consider inflow or outflow within the domain. However, it is important to note that each additional parameter increases the model's complexity, so the number of inputs should be tailored to the study's objectives.

For this reason, the model used in this study has these characteristics. Despite its simplicity, it serves as a foundation for further analyses aimed at gaining more information on the introduction of MAR systems in specific locations.

5 Conclusions

The objective of this study was to perform a sensitivity analysis using FEFLOW software on an unconfined aquifer system subjected to seasonal recharge through a Managed Aquifer Recharge (MAR) system. Two configurations were examined: one featuring a trench representing the MAR system, and the other comprising a series of eleven wells replacing the trench. A simplified 3D model was adopted, consisting of three layers: the upper unsaturated layer, the intermediate saturated layer, and the lower impermeable layer at the base of the domain.

The sensitivity analysis aimed to determine which factors most significantly affect the recharge, thereby increasing the hydraulic head at the extraction well. To achieve this, various scenarios were considered in which parameters such as hydraulic conductivity, hydraulic gradient, the distance between the extraction well and the injection point, and the injected flow rate were varied. The goal was to identify the optimal scenario that yields the highest increase in hydraulic head at the extraction well, consequently enhancing the available extracted flow rate.

To determine which parameters have the greatest impact, the evolution of the hydraulic head over time was observed. These hydraulic head curves were crucial in evaluating the performance of the wells, particularly in terms of the increase in hydraulic head following recharge. Additionally, the extraction flow rate was assessed by increasing the pumping rate until the hydraulic head curve under recharge conditions matched the curve under no-recharge conditions on day 210 through a trial-and-error process.

From the analysis conducted, it was determined that the optimal distance for the extraction well from the injection point is 600 meters, within a range of 200 to 1200 meters. The impact of the well distance from the recharge zone becomes evident, even if not significantly, when considering the reduction of hydraulic head gains in the wells that precede and follow the well under consideration. Specifically, hydraulic head gains of 37 cm were observed with a hydraulic conductivity value of 5×10^{-4} m/s, and gains of 17 cm were observed with a hydraulic conductivity value of 1×10^{-3} m/s. However, assessing the true influence of the distance between the pumping well and the injection point remains challenging due to the presence of other affecting parameters. This configuration was evaluated to assess the potential increase in pumping rate following the recharge. After establishing the new pumping rate under various conditions for each configuration, the storage efficiency was calculated as the ratio between the additional volume extracted with the increased flow rate and the amount of water previously injected into the aquifer. The results indicated that storage efficiency was higher in scenarios with low hydraulic conductivity, regardless of the hydraulic gradient and the MAR system considered.

However, based on the storage efficiency values obtained, it is difficult to determine whether these results are favourable for the technology used, as there are no comparable values available in the scientific literature. In an economic analysis, however, one could consider the difference of costs between a MAR infrastructure and a reservoir to achieve the same gain in water volumes available for the irrigation season.

Aiming to improve storage efficiency, an additional scenario was considered in which the injection rate was reduced. As expected, this adjustment results in lower hydraulic head gains, but it effectively increased the efficiency value, particularly in the case of low hydraulic conductivity, regardless of the hydraulic gradient and the MAR system considered.

Further studies are necessary to identify other parameters and configurations that could be crucial in enhancing the controlled aquifer recharge process. For instance, it is important to investigate how the configuration of the MAR system and its parameterization can affect recharge. Introducing non-steady-state boundary conditions would introduce variability into the model, making it more accurate. Additionally, incorporating the stratigraphy of the area of interest and using more site-specific data, such as considering inflow or outflow, would provide a more detailed understanding of the process.

The approach applied in this study can contribute to a comprehensive understanding of the factors influencing recharge efficiency and provide insights into optimizing the MAR system for improved groundwater management.

References

1. Gleeson T, Wada Y, Bierkens MFP, van Beek LPH. Water balance of global aquifers revealed by groundwater footprint. *Nature*. 2012;488(7410):197-200. doi:10.1038/nature11295
2. Gleick PH. Water in crisis. *Pac Inst Stud Dev Environ Secur Stockb Env Inst Oxf Univ Press* 473p. 1993;9:1051-0761.
3. Casanova J, Devau N, Pettenati M. Managed aquifer recharge: an overview of issues and options. *Integr Groundw Manag Concepts Approaches Chall*. Published online 2016:413-434.
4. Alam S, Borthakur A, Ravi S, Gebremichael M, Mohanty SK. Managed aquifer recharge implementation criteria to achieve water sustainability. *Sci Total Environ*. 2021;768:144992. doi:10.1016/j.scitotenv.2021.144992
5. Siebert: Groundwater use for irrigation—a global inventory - Google Scholar. Accessed December 11, 2023. https://scholar.google.com/scholar_lookup?hl=en&volume=14&publication_year=2010&pages=1863-1880&journal=Hydrol.+Earth+Syst.+Sci.&author=S.+Siebert&author=J.+Burke&author=J.+M.+Faures&author=K.+Frenken&author=J.+Hoogeveen&author=P.+Doll&author=F.+T.+Portmann&title=Groundwater+use+for+irrigation%3A+A+global+inventory
6. Falkenmark M, Folke C, Foster SSD, Chilton PJ. Groundwater: the processes and global significance of aquifer degradation. *Philos Trans R Soc Lond B Biol Sci*. 2003;358(1440):1957-1972. doi:10.1098/rstb.2003.1380
7. Famiglietti JS. The global groundwater crisis. *Nat Clim Change*. 2014;4(11):945-948. doi:10.1038/nclimate2425
8. Zektser IS, Everett LG. Groundwater resources of the world and their use. Published online 2004. Accessed December 11, 2023. <https://policycommons.net/artifacts/8956437/groundwater-resources-of-the-world-and-their-use/9822992/>
9. Wada Y, van Beek LPH, van Kempen CM, Reckman JWTM, Vasak S, Bierkens MFP. Global depletion of groundwater resources. *Geophys Res Lett*. 2010;37(20). doi:10.1029/2010GL044571
10. Wada Y. Modeling Groundwater Depletion at Regional and Global Scales: Present State and Future Prospects. *Surv Geophys*. 2016;37(2):419-451. doi:10.1007/s10712-015-9347-x
11. Lee CH. *The Determination of Safe Yield of Underground Reservoirs of the Closed-Basin Type.*; 1914.
12. Alley WM, Leake SA. The Journey from Safe Yield to Sustainability. *Groundwater*. 2004;42(1):12-16. doi:10.1111/j.1745-6584.2004.tb02446.x
13. Alley WM, Reilly TE, Franke OL. *Sustainability of Ground-Water Resources*. Vol 1186. US Department of the Interior, US Geological Survey; 1999. Accessed December 12, 2023. [https://books.google.com/books?hl=it&lr=&id=UKdIgfFWH6g4C&oi=fnd&pg=PA1&dq=%2BAley,+W.+M.,+T.+E.+Reilly,+and+O.+L.Franke+\(1999\),+Sustainability+of+ground-](https://books.google.com/books?hl=it&lr=&id=UKdIgfFWH6g4C&oi=fnd&pg=PA1&dq=%2BAley,+W.+M.,+T.+E.+Reilly,+and+O.+L.Franke+(1999),+Sustainability+of+ground-)

water+resources,+U.S.+Geol.+Surv.+Circ.,+1186,+79+pp.&ots=q__tnUgEaY&sig=0n5-R2pT1Dy_WEZEX91rLPBp5uM

14. Morris BL, Lawrence AR, Chilton PJC, Adams B, Calow RC, Klinck BA. Groundwater and its susceptibility to degradation: a global assessment of the problem and options for management. Published online 2003. Accessed December 13, 2023. <https://nora.nerc.ac.uk/id/eprint/19395/>
15. Chowdary VM, Rao NH, Sarma PBS. Decision support framework for assessment of non-point-source pollution of groundwater in large irrigation projects. *Agric Water Manag.* 2005;75(3):194-225.
16. Dwivedi AKr, Vankar PS. Source identification study of heavy metal contamination in the industrial hub of Unnao, India. *Environ Monit Assess.* 2014;186(6):3531-3539. doi:10.1007/s10661-014-3636-6
17. Hillel D. *Salinity Management for Sustainable Irrigation: Integrating Science, Environment, and Economics.* World Bank Publications; 2000. Accessed December 13, 2023. [https://books.google.com/books?hl=it&lr=&id=XZYG0e2WcdkC&oi=fnd&pg=PP8&dq=Hillel+D+\(2000\)+Salinity+management+for+sustainable+irrigation:+integrating+science,+environment,+and+economics.+World+Bank+Publications,+Washington,+DC,+USA&ots=JLgPAnHdfv&sig=bX_Jjm8QorPjC8Gb6JGrM-8bT_s](https://books.google.com/books?hl=it&lr=&id=XZYG0e2WcdkC&oi=fnd&pg=PP8&dq=Hillel+D+(2000)+Salinity+management+for+sustainable+irrigation:+integrating+science,+environment,+and+economics.+World+Bank+Publications,+Washington,+DC,+USA&ots=JLgPAnHdfv&sig=bX_Jjm8QorPjC8Gb6JGrM-8bT_s)
18. Werner AD, Bakker M, Post VE, et al. Seawater intrusion processes, investigation and management: Recent advances and future challenges. *Adv Water Resour.* 2013;51:3-26.
19. Dominguez-Faus R, Powers SE, Burken JG, Alvarez PJ. The Water Footprint of Biofuels: A Drink or Drive Issue? *Environ Sci Technol.* 2009;43(9):3005-3010. doi:10.1021/es802162x
20. Vidic RD, Brantley SL, Vandenbossche JM, Yoxtheimer D, Abad JD. Impact of Shale Gas Development on Regional Water Quality. *Science.* 2013;340(6134):1235009. doi:10.1126/science.1235009
21. Badiani R, Jessoe KK, Plant S. Development and the Environment: The Implications of Agricultural Electricity Subsidies in India. *J Environ Dev.* 2012;21(2):244-262. doi:10.1177/1070496512442507
22. Gorelick SM, Zheng C. Global change and the groundwater management challenge. *Water Resour Res.* 2015;51(5):3031-3051. doi:10.1002/2014WR016825
23. IPCC_AR6_SYR_LongerReport.pdf. Accessed December 15, 2023. https://report.ipcc.ch/ar6syr/pdf/IPCC_AR6_SYR_LongerReport.pdf
24. Piao S, Ciais P, Huang Y, et al. The impacts of climate change on water resources and agriculture in China. *Nature.* 2010;467(7311):43-51. doi:10.1038/nature09364
25. Okkonen J, Kløve B. A sequential modelling approach to assess groundwater–surface water resources in a snow dominated region of Finland. *J Hydrol.* 2011;411(1):91-107. doi:10.1016/j.jhydrol.2011.09.038
26. Kløve B, Ala-Aho P, Bertrand G, et al. Climate change impacts on groundwater and dependent ecosystems. *J Hydrol.* 2014;518:250-266. doi:10.1016/j.jhydrol.2013.06.037

27. Hrdinka T, Novický O, Hanslík E, Rieder M. Possible impacts of floods and droughts on water quality. *J Hydro-Environ Res.* 2012;6(2):145-150. doi:10.1016/j.jher.2012.01.008
28. Herbert C, Döll P. Global Assessment of Current and Future Groundwater Stress With a Focus on Transboundary Aquifers. *Water Resour Res.* 2019;55(6):4760-4784. doi:10.1029/2018WR023321
29. Rodell M, Famiglietti JS, Wiese DN, et al. Emerging trends in global freshwater availability. *Nature.* 2018;557(7707):651-659. doi:10.1038/s41586-018-0123-1
30. Bierkens MFP, Wada Y. Non-renewable groundwater use and groundwater depletion: a review. *Environ Res Lett.* 2019;14(6):063002. doi:10.1088/1748-9326/ab1a5f
31. Zhang H, Xu Y, Kanyerere T. A review of the managed aquifer recharge: Historical development, current situation and perspectives. *Phys Chem Earth Parts ABC.* 2020;118:102887.
32. Wang W, Zhou Y, Sun X, Wang W. Development of managed aquifer recharge in China. *Bol Geol Min.* 2014;125(2):227-233.
33. Gammie G, De Bievre B, Guevara O. Assessing green interventions for the water supply of Lima, Peru. *For Trends.* Published online 2015. Accessed December 19, 2023. <https://www.forest-trends.org/wp-content/uploads/imported/Assessing%20Green%20Interventions%20for%20the%20Water%20Supply%20of%20Lima%2C%20Peru.pdf>
34. The relation between the lowering of the Piezometric surface and the rate and duration of discharge of a well using ground-water storage. *Eos Trans Am Geophys Union.* 1935;16(2):519-524. doi:10.1029/TR016i002p00519
35. Ringleb J, Sallwey J, Stefan C. Assessment of managed aquifer recharge through modeling—A review. *Water.* 2016;8(12):579.
36. Dillon P, Stuyfzand P, Grischek T, et al. Sixty years of global progress in managed aquifer recharge. *Hydrogeol J.* 2019;27(1):1-30. doi:10.1007/s10040-018-1841-z
37. 2008_IGRAC_Global MAR Inventory Report.pdf. Accessed December 20, 2023. https://www.un-igrac.org/sites/default/files/resources/files/2008_IGRAC_Global%20MAR%20Inventory%20Report.pdf
38. DEEPWATER-CE. Interreg CENTRAL EUROPE. Accessed December 21, 2023. <http://programme2014-20.interreg-central.eu/Content.Node/DEEPWATER-CE.html>
39. Maliva R, Missimer T. *Arid Lands Water Evaluation and Management.* Springer Science & Business Media; 2012. Accessed December 20, 2023. https://books.google.com/books?hl=it&lr=&id=Tx-gqLgdz0YC&oi=fnd&pg=PR5&dq=Maliva,+R.G.,+Missimer,+T.,+2012.+Managed+Aquifer+r+Recharge.+Arid+Lands+Water+Evaluation+and+Management,+pp.+559%E2%80%933630.&ots=Z0yhn5xVPA&sig=Q_tIW3S6kLR1KpzKYq9lFf08Cu8
40. Kim RH, Lee S, Lee JH, Kim YM. Design of rainwater management system for eco-housing complex. In: *Rainwater and Urban Design 2007.* Engineers Australia [Barton, ACT];

- 2007:634-639. Accessed December 20, 2023. <https://search.informit.org/doi/abs/10.3316/informit.887478029796157>
41. Middleton N, Thomas DS. *World Atlas of Desertification*. Vol 182. Arnold London; 1997. Accessed January 2, 2024. <https://library.wur.nl/WebQuery/titel/951815>
 42. Esfahani AR, Batelaan O, Hutson JL, Fallowfield HJ. Combined physical, chemical and biological clogging of managed aquifer recharge and the effect of biofilm on virus transport behavior: A column study. *J Water Process Eng*. 2020;33:101115.
 43. Bachtouli S, Comte JC. Regional-scale analysis of the effect of managed aquifer recharge on saltwater intrusion in irrigated coastal aquifers: Long-term groundwater observations and model simulations in NE Tunisia. *J Coast Res*. 2019;35(1):91-109.
 44. Maassen S, Richter E, Coors A, Guimarães B, Balla D. Dissipation of micropollutants in a rewetted fen peatland: a field study using treated wastewater. *Water*. 2017;9(6):449.
 45. American Society of Civil Engineers. *Standard Guidelines for Artificial Recharge of Ground Water*. American Society of Civil Engineers; 2001. doi:10.1061/9780784405482
 46. Händel F, Liu G, Dietrich P, Liedl R, Butler Jr JJ. Numerical assessment of ASR recharge using small-diameter wells and surface basins. *J Hydrol*. 2014;517:54-63.
 47. Maliva RG, Herrmann R, Coulibaly K, Guo W. Advanced aquifer characterization for optimization of managed aquifer recharge. *Environ Earth Sci*. 2015;73(12):7759-7767. doi:10.1007/s12665-014-3167-z
 48. Available Version (via Google Scholar). Accessed March 14, 2024. <https://pubs.usgs.gov/publication/twri06A1>
 49. Diersch HJ, Kolditz O. Variable-density flow and transport in porous media: approaches and challenges. *Adv Water Resour*. 2002;25(8-12):899-944.
 50. Langevin CD, Thorne Jr DT, Dausman AM, Sukop MC, Guo W. *SEAWAT Version 4: A Computer Program for Simulation of Multi-Species Solute and Heat Transport*. Geological Survey (US); 2008. Accessed March 14, 2024. <https://pubs.usgs.gov/publication/tm6A22>
 51. Sahoo GB, Ray C, De Carlo EH. Calibration and validation of a physically distributed hydrological model, MIKE SHE, to predict streamflow at high frequency in a flashy mountainous Hawaii stream. *J Hydrol*. 2006;327(1-2):94-109.
 52. Thiéry D. Software MARTHE. Modelling of Aquifers with a Rectangular Grid in Transient state for Hydrodynamic calculations of hEads and flows. Release 4.3. *Rep BRGM S*. 1990;4.
 53. Available Version (via Google Scholar). Accessed March 14, 2024. https://www.researchgate.net/profile/Jiri-Jirka-Simunek/publication/236901785_The_HYDRUS-2D_Software_Package_for_Simulating_Water_Flow_and_Solute_Transport_in_Two_Dimensional_Variably_Saturated_Media_Version_20/links/565dc02108aeafc2aac88886/The-HYDRUS-2D-Software-Package-for-Simulating-Water-Flow-and-Solute-Transport-in-Two-Dimensional-Variably-Saturated-Media-Version-20.pdf

54. Bao YB, Thunvik R. Sensitivity Analysis of Groundwater Flow: Paper presented at the Nordic Hydrological Conference (Kalmar, Sweden, August-1990). *Hydrol Res.* 1991;22(3):175-192.
55. Razavi S, Jakeman A, Saltelli A, et al. The future of sensitivity analysis: an essential discipline for systems modeling and policy support. *Environ Model Softw.* 2021;137:104954.
56. Engelbrecht AP, Cloete I, Zurada JM. Determining the significance of input parameters using sensitivity analysis. In: Mira J, Sandoval F, eds. *From Natural to Artificial Neural Computation.* Vol 930. Lecture Notes in Computer Science. Springer Berlin Heidelberg; 1995:382-388. doi:10.1007/3-540-59497-3_199
57. Rodriguez JD, Perez A, Lozano JA. Sensitivity analysis of k-fold cross validation in prediction error estimation. *IEEE Trans Pattern Anal Mach Intell.* 2009;32(3):569-575.
58. Maxwell RM, Miller NL. Development of a coupled land surface and groundwater model. *J Hydrometeorol.* 2005;6(3):233-247.
59. Haghnegahdar A, Razavi S, Yassin F, Wheeler H. Multicriteria sensitivity analysis as a diagnostic tool for understanding model behaviour and characterizing model uncertainty. *Hydrol Process.* 2017;31(25):4462-4476. doi:10.1002/hyp.11358
60. Bao YB, Thunvik R. Sensitivity Analysis of Groundwater Flow: Paper presented at the Nordic Hydrological Conference (Kalmar, Sweden, August-1990). *Hydrol Res.* 1991;22(3):175-192.
61. Gan Y, Duan Q, Gong W, et al. A comprehensive evaluation of various sensitivity analysis methods: A case study with a hydrological model. *Environ Model Softw.* 2014;51:269-285.
62. Kuczera G, Parent E. Monte Carlo assessment of parameter uncertainty in conceptual catchment models: the Metropolis algorithm. *J Hydrol.* 1998;211(1-4):69-85.
63. Norton EC, Wang H, Ai C. Computing Interaction Effects and Standard Errors in Logit and Probit Models. *Stata J Promot Commun Stat Stata.* 2004;4(2):154-167. doi:10.1177/1536867X0400400206
64. Reiter R. A theory of diagnosis from first principles. *Artif Intell.* 1987;32(1):57-95.
65. Devak M, Dhanya CT. Sensitivity analysis of hydrological models: review and way forward. *J Water Clim Change.* 2017;8(4):557-575.
66. van Griensven A van, Meixner T, Grunwald S, Bishop T, Diluzio M, Srinivasan R. A global sensitivity analysis tool for the parameters of multi-variable catchment models. *J Hydrol.* 2006;324(1-4):10-23.
67. Gorelick SM. A review of distributed parameter groundwater management modeling methods. *Water Resour Res.* 1983;19(2):305-319. doi:10.1029/WR019i002p00305
68. FEFLOW_Flyer.pdf.
69. Fouad M, Hussein EE, Jirka B. Assessment of numerical groundwater models. *Int J Sci Eng Res.* 2018;9(6):951-974.